DYNAMIC LOADING EFFECTS OF TRACKED AND WHEELED MILITARY VEHICLES ON A MODULAR TRUSS BRIDGE

AMPLIFICATION DYNAMIQUE DES VÉHICULES MILITAIRES À CHENILLES ET À ROUES SUR UN PONT À TREILLIS MODULAIRE

A Thesis Submitted to the Division of Graduate Studies
of the Royal Military College of Canada
by

Brandon Pinkney, rmc, P.Eng.
Captain

In Partial Fulfillment of the Requirements for the Degree of
Master of Applied Science

April, 2020

ACKNOWLEDGEMENTS

I would like to recognize the guidance, assistance, and effort I received from my supervisors, Dr. Gordon Wight and Dr. Marc-André Dagenais, throughout all phases of this research endeavour. Whether reviewing analysis results indoors or recording experimental data in freezing conditions outside, their expertise, knowledge, and time were key to ensuring the quality of information present in this document.

Field testing, including all preparations, execution, and post-activity tasks would not have been remotely successful if it wasn't for the efforts of technicians Mr. Dexter Gaskin and Mr. Steve Vanvolkingburgh. Their familiarity with testing equipment, problem-solving skills, and focus on completing the task correctly the first time, enabled smooth conduct of all phases of experimental testing.

This research was made possible through the funding support provided by Director Combat Support Equipment Management (DCSEM) 3. This research work is a component of a larger project sponsored by DCSEM which includes the development of the Military Load Classification (MLC) Software Suite for both the Canadian Armed Forces and North Atlantic Treaty Organization. This particular work is intended to provide a better understanding and improvement of doctrine related to the MLC system.

Because field testing was conducted in Wainwright, Alberta, the support of nearby military units was crucial to ensure appropriate vehicles were available when required. Without personnel and vehicle support from 1 Combat Engineer Regiment, and vehicle support from Lord Strathcona's Horse (Royal Canadians), this research would not have been possible. Similarly, the willingness of Real Property Operations Detachment Wainwright to facilitate testing on the Battle Bridge was key to realizing research objectives.

Maintenance of personal efficiency, focus, and general sanity must be recognized as the results of effort put forward by my fiancée, Tiffany. She patiently supported me through numerous presentation practices and draft document revisions, all with a willingness to learn about my research.

ABSTRACT

In the context of bridge assessment, application of inaccurate factors accounting for the dynamic loading effects of vehicles can have significant impact on the predicted structural capacity of a bridge. Currently there is no guidance in bridge design codes to assist engineers in differentiating between the dynamic loading effects of tracked and wheeled vehicles; present codes solely consider wheeled vehicle traffic, and therefore offer guidance on dynamic impact factors for this one vehicle type. Internationally, factors that account for dynamic loading are referred to as Dynamic Load Allowance (DLA), Dynamic Amplification Factor (DAF), Dynamic Load Factor (DLF), dynamic impact factor (IM), or impact fraction (I).

In the North Atlantic Treaty Organization (NATO) Military Load Classification (MLC) system, load effects and structural capacities are compared to determine the feasibility of vehicles crossing bridges, rafts, and ferries. While the MLC system differentiates between tracked and wheeled vehicle effects, it does not make recommendations for the application of separate dynamic load factor values. Canadian Armed Forces (CAF) and United States Army bridge assessment manual recommendations indicate that a single load factor should be applied in all loading cases, which imposes strategic mobility restrictions on tracked vehicles, specifically main battle tanks.

Experimental testing was conducted on a fully instrumented modular pony truss bridge to compare dynamic loading effects of two tracked military vehicles and two wheeled military vehicles. Vehicle speed and deck condition were controlled to determine the relationship between dynamic bridge response and speed over smooth and rough surfaces. Using data gathered from eighty-six test iterations, appropriate DLA values were calculated for each vehicle, as well as each vehicle category. A comparison of international bridge code factors was completed to assess the validity of calculated values.

Analysis showed dynamic loading effects due to tracked vehicles were approximately half of those generated by wheeled traffic. Variation of surface condition showed that both vehicle types caused increased dynamic effects in the bridge under degraded deck conditions or obstacle emplacement. The dynamic loading effects of tracked vehicles associated with the rough deck conditions were significantly lower than those observed for wheeled vehicles. Recommendations were made regarding appropriate DLA values for use in the MLC system, as well as respective Canadian and American national bridge codes.

RÉSUMÉ

L'évaluation de la capacité structurale d'un pont implique l'utilisation de coefficients de pondération de charges et de coefficient de tenues. Ces coefficients peuvent avoir un impact significatif sur l'évaluation particulièrement lorsqu'ils sont surestimés ou encore inexacts. Actuellement, il n'y a pas de distinction dans les normes sur le calcul des ponts routiers entre l'effet dynamique causé par un véhicule à chenilles versus un véhicule à roues. Les normes, dont la norme canadienne CSA-S6, sont basées uniquement sur les camions ou véhicules à roues. Ainsi les coefficients de majorations dynamiques fournies par ces normes sont applicables uniquement à ce type de véhicule alors qu'aucune recommandation n'est apportée pour les véhicules à chenilles. Il existe plusieurs termes pour désigner l'effet dynamique d'une charge mobile soit : coefficient de majoration dynamique, coefficient d'amplification dynamique, coefficient de charge dynamique et coefficient d'impact dynamique.

Dans le système de Classification des ponts et véhicules utilisé par l'Organisation du traité de l'Atlantique Nord (OTAN), les effets des charges et la capacité structurale sont comparés afin de déterminer la faisabilité d'une traversée d'un pont, d'un radeau ou encore d'un traversier. Même si ce système fait la différentiation entre les véhicules à chenilles et les véhicules à roues, il n'y a pas de recommandations précises sur l'application de coefficients de majoration dynamique propre à chaque type de véhicule. Les manuels d'évaluation des ponts utilisés par les Forces armées canadiennes et par l'armée américaine prescrivent l'utilisation d'un coefficient unique devant être appliqué dans tous les cas de chargement, ce qui impose des restrictions stratégiques sur la mobilité des véhicules à chenilles, particulièrement pour les chars de combat.

Des essais expérimentaux ont été effectués sur un pont à treillis modulaire entièrement instrumenté afin de comparer les effets dynamiques causés par deux véhicules militaires à chenilles et deux véhicules militaires à roues. La réponse dynamique du pont a été évaluée selon différents paramètres : la vitesse des véhicules et la condition de la surface de roulement sur le tablier du pont, surface lisse ou irrégulière. En utilisant les données recueillies à partir de quatre-vingt-six essais, les valeurs appropriées du coefficient de majoration dynamique ont été déterminées pour chaque type de véhicule. Ces valeurs expérimentales ont été validées et comparées aux facteurs utilisés par différentes normes de calcul sur les ponts routiers.

L'analyse des données expérimentales a démontré que les effets dynamiques causés par les véhicules à chenilles sont environ la moitié de ceux causés par les véhicules à roues. La variation de la condition de surface, simulant une chaussée endommagée et la présence d'obstacle, a permis d'observer une augmentation de l'effet dynamique induit par les deux types de véhicules. Cependant, les effets dynamiques induits par les véhicules à chenilles ont été nettement inférieurs à ceux induits par les véhicules à roues pour une condition de surface irrégulière. Des recommandations ont été faites concernant les valeurs appropriées du coefficient de majoration dynamique à utiliser dans le système de Classification militaire des ponts et véhicules, ainsi que pour les normes sur le calcul des ponts routiers canadien et américain.

CO-AUTHORSHIP STATEMENT

This thesis document is written in the manuscript-based format as laid out in the Royal Military College of Canada Thesis Preparation Guidelines, dated May 2015. The author of this thesis document, Brandon Pinkney, was the main author for both manuscripts (Chapter 3 and Chapter 4) contained within this document; co-authors (supervisors) provided guidance, advice, and feedback throughout all steps of analysis and manuscript writing. As the author plans to submit both manuscripts contained in this document for publication in peer-reviewed journals, each individual article submission will note both supervisors as co-authors.

Chapter 3 – Manuscript 1: Testing Procedures for Experimental Assessment of a Modular Truss Bridge is planned for submission to the American Society of Civil Engineers (ASCE) Journal of Bridge Engineering, in the category of data paper submission.

Chapter 4 – Manuscript 2: Dynamic Load Testing of a Modular Truss Bridge Using Military Vehicles is planned for submission to the ASCE Journal of Bridge Engineering.

TABLE OF CONTENTS

LIST OF FIGURES

LIST OF TABLES

LIST OF ACRONYMS

AASHO	American Association of State Highway Officials
AASHTO	American Association of State Highway and Transportation Officials
AEV	Armoured Engineer Vehicle
AREA	American Railway Engineering Association
ASCE	American Society of Civil Engineers
BBF	Bottom of bottom flange
BTC	Bottom of top chord
BTF	Bottom of top flange
CAF	Canadian Armed Forces
CDSB	Canadian Division Support Base
CL	Canadian Loading
CHBDC	Canadian Highway Bridge Design Code
DA	Dynamic Amplification
DAF	Dynamic Amplification Factor
DLA	Dynamic Load Allowance
DLF	Dynamic Load Factor
DND	Department of National Defence
EMPA	Swiss Federal Laboratories for Materials Testing and Research (Eidgenössische Materialprüfungs- und ForschungsAnstalt)
FLS	Fatigue Limit State
GVWR	Gross Vehicle Weight Rating
I	Impact Fraction
IM	Dynamic Impact Factor
LHS	Load Handling System
LRFD	Load and Resistance Factor Design
MBT	Main Battle Tank
MLC	Military Load Classification
MSVS	Medium Support Vehicle System

NATO	North Atlantic Treaty Organization
OHBDC	Ontario Highway Bridge Design Code
PA	Annual or project vehicle permit
PB	Bulk haul vehicle permit
PC	Controlled vehicle permit
PS	Single trip vehicle permit
SBS	Side of bridge support
SLS	Serviceability Limit State
SP	String potentiometer
STANAG	Standardization Agreement
TAPV	Tactical Armoured Patrol Vehicle
TBC	Top of bottom chord
TTC	Top of top chord
UDL	Uniformly Distributed Load
ULS	Ultimate Limit State
US	United States
WA	Web rosette, 45° angle to horizontal
WH	Web rosette, horizontal
WV	Web rosette, vertical

LIST OF SYMBOLS

A	Activity factor
$A_{0...n}$	Response amplitude at the specified number of periods of oscillation
A_{dyn}	Dynamic response
A_{stat}	Static response
c	Damping coefficient
D	Distance between instrumented location and driving axis
f	Fundamental frequency
$F(t)$	External force applied to a system (function)
H	Height of bridge cross section at instrumented location
k	Stiffness coefficient
K	Calibration constant
L	Span length
m	Lumped mass
MLC_T	Military Load Classification (tracked vehicle)
MLC_W	Military Load Classification (wheeled vehicle)
n	Number of periods
n_r	Number of people at risk
N	Number of input variables
p	Percentage of critical damping
p_{lam}	Percentage of timber deck lamination
P_F	Notional probability of failure
R_{dyn}	Dynamic bridge response
R_{sta}	Static bridge response
s	Separation factor for dynamic loading
S_s	Stringer spacing
t_d	Deck thickness
t_{dr}	Required and effective timber deck thickness

u	Displacement of a system
$\dot{u}$	Velocity of a system
$\ddot{u}$	Acceleration of a system
$u(x_i)$	Standard uncertainty for input variable x_i
$u(x_i,x_j)$	Covariance of input variables x_i, x_j
$u(y)$	Combined uncertainty of the measurement y
V	Vehicle speed
w	Warning factor
W	Vehicle width
x_i, x_j	Input variables (for uncertainty)
y	Measured quantity
α	Zone of influence parameter
α_L	Live load factor
β	Reliability index
δ	Logarithmic decrement
δ_D	Dynamic deflection
δ_S	Static deflection
ε	Strain
$\varepsilon_{max,min}$	Principal strains
ε_α, ε_β, ε_γ	Strains from rosette gauges α, β, and γ, respectively
θ_p	Angle of principal strain
ν	Coefficient of variation
ν_{DAF}	Coefficient of variation of the Dynamic Amplification Factor
ν_{DLA}	Coefficient of variation of the Dynamic Load Allowance
σ	Standard deviation
Φ	Dynamic amplification factor

CHAPTER 1 INTRODUCTION

1.1 Background

Effectively executing bridge lifecycle management is a task that requires significant technical knowledge. To facilitate the management of over 47,000 publicly owned bridges across the country [1], Canada applies the Canadian Highway Bridge Design Code (CHBDC), ensuring national standardization of design, construction, and maintenance of these structures. It does this by applying limit states philosophy, which, broadly speaking, ensures acceptability of design through the comparison of appropriate factored loading effects and factored structural resistance [2].

To account for the variable effects of moving vehicle loads, the CHBDC outlines the requirement for a Dynamic Load Allowance (DLA) factor. Transitory loads such as those imposed by vehicle traffic are comprised of static and inertial elements [3]; the inertial component can be estimated as a portion of the static load effect [4]. The DLA is a quantification of this dynamic load estimate.

The North Atlantic Treaty Organization (NATO) provides guidance on bridge assessment in a military context through NATO AEP-3.12.1.5 (Standardization Agreement (STANAG) 2021). This document, which outlines details of the Military Load Classification (MLC) system, allows military engineers to place a numerical value on the relationship between vehicle load effects and load-carrying capacity of bridges, rafts, and ferries. Similar to the CHBDC, the MLC system requires the incorporation of a DLA factor in certain cases. However, due to the international audience to which this document is focussed, dictation of a specific DLA value is not made, but a recommendation is made to follow the standard practice of the nation expected to use the bridge [5].

Unlike the CHBDC, the MLC system provides differentiation between tracked and wheeled vehicle types for classification of their loading effects on bridges, which allows more accurate determination of mobility limits than considering only a wheeled vehicle loading scenario. However, in the context of military bridge engineering in the Canadian Armed Forces (CAF) and United States (US) Army, a DLA value of 0.15 is used to account for dynamic loading in all cases [6], [7]; there is no differentiation of factor value based on vehicle type.

Use of a DLA value that is applicable in all loading scenarios may be inappropriate due to the typical difference in dynamic properties of tracked and wheeled vehicle types. Application of a unique, reduced value of the factor for tracked vehicle traffic could see a notable increase in the mobility of tracked vehicles, such as main battle tanks (MBTs), across existing bridge infrastructure globally.

This research is part of a larger study aimed at understanding the effects of dynamic tracked and wheeled vehicle loading on various bridge types. As such, this investigation will build on the

limited research conducted previously, which focussed on determining dynamic load effects due to military traffic on a continuous composite concrete-steel bridge [8].

1.2 Aim

The aim of this research was threefold: first, to validate the difference in the dynamic loading effects of tracked and wheeled vehicle loading on a bridge; second, to quantify this behaviour through the generation of appropriate DLA values; and third, to examine the effects of an irregular surface on the dynamic loading effects.

1.3 Scope

To accomplish the stated goals of this investigation, a comprehensive experimental testing programme was developed. This programme was limited to analyzing the effects of vehicle crossings over a specific bridge at controlled speeds, with controlled deck conditions.

An ACROW modular pony truss bridge was identified for use in this testing programme, as shown in Figure 1.1. Located at 3rd Canadian Division Support Base (CDSB) Wainwright, the Battle Bridge spans 39.62 m across the Battle River, has a deck width of 5.00 m, and is used almost exclusively by military vehicles on an unpaved road.

Figure 1.1 - Battle Bridge

In total, thirty-nine instruments gathered data during testing iterations at a sample rate of 1200 Hz. These instruments included strain gauges and displacement transducers; strain gauges were placed at mid-span truss chords, on end-span stringers, and above superstructure bearing pads; linear displacement potentiometers were located at mid- and quarter-span.

Four vehicles were used for the conduct of iterative tests, including two tracked vehicles, and two wheeled vehicles. To begin, smooth-surface test iterations took place; static load tests were conducted to determine the static response of the bridge, which were then compared with responses due to vehicles crossing at controlled speeds ranging from 10 km/h to 50 km/h. A total of eighty-

six tests were conducted. Using the data captured from the installed instruments, dynamic effects were quantified, and a code calibration process was applied to determine statistically relevant DLA values for each vehicle. Next, bridge responses to vehicular loading over rough deck conditions were recorded using the same controlled crossing speeds.

A comparison of DLA values by vehicle type was completed to determine the validity of applying separate values for tracked and wheeled vehicles. To determine the effects of deck condition on bridge response, a comparison of dynamic load response due to smooth and rough surface condition was conducted.

1.4 Document Organization

This document is written in the manuscript, or article, style format [9], and includes six chapters.

Chapter 1 – Introduction contains specific background information on the research conducted, including information related to the broader research initiative that formed the requirement for this investigation, as well as aim and scope of research.

Chapter 2 – Literature Review delivers a detailed summary of concepts, past experimentation, and guidance taken from published engineering documents related to bridge dynamics, the MLC system, and experimental testing and analysis considerations.

Chapter 3 – Manuscript 1: Testing Procedures for Experimental Assessment of a Modular Truss Bridge gives a detailed account of the experimental setup used for the collection of data. This chapter is the first manuscript that has been submitted in the category of a data paper to an appropriate engineering journal and as such, contains a short literature review pertinent to the content of the manuscript. Additionally, this chapter contains a separate reference list, to facilitate submission as a standalone document.

Chapter 4 – Manuscript 2: Dynamic Load Testing of a Modular Truss Bridge Using Military Vehicles presents details related to the analysis of experimental data. This manuscript aims to determine the validity of establishing unique DLA values for tracked and wheeled military vehicles. Similar to Chapter 3, this chapter has been submitted to a journal as a standalone article; as such, it contains a short literature review and reference list of its own.

Chapter 5 – Conclusions and Recommendations provides a summary of the entire research endeavour, with a focus on the key conclusions from analysis of the data. As this study is made in the context of a larger research objective, suggestions are made to guide future researchers in similar investigations.

Finally, Chapter 6 – References lists all cited sources of information used throughout this document, and does not differentiate between those sources used in standalone manuscripts and those in other chapters.

Appendices follow Chapter 6. While general information related to the conduct of the experimental testing and data analysis are indicated in appropriate chapters of the main document, appendices include additional information that may be useful in recreating the experimental testing programme, following the details associated with post-testing analysis, or are of use in application of classification systems outlined in this document.

Appendix A – Characteristics of Military Load Classification Hypothetical Vehicles contains dimensions, weights, and other load characteristics of the hypothetical vehicles used to classify vehicle effects and bridge, ferry and raft capacities in the NATO MLC system.

Appendix B – Standard Military Load Classification Curves contains graphs that can be used to assign MLC ratings to vehicles based on the span of the bridge being assessed, as well as the vehicle type, and load effects (bending moment and shear force).

Appendix C – Data Manipulation outlines additional theory relevant to the modification of experimental data. This includes application of appropriate data filters, calculation and propagation of errors and uncertainties, and calculation of principal strains given specific strain sensor layouts.

Appendix D – Instrumentation Identifiers and Associated Data Acquisition Channels contains information on the data acquisition system used during field testing. Channel names associated with specific data acquisition units are coupled to instrument identifiers to indicate where each instrument was located on the bridge.

Appendix E – Vehicle Properties contains technical information of vehicles used during testing. Note that this is considered RESTRICTED information; this appendix will only be included in a limited distribution copy of this document, and will not be made available for online publication.

Appendix F – Iterative Testing Plan contains details related to the experimental programme generated for field testing. This appendix indicates, for each serial of testing, which vehicle was used, speed and direction of crossing, and deck surface condition.

Appendix G – Model Validation outlines the calculations that were made to validate the simplified numerical model with raw data gathered during field testing. This includes validation using both strain and displacement data.

Appendix H – Data Filter Convergence Test Results contains graphical information related to the selection of data filter cut-off frequency that was applied during data analysis to isolate the effects of static loads on bridges.

Appendix I – Bridge Dynamic Load Allowance Comparison contains information on calculation of DLA values using the equations and values outlined in multiple national bridge codes and military bridge manuals. These calculated values are made based on the properties of the bridge used in experimental testing.

CHAPTER 2 LITERATURE REVIEW

2.1 General

This chapter focusses on reviewing relevant literature available on the topics of bridge load factors, DLA, the MLC system, and considerations for experimental testing of bridge-vehicle interaction. Each manuscript included in this document has a standalone, focussed literature review section relevant to the information being presented; this chapter focuses on providing a background on all topics covered in each manuscript.

Some theories introduced in this document are applicable across multiple engineering disciplines; those outlined herein will be done so within the context of structural engineering of bridges.

2.2 Limit States Philosophy

Bridge design and assessment are governed in Canada by the CHBDC. This document applies the limit states philosophy to the processes of bridge design and analysis [2], which has as its main objective the achievement of more uniform structural safety formats than the previous working stress methods. This philosophy involves the identification of potential failure modes, determination of acceptable levels of safety, and allows the designer to consider specific limit states that may be of significance to the scenario being investigated [10].

With the application of limit states design philosophy comes the distinct design and analysis states themselves: Serviceability Limit State (SLS), Ultimate Limit State (ULS), and Fatigue Limit State (FLS). SLS design is concerned with potential interruptions to the functional use of the bridge [10] (due to vibration, superstructure acceleration, and sway, among others [4]). ULS design focuses on maximum load carrying capacity of a bridge, in which load factors are applied to bridge loads to increase their effects, while performance factors are applied to the bridge strength and resistance metrics in order to decrease capacity estimates [10]. This allows for designing engineers to incorporate a controllable degree of conservatism into the design and assessment of bridges. An acceptable ULS design sees factored resistances being larger than factored applied loads [2]. Finally, FLS design focuses specifically at ensuring the cumulative fatigue effect due to a predetermined number of standard cyclic transient loads is equivalent to that caused by the expected variable transient loads over the expected life of a bridge, without causing failure [4]. For the purpose of this analysis, ULS design will be investigated further.

2.2.1 Reliability Index

To control the level of conservatism applied to structural design, a reliability index (given as β) is used to quantify structural safety with current probabilistic design methods [10]. This is accomplished through a relationship with a notional probability of failure, used to quantify the risks of structural failure causing injury or loss of life, as given in Equation 2.1 [4]:

$$P_F = \frac{AK}{w\sqrt{n_r}} \quad 2.1$$

where P_F is the notional probability of failure;
A is the activity factor relating risk to human life with activities related to structural use;
K is a calibration constant related to existing experience known to provide satisfactory life safety;
w is a warning factor corresponding to the probability of an individual being killed or seriously injured due to structural failure; and
$\sqrt{n_r}$ is an aversion factor based on the number of people (n_r) at risk if failure occurs [11].

The P_F term is considered notional since it is calculated with various factors and constants used to statistically describe risk, rather than being calculated from measured results [11]. For the purposes of this investigation, knowledge of the quantifiable nature of the terms used to determine the notional probability of failure is adequate; a detailed investigation into the values selected for each term will not be completed.

The level of safety used in the Canadian code has an inversely proportional relationship to the notional probability of failure [4], [11]. Table 2.1 [4] outlines various reliability index values, along with the corresponding notional probability of failure. Canadian code dictates that new bridge construction achieves a lifetime target reliability index of 3.50 [4], with design life being 75 years [2], [4].

For assessments of existing structures, system and element characteristics can be used to determine an appropriate reliability index, which in turn can prescribe specific strength and resistance factors applicable to ongoing analysis. Determination of load factor values for new construction is accomplished with the identification of appropriate codified load combinations and the type of limit state analysis being conducted [2].

Table 2.1 - Notional probability of failure for various reliability indices [4]

Reliability Index (β)	Notional Probability of Failure (P_F)		
2.00	2.3×10^{-2}	or	1:44
2.25	1.2×10^{-2}	or	1:81
2.50	6.2×10^{-3}	or	1:160
2.75	2.8×10^{-3}	or	1:360
3.00	1.4×10^{-3}	or	1:740
3.25	5.6×10^{-4}	or	1:1,800
3.50	2.3×10^{-4}	or	1:4,300
3.75	8.8×10^{-5}	or	1:11,000
4.00	3.2×10^{-5}	or	1:31,500
4.25	1.1×10^{-5}	or	1:93,500
4.50	3.4×10^{-6}	or	1:294,000

2.2.2 Load Factors and Allowances

Load factors allow for consideration of the variability of loads, lack of analysis precision related to the effects of loading, and the reduced likelihood of loads acting on the structure from different sources concurrently. The CHBDC uses these factors for various applications, forming three groups: permanent, exceptional, and transitory loads [2].

Permanent loads include dead load, earth and hydrostatic pressure, and secondary prestress effects. These focus on all structural and non-structural components of the bridge [2]. Forms should be taken into account, and future additions should be considered [4], such as an as-yet-uninstalled bituminous road surface layer, for example.

Exceptional loads either are expected to occur, or achieve the magnitude specified, only in rare instances [4]. These include earthquake, stream, ice, or debris loads, or vehicle or vessel collision [2]. Not including earthquake loads, CHBDC ultimate limit state analysis sees the maximum effect of a specified exceptional load multiplied by its corresponding load factor having a probability of exceeding bridge capacities in the region of 1% over a 75 year design life [4].

Transitory loads are either present only occasionally, or vary in magnitude, position, or direction [4]. This transitory load category considers effects due to live loads (applied either independently, or in conjunction with a DLA when applicable), strain, deformation or displacement effects, wind load (both on the structure and on traffic), and differential foundation settlement or movement [2]. Highway traffic would be considered a live load [4], as the load from a passing truck would only act on the structure for a limited time. Similarly, strain or deformation effects could occur due to temperature variation, shrinkage, or creep [2].

Dynamic assessment on bridges inherently focuses on the effects transitory loads have on the structure. A complete bridge response to moving traffic is comprised of two components: the static response caused by the weight of the vehicle in question, and the dynamic response due to the vehicle's inertia [3]. To account for the increase in loading due to vehicular inertia, a dynamic load factor is applied to the design. The dynamic and vibratory vehicle effects are defined as being equivalent to a portion of the static load effects [4], such that the static effect multiplied by the dynamic amplification factor will give a good approximation of the full dynamic loading experienced by the bridge [12], [13]. This is summarized through Equation 2.2 [3], [12], [14], [15]:

$$R_{dyn} = R_{sta}(1 + DA) \tag{2.2}$$

where R_{dyn} is the maximum dynamic response of the bridge;
R_{sta} is the maximum static response of the bridge; and
DA (Dynamic Amplification) is a ratio of dynamic response to static response [16].

To better understand the concept of dynamic response increases due to moving loads, a graphical representation is appropriate. Consider Figure 2.1 [17], which shows a simply supported bridge. The static response of the bridge is indicated by a dashed line, with the solid line representative of the maximum dynamic response. It can be seen that the maximum dynamic response exceeds that of the static response.

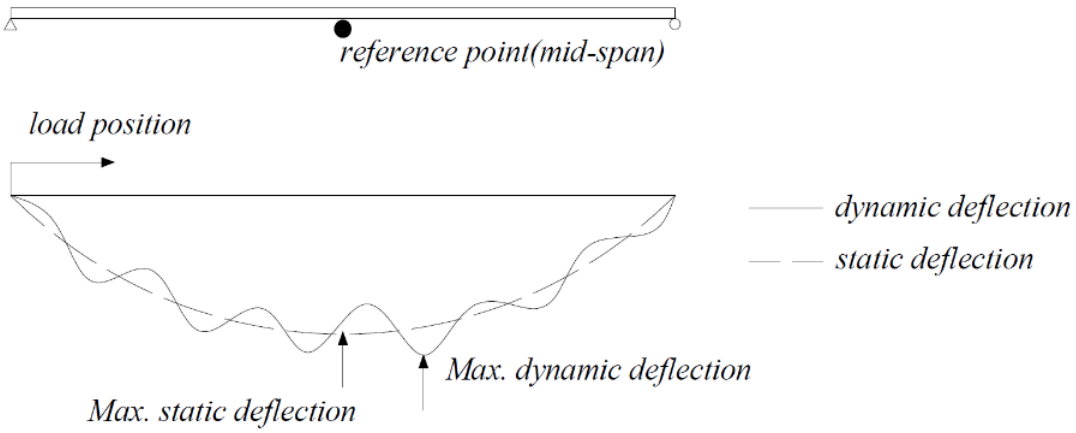

Figure 2.1 - Simple bridge deflection due to a moving load [17]

2.3 Dynamic Load Allowance

2.3.1 Nomenclature

Nomenclature for dynamic load effects is varied, and continues to change with time. Some terms that have been, and continue to be used include Dynamic Load Allowance (DLA) [2], Dynamic Amplification Factor (DAF) [18], [19], dynamic impact factor (IM) [14] or impact fraction (I) [20], and Dynamic Load Factor (DLF) [21], [22]. The relationship between these factors is summarized in Equation 2.3 [8]:

$$DLA \approx IM \approx DA \approx DAF - 1 \approx DLF - 1 \tag{2.3}$$

It is important to note that there is a differentiation between code-based dynamic factors and those derived through experimental means. DLA, DLF, and IM are generally representative of code-based values [12], [21], while DA is derived through testing [12]. The DAF term is used in some international codes [21], while other research has used it to represent experimentally determined responses [12].

For the purposes of this research, the term DA will represent the dynamic amplification term calculated with experimental data, and DLA will represent the dynamic amplification term given in published design and analysis codes.

2.3.2 History

Dynamic load effects were not always considered in bridge design. A rail bridge collapse in Britain in 1849 spurred what is presumably the first recorded dynamic load testing aimed at determining the effects of a test vehicle crossing cast iron beams [18], [23]. From these tests, it was determined that a moving load has an increased effect on the beams when compared to the same load's static effect. An equation was put forward that accounted for this amplification, as given in Equation 2.4 [18]:

$$\Phi = \frac{\delta_D}{\delta_S} \tag{2.4}$$

where Φ is the DAF;
δ_D is the largest dynamic deflection; and
δ_S is the static deflection.

Continued interest in dynamic effects was the result of further bridge collapses in the following decades. Development of the field saw modifications to this DAF definition, such that Equation 2.5 [18] was used by the Swiss Federal Laboratories for Materials Testing and Research (EMPA) over the 1924-1949 time period:

$$DA = \frac{A_{dyn} - A_{stat}}{A_{stat}} \times 100\% \quad (2.5)$$

where A_{dyn} is the maximum dynamic response; and
A_{stat} is the static response.

Considering the definition of dynamic effect terms given in Equation 2.3, comparison of Equations 2.4 and 2.5 indicate that the $DA \approx DAF - 1$ relationship exists between these two early definitions of bridge dynamics.

Attempts to codify dynamic impact factors in North America originate with the rail industry, with the American Railway Engineering Association (AREA) adopting a span length-based definition in 1922, as given in Equation 2.6 [24], and the American Association of State Highway Officials (AASHO) suggesting a modified equation for use in highway applications, shown in Equation 2.7 [24]. A joint AREA/AASHO conference in 1927 led to the adoption of Equation 2.8 [20], [24]:

$$I = \frac{50}{L + 150} \quad (2.6)$$

$$I = \frac{L + 250}{10\,L + 500} \quad (2.7)$$

$$I = \frac{50}{L + 125} \quad (2.8)$$

where I is the impact factor (not to exceed 0.30); and
L is the span of the bridge in feet.

Continued testing using various instrumentation yielded the conclusion that the dynamic increment was not the same when determined experimentally with strain and displacement data [18], with indications that dynamic bridge response factors calculated using displacement data were typically larger than those same factors calculated with strain data [14]. There is some conflict within the literature on the best way to determine the dynamic amplification factor of a structure; some sources outline moment-based calculation should be used [17] (which can be accomplished via measurement of strain [14], [25]), and others indicate standard tests that have been developed using deflection as a primary data collection source, with strain measurement as an alternate only [14], [18].

North American studies conducted through the 1950s and 1960s began identifying various factors that had an effect on the dynamic response of bridges. These included road surface roughness, condition of approaches, and the ratio of axle spacing to bridge span [24]. Further studies have

identified a significant list of factors that affect dynamic responses; these are covered in more detail in Section 2.3.3.1.

Data analyzed from EMPA tests in 1975 indicated that placement of the measuring instruments in relation to the vehicle location on the bridge was of significant importance when considering dynamic effects as a result of different deflection distribution across bridge cross-sections for static and dynamic tests [18]. To account for this phenomenon, a zone of influence is defined as extending from the outer edge of the wheel contact surface through the bridge cross-section at a 45° angle [14], [18]. Roughly speaking, a point of instrumentation is considered within the zone of influence if it lies within this boundary. To better quantify this scenario, the zone of influence parameter α is introduced as per the modified Equation 2.9 [18]. A graphical representation is of assistance in furthering understanding of this definition, as given in Figure 2.2 [18]:

$$\alpha = \frac{D}{H + 0.5W} \tag{2.9}$$

where α is the zone of influence parameter;
D is the distance between the instrumented location and the driving axis (in metres);
H is the height of the cross section at the instrumented location (in metres); and
W is the width of the vehicle (in metres) [14].

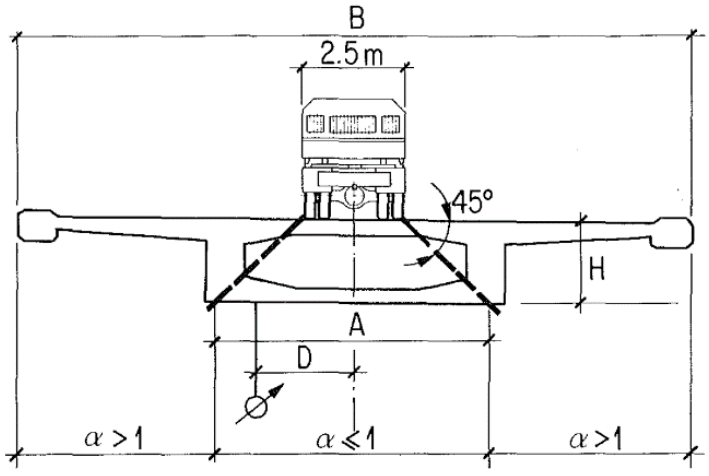

Figure 2.2 - Graphical definition of the zone of influence parameter [18]

Equation 2.9 is noted in literature with the denominator $(H + 1.25)$ [14], [18]; with initial tests having been completed by a vehicle with a width of 2.5 m, the half-width is simplified in the equation to 1.25. This simplification is parameterized by the term $0.5W$ here to allow for application to vehicles of any width.

If $\alpha > 1.0$ it can be said that the calculated DA value will be larger than realistic due to the low static response (A_{stat}) value. Therefore, data gathered for the instrument located in this area should be disregarded and not used to calculate DA, as proper dynamic effects are not felt in this area. A value of $\alpha \leq 1.0$ indicates the measurement location lies within the zone of influence, and the gathered data is usable for DA determination [14], [18].

Bridges that allow for transverse load distribution, such as a pony truss design, will not be able to have this simplified zone of influence definition applied. In instances such as this, it may be more appropriate to use data from whichever instrumented location experiences the maximum static response across the entire cross-section [14].

Aside from the relationship between instrument location and the transverse placement of the load during dynamic testing, there are a multitude of other factors that influence dynamic response of bridges to vehicle traffic.

2.3.3 Structural Dynamics

The way a structure will dynamically respond to loading is dependent on the unique design of the edifice in question. Therefore, an engineer will often have an extensive number of combinations of design options available to respond to expected loading scenarios. While the specific methods of reaction may be distinctive between structures, a general equation of motion can be summarized by Equation 2.10 for a simplified unforced system, and Equation 2.11 for a simplified system subjected to an external force [26]:

$$m\ddot{u} + c\dot{u} + ku = 0 \tag{2.10}$$

$$m\ddot{u} + c\dot{u} + ku = F(t) \tag{2.11}$$

where m is the lumped mass of the system;
c is the damping coefficient defining damping within the entire system;
k is the stiffness coefficient defining stiffness of the entire system;
$\ddot{u}$ is the acceleration of the system;
$\dot{u}$ is the velocity of the system;
u is the displacement of the system; and
$F(t)$ defines the external force applied to the system.

In the context of bridge dynamics, one must consider an equation of motion for the entire bridge system that accounts for the dynamic properties of both the bridge as well as the load (vehicle). Therefore, an understanding of which physical properties influence bridge and vehicle dynamic responses is appropriate.

2.3.3.1 Vehicle Dynamic Effects

Structural dynamics is a complex field, with a host of factors potentially impacting the dynamic loading of bridges, and indeed impacting how other potential factors form part of the dynamic system. Writ large, these factors could be categorized such that they include the dynamic properties of the vehicle, the dynamic properties of the bridge, and the roughness of the road itself [27], [28].

Vehicle dynamics account for various design options used in each vehicle crossing the bridge. Suspension characteristics, axle spacing, gross vehicle weight, vehicle speed [16], [29], and even tire stiffness and production methods [30] each play a role in how the load is transferred to the bridge. For example, it has been shown that air-spring damping systems in vehicles result in lower dynamic effects than vehicles using leaf-spring systems [21], [24], [31]–[33], and increased vehicle weight results in a smaller calculated DA value [14], [21], [31]. Typically vehicle damping, achieved through the suspension system, has a much larger impact on the dynamic response of the system than bridge damping [34]. Some research has shown that mass variation does not change the DA value calculated through experimentation, but rather changes the speed at which maximum DA occurs [16].

While there is limited disagreement in the literature [17], the majority of research has found that the speed of vehicles crossing the bridge does have measurable impact on the dynamic response of the structure [16], [21], [35]. For example, test speed was an important parameter in testing conducted with bridges of average and poor surface condition, but good condition deck surfaces did not see dynamic response factor growth with vehicle speed increases [30]. Such disagreement could be the result of a complex relationship between the vehicle speed on a bridge and the dynamic effects experienced by the structure [21], indicating that tests should be conducted with crossings made at multiple different speeds where possible. Additionally, variation in vehicle motion while crossing a bridge could impact the dynamic response of the bridge [16], [21], [29]. This requires testing constraints on vehicles, such as maintenance of consistent speed and direction of travel for the duration of each crossing to ensure the generation of quality data.

Vehicle speed and initial excitation specifically upon entering the bridge should be considered some of the more important factors to consider when analyzing dynamic bridge loading [16], [34], but are difficult to assess [24]. While loads lacking any sort of suspension see speed being the most important factor affecting dynamic response [16], this investigation will focus on loads that have their own intrinsic suspension systems.

Axle and vehicle spacing is an additional factor that has a notable impact on dynamic bridge response. Ensuring axles are spaced to avoid being in phase with bridge superstructure response will have significant effect on moderating dynamic impacts [24], [36]. This occurs because the spacing of vehicle axles affects the amplitude of the static bridge response [16]; when considering a multiple lane or multiple vehicle loading scenario, it is unlikely that axles will be in phase [2]–[4], and the added static load effect results in a reduced DA value [14], [21].

In the context of this research, it is important to outline an exception to the expected trend of axle spacing effects. MBTs are often transported using prime movers when travelling between established bases and off-site training areas, as shown in Figure 2.3. In the case where a long vehicle having regularly spaced axles passes across a short span, even at low speeds, the response generated by the vehicle could cause a resonance effect within the structure. For special vehicles seeking transportation permits where the axle spacing is such that this synchronization of response with the natural frequency of the bridge occurs, it is prudent to consider increased dynamic amplification within the structure due to the load [37]. This is counter-intuitive to the previously mentioned trend of heavier vehicles imparting lower dynamic effects.

Figure 2.3 - Canadian Army tank hauler

2.3.3.2 Bridge Dynamic Effects

Similar to vehicle properties affecting dynamic characteristics, specific bridge properties will dictate how a bridge will react to dynamic loads. These include damping, span length, natural frequency, and road surface irregularities [14], [16], [21], [24]. Additional materials used to facilitate the construction of a bridge were not found to impact the DA values [16].

Considering the bridge itself, two types of damping can be considered: material and structural. Material damping is an inherent material property [18], [38]; for example, the ability of wood to mitigate vibrations has resulted in the application of an additional dynamic reduction factor in Canadian code [2], [21]. Structural damping is a function of the bridge type, bearings used, and the types and quantities of connections within the structure, among others [18], [38]. In this example, a modular bridge with many pinned connections will experience significantly more damping than one that is a continuous structure with minimal connections incorporated into the design. System damping, due to external influence, is sometimes considered as an additional damping category, resulting from such factors as bridge interactions with vehicle suspensions or soil around the foundations [18]. Quantification of damping occurs with the application of the logarithmic decrement, given in Equation 2.12 [18], [38], which is related to the percentage of critical damping as outlined in Equation 2.13 [18]:

$$\delta = \frac{1}{n} \ln \frac{A_0}{A_n} \quad 2.12$$

$$p = \frac{\delta}{2\pi} \times 100\% \quad 2.13$$

where δ is the logarithmic decrement;
n is the number periods over which decaying oscillations are measured;
$A_{0\ldots n}$ is the response amplitude at the specified number of periods of measurement; and
p is the percentage of critical damping.

Although use of the logarithmic decrement implies viscous damping throughout the system, in reality bridges experience both viscous and friction damping. Despite this detail, it has been found that the logarithmic decrement is still an appropriate quantification of damping [38].

For spans less than 75 m, testing conducted in Ontario has shown that the logarithmic decrement is typically in the range of 0.040 to 0.150 [36], while EMPA measurement has found the logarithmic decrement between 0.030 and 0.300 [18]. Tests on various bridge spans have shown that spans greater than 20 m have lower damping ratios than shorter bridges [4]. Generally, bridges with closed cross-sections, bridges without skew, and narrow bridges have been found to have less structural damping capacity than bridges with alternate characteristics [18].

A relationship between span length and dynamic amplification has been found through multiple testing regimes. It has been noted that longer-span bridges tend to have smaller dynamic responses than short-span bridges, and could potentially be neglected due to the effect of larger dead load and diminished proportion of total live load generated by a single vehicle [21], [24], [39]. Vehicle characteristics and road surface irregularities tend to have diminished impact on dynamic response for long-span bridges [16]. Various equations outlining a relationship between the span length and first natural frequency of a bridge have been presented in the literature. It has been found that an estimate of the first fundamental frequency can be given by Equation 2.14 [18], [27], and is especially useful for structures with extremely complex geometry:

$$f = 95.4\, L^{-0.933} \quad 2.14$$

where f is the bridge fundamental frequency in Hertz; and
L is the bridge span in metres.

The natural frequencies of a structure should always be considered when assessing dynamic responses. When loading functions on a structure have the same or similar natural frequencies, resonance or quasi-resonance can occur, increasing the loading effects above normal response

levels. In the context of bridge traffic, the dynamic wheel load frequency of traffic tends to be in the range of 2 Hz to 5 Hz [16], [18], [21], [24], [28], [31].

Finally, the state of the road surface plays an important part in the vehicle-bridge relationship, both on the span and in the approach to the bridge. It has been found that surface roughness increases the dynamic effects in the bridge structure [3], [14], [16], [18], although some research has indicated it is more likely to cause local material distresses than a global dynamic response increase [23], [40]. Increases measured from rough surface profiles are likely the result of vehicle excitation occurring at frequencies near the vehicle natural frequency, inciting larger forces to be imparted onto the bridge structure, resulting in larger recorded dynamic bridge response [29].

2.3.4 Calculation of Dynamic Load Allowance

The DLA values listed in codes are not generated directly from physical testing. Instead, the results from experimental testing (individual DA values) are aggregated, and select factors are applied to generate a statistically relevant DLA value.

There is some discussion within the literature on the optimal equation to apply to calculate DA values. To determine dynamic amplification from known experimental results, the maximum dynamic response of all measured data is compared with the maximum static response of the structure [31], [41], even if measurements are captured with sensors at different locations [41], using Equation 2.15 [3], [13], [14], [16], [33], [41], [42]:

$$DA = \frac{R_{dyn} - R_{sta}}{R_{sta}} \tag{2.15}$$

where R_{dyn} is the maximum dynamic bridge response; and
R_{sta} is the maximum static bridge response.

This calculation of DA can be completed for each test run made on a bridge by the test vehicle. Considerations to be made when generating a testing programme are outlined in Section 2.5. To calculate a statistically relevant DLA, multiple DA values are averaged and applied to Equation 2.16 [14], [18], [31]:

$$DLA = \frac{\overline{DA}(1 + \nu s\beta)}{\alpha_L} \tag{2.16}$$

where $\overline{DA}$ is the average value of the calculated DA terms acquired through testing;
ν is the coefficient of variation of the measured quantity, in this case DA;
s is the separation factor for dynamic loading;
β is the reliability index; and
α_L is the live load factor.

The coefficient of variation can also be defined as the ratio of standard deviation to mean of the data being considered [4], [14], which is the experimentally calculated DA values in this case. The separation factor, sometimes referred to as the sensitivity factor, outlined for DLA calibration has been shown to have a value of 0.57 [14], [18].

Some discussion exists related to the relevance of this approach to DLA calibration from experimental data. Ideally, the denominator of Equation 2.16 should account for the variability of static loads rather than equate to the live load factor itself, as the live load factor does not solely define the static load variations [14]. Without additional detailed analysis, a value for α_L of 1.4 is recommended [14], [18].

2.3.5 Dynamic Load Allowance in Codes

There is a lack of uniformity internationally with regards to implementing a single method to determine DLA in design codes. There are, however, similar independent variables indicated across national and international codes that define this factor.

One common way of defining dynamic factors is via span length [12], [16], [17], [21], [28]. It has been found that shorter spans tend to exhibit higher DLA values than longer spans [4], [24], [30]. This is possibly one of the oldest methods of defining dynamic impacts. It should be noted that the definition of dynamic response based on this parameter does not account for characteristics of the vehicle, nor the multitude of other bridge properties noted in Section 2.3.3.1 [16]. The AASHO 1973 bridge code defines dynamic impact in terms of span length, as given in Equation 2.8 above [20]. The New Zealand code takes the same approach, providing a graphical relationship between span and DLF as well as the corresponding numerical relationship given in Equation 2.17 [22]:

$$DLF = \begin{cases} 1.30, & L \leq 12\ m \\ 1 + \dfrac{15}{L + 38}, & L > 12\ m \end{cases} \qquad 2.17$$

where L is the bridge span for positive moment, and average of adjacent span lengths for negative moment, in metres.

The second way DLA is typically defined is in terms of the fundamental frequency of the bridge [12], [16], [17], [21], [24], [40], [43]. This definition of DLA accounts for quasi-resonance effects noted previously, where the vehicle and bridge frequencies are sufficiently close to each other to cause increased bridge response to vehicle traffic [16], [18], [21], [24], [28], [31]. The Ontario Highway Bridge Design Code (OHBDC) defined DLA in this manner; more detailed studies completed after the 1979 first edition was published resulted in a lower calibrated DLA value set being codified in the 1983 second edition, as outlined in Figure 2.4 [43].

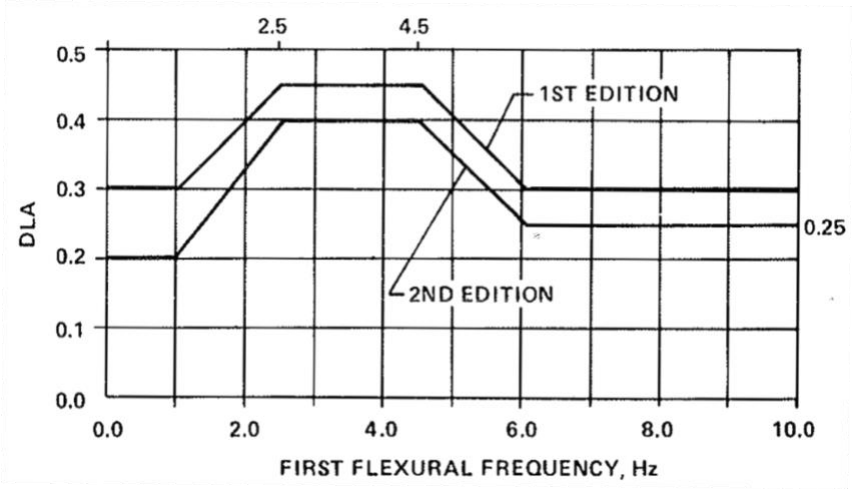

Figure 2.4 - DLA as given in OHBDC editions [43]

China's 2004 bridge design code also uses flexural frequency to define dynamic impacts on the bridge using the IM nomenclature. Instead of using a graphical approach, the code presents the relationship in a mathematical format through Equation 2.18 [21]:

$$IM = \begin{cases} 0.05, & f < 1.5\ Hz \\ 0.1767 \ln f - 0.0157, & 1.5\ Hz \leq f \leq 14\ Hz \\ 0.45, & f > 14\ Hz \end{cases} \quad 2.18$$

where f is the bridge fundamental frequency in Hertz.

Finally, traffic loading models can be used to define appropriate DLAs to different expected loading scenarios [21]. Canadian code dictates DLA based either on element type, or number of axles of a specified standard vehicle loading a superstructure, and restricts application altogether in cases where the standard lane loading is being considered for design and analysis purposes [2], [4]. Table 2.2 summarizes these provisions for components other than buried structures.

Table 2.2 - CHBDC DLA provisions [2]

Loading Model	DLA
Deck joints	0.50
One Canadian Loading-W (CL-W)/Special Truck axle	0.40
Any two axles of the CL-W Truck, or axle nos. 1 to 3 of the CL-W Truck or the tandem or tridem of the Special Truck(s)	0.30
Three axles of the CL-W Truck, except for axles nos. 1 to 3, or more than three axles of the CL-W Truck, or more than one axle unit of the Special Truck(s)	0.25

In Canada, special permits can be granted for vehicles with loads or dimensions that exceed regulations to use transport infrastructure such as bridges. Additional guidance on DLA modification is applied to such vehicles, as there is increased knowledge of the loads and dimensions [4]. Four categories of permits exist under the CHBDC: annual or project permit (PA), bulk haul permit (PB), controlled permit (PC), or single trip permit (PS). PA vehicles include vehicles with an indivisible load authorized by the annual permit for unsupervised transit mixed with uncontrolled traffic. PB vehicles are made of bulk haul, divisible loads permitted for multiple trips while mixed with uncontrolled traffic, where axle loads restrictions are rigorously applied, but gross vehicle weights may exceed established limits. PC vehicles may carry an indivisible load along an established route under supervision, with specific travel conditions applied based on the scenario in question. Finally, PS vehicles may carry an indivisible load for a single trip, while mixed with uncontrolled traffic under supervision, where axle loads and gross vehicle weight may exceed established restrictions. All permit classes specify unique loading conditions to apply during structural analysis. Based on these categories, the DLA used for assessment of restricted-speed vehicles must be modified by the factors noted in Table 2.3 [2].

Table 2.3 - DLA modification factors for permit vehicle loads [2]

Vehicle Speed (V, km/h)	DLA Modification Factor
$V \leq 10$	0.30
$10 < V \leq 25$	0.50
$25 < V \leq 40$	0.75
$V > 40$	1.00

The British and Australian codes follow a similar loading model approach to that of Canada [44], [45]. While the CHBDC code does not consider lane loading in conjunction with DLA application, some Australian scenarios incorporate a uniformly distributed load (UDL) for traffic in conjunction with standard vehicle axle loads [21], [44]. Table 2.4 outlines the Australian DLA application.

Table 2.4 - Australian code DLA provisions [21], [44]

Loading Model	DLA
W80 wheel load	0.40
A160 axle load	0.40
M1600 tri-axle group (including traffic load UDL)	0.35
M1600 load (including traffic load UDL)	0.30
S1600 load (including traffic load UDL)	0
HLP loading	0.10

Considering regulations other than national-level bridge codes, the Canadian military has published a bridge manual for use on operational deployments. In this document, a global DLA of 0.15 is specified for all bridge types and span lengths, with the exception of timber stringer and floating bridges, which have no amplification factor applied for dynamic loading. This DLA is rationalized by the fact that military convoys maintain strict vehicle spacing and relatively low speeds compared to normal civilian traffic. This document does recommend increasing the DLA up to 30% under extremely unfavourable road surface conditions, or 40% for extremely unfavourable surface conditions for short elements where only one axle loads the span [6].

Similarly, a design and test code used by select NATO allies to guide military bridging and gap-crossing equipment procurement indicates a DLA of 0.15 for interior portions of the equipment, and 0.2 for ramps [46] (assuming differentiation between the ramp and interior components of gap-crossing equipment).

2.4 Military Load Classification System

Design and construction of bridges for unrestricted use is a very detailed process. While appropriate for application in civilian environments, the level of detail is not always appropriate to military applications. As such, an alternate method is employed by NATO member state militaries, called the MLC system, through NATO AEP-3.12.1.5 (STANAG 2021). This method allows for the clear relation of vehicle-induced load effects with the structural load capacity of bridges, military rafts, or military ferries [5]. In the context of this research, focus will be maintained on bridge effects, and considerations for military rafts and ferries will not be investigated.

With the unavoidable requirement of military traffic to use civilian bridges, whether for peacetime transition between military establishments or wartime combat missions, knowledge of vehicle load effects and bridge capacities is critical to maintaining manoeuvrability. The MLC system is key in allowing military commanders to generate informed direction for subordinates related to route identification and selection during operations, as it gives clear indication on which bridges can support the required military traffic. With the flexibility afforded by this classification method, military engineers can identify MLC ratings of any bridge that may lie within a specified area of operations, further assisting the commander in protecting existing structures against overloading, protecting vehicles, crew, and cargo, and prioritizing bridge strengthening and replacement [6].

The MLC system indicates which vehicles can pass over a specified bridge, and which need to be diverted. Under normal crossing conditions, if the MLC rating of a vehicle is less than or equal to that of the bridge, it can pass; if the vehicle possesses an MLC rating greater than that of the bridge, it must be diverted to an alternate crossing point [5]. Exceptional crossing conditions are possible, and will be outlined in detail in Section 2.4.2.3.

2.4.1 Classification of Vehicles

AEP-3.12.1.5 (STANAG 2021) introduces 32 standard hypothetical vehicles to facilitate classification; 16 tracked, and the corresponding 16 wheeled vehicles. The MLC rating numbers are based on the short ton (907 kg) mass of the hypothetical tracked vehicle, scaled from MLC 4 to MLC 150; maximum vehicle characteristics are also listed for both the tracked and wheeled hypothetical vehicles of each MLC. An example of the MLC 50 hypothetical tracked vehicle is given in Figure 2.5, with the corresponding MLC 50 hypothetical wheeled vehicle parameters listed in Table 2.5 [5]. A complete list of hypothetical vehicles can be found in Appendix A – Characteristics of Military Load Classification Hypothetical Vehicles.

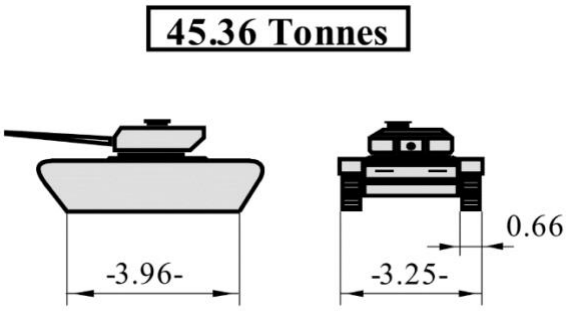

Figure 2.5 - MLC 50 hypothetical tracked vehicle parameters (m) [5]

Due to the difference in load distribution mechanics of wheeled and tracked vehicles, a similar MLC rating for tracked and wheeled vehicles will correspond to vehicles of different overall masses [6]. For example, as noted in Figure 2.5 and Table 2.5, a tracked vehicle rated at MLC 50 has a mass of 45.36 t, with the wheeled MLC 50 vehicle massing 52.62 t. The hypothetical wheeled vehicle as a consequence of the distance over which vehicle mass is distributed (vehicle length);; Figure 2.6 outlines this relationship in a graphical context [7].

Table 2.5 - MLC 50 hypothetical wheeled vehicle parameters [5]

Axle Load (Tonnes) and Spacing (m)	Maximum Single Axle Load	Tire Load and Nominal Ground Contact Width (m)	Axle Load and Nominal Ground Contact Width (m)	Axle Wheel Spacing and Nominal Ground Contact Width (m)
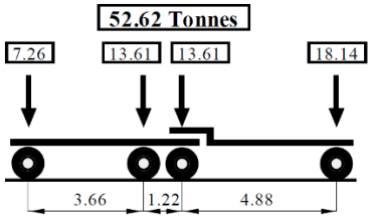	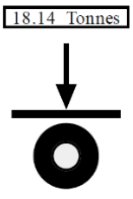	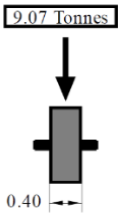	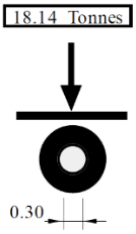	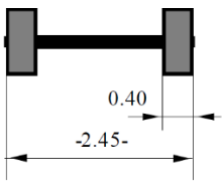

It is important to note that the MLC value associated with vehicles is only a number, and does not represent the mass of the vehicle being analyzed [5]–[7]. Similarly, the hypothetical vehicles are not representative of vehicles in service with any NATO member militaries; rather, real military vehicles can be related to the established hypothetical vehicle effects, thus enabling classification [47].

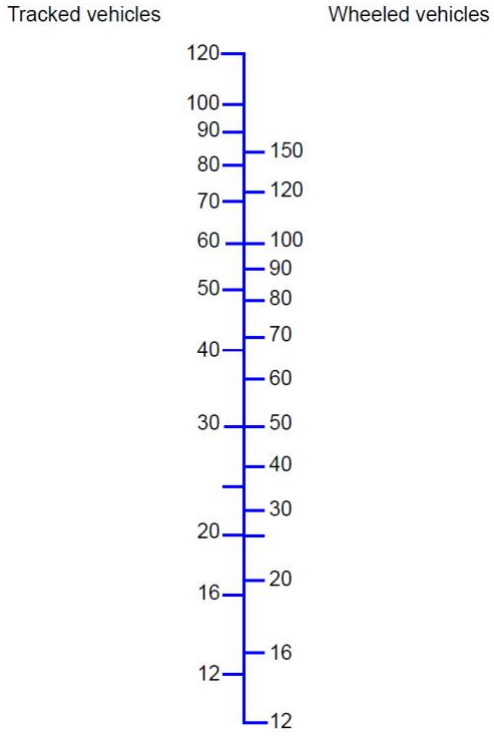

Figure 2.6 - MLC comparison of hypothetical tracked and wheeled vehicles based on equivalent mass [7]

As noted previously, wheeled and tracked vehicles distribute load differently; the effect is sufficiently significant that categorization must be completed for each vehicle type independently [5]–[7]. To accomplish this, the effects on spans from 1 m to 100 m due to trafficking of the hypothetical vehicles have been determined and plotted. Effects include unit bending moment, calculated by dividing the maximum bending moment by the span length being assessed, as well as the shear force imparted on the structure. An example of the resultant curves for wheeled vehicles is shown in Figure 2.7 [6]. Four plots exist: two for hypothetical tracked vehicles, and two for hypothetical wheeled vehicles (one each for unit bending moment, and one each for shear force). All plots can be found in Appendix B – Standard Military Load Classification Curves, with the associated tabulated values found in NATO AEP-3.12.1.5 (STANAG 2021) [5].

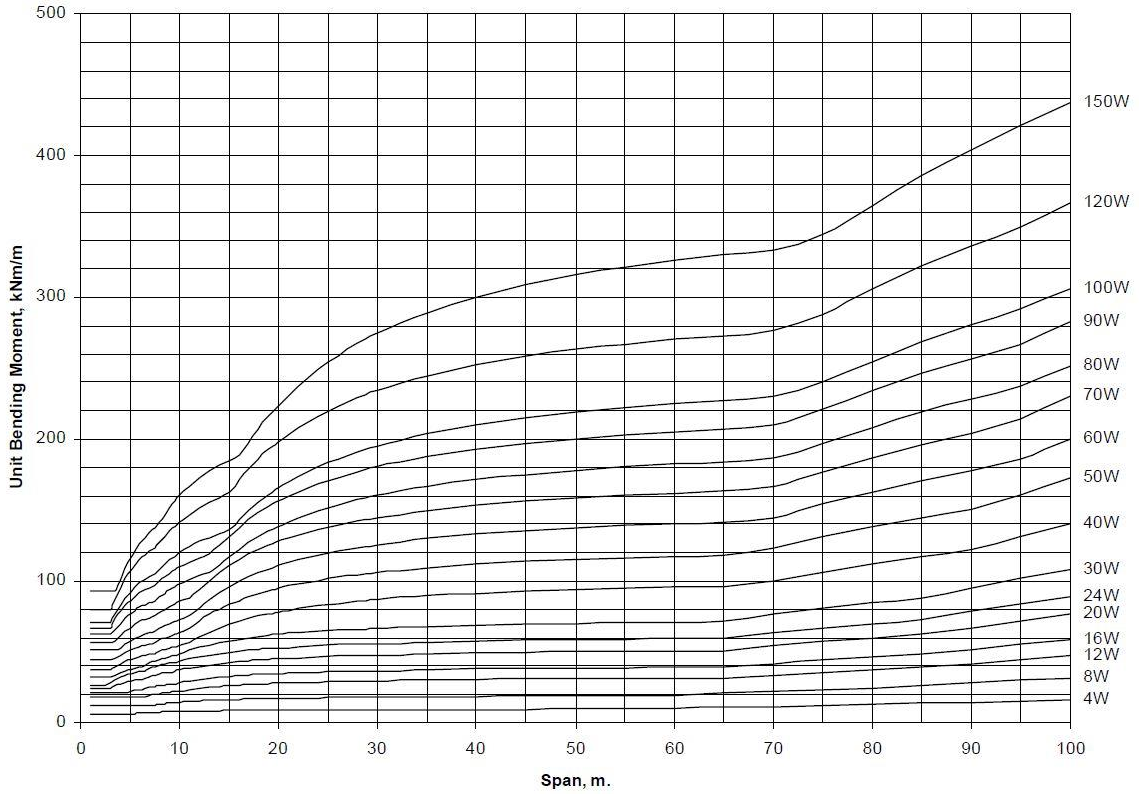

Figure 2.7 - Unit bending moment due to theoretical wheeled vehicles for spans from 1 to 100 m [6]

In generating the standard unit effect curves, various assumptions have been made. First, a NATO-standard spacing of 30.5 m between the trailing axle of one vehicle and leading axle of the subsequent vehicle is applied to convoys. Next, no dynamic loading coefficient is applied to analysis. Finally, analysis is completed on single-span, simply supported bridges [5], [6].

When classifying a specific real vehicle, the unit effects caused by the vehicle in question are determined for spans of 1 m to 100 m, and compared with the established unit effect curves of the same type of standard theoretical vehicle. The real vehicle is given a rating based on the maximum MLC attained on the graph, rounded to the nearest integer, with linear interpolation allowing for the determination of MLC between the established theoretical vehicle curves [5], [6].

For vehicles narrower than their theoretical counterparts, a width correction factor must be applied to the MLC, as given in Figure 2.8. This correction accounts for the production of higher overloading forces for individual structural components by narrow vehicles [6]. To determine the deviation from the width of the standard vehicle, first the width across ground contact points of the hypothetical vehicle of equivalent MLC must be known. For MLC ratings that lie between the established hypothetical vehicles, linear interpolation can be completed to determine an acceptable width. Once known, the width of the vehicle to be classified is subtracted from the standard hypothetical vehicle width, and an MLC correction factor is applied [5], [6].

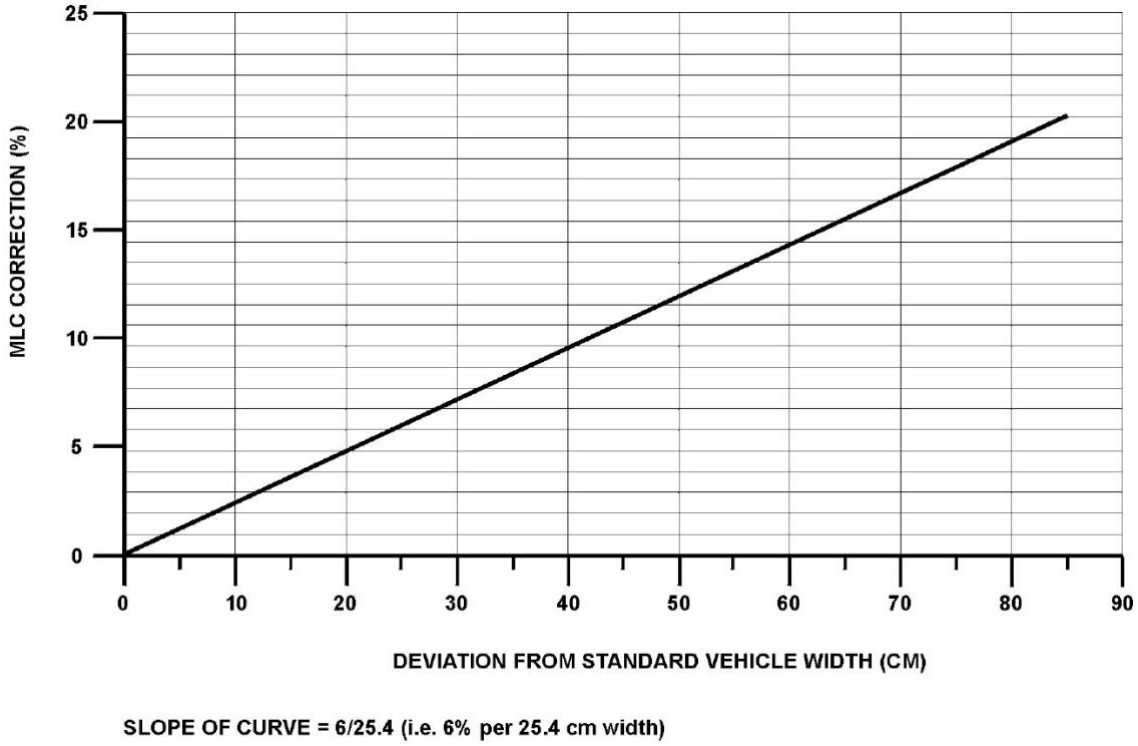

Figure 2.8 - Narrow vehicle width correction factor [6]

Vehicle MLC rating can be accomplished in unique scenarios. For example, an empty or partially-loaded vehicle can be assigned a temporary MLC. Additionally, multi-unit vehicles can receive a temporary MLC rating for the entire train. Where individual units in a train vary between tracked and wheeled components, MLC is computed based on the leading vehicle type. For a towed vehicle setup, a combined MLC greater than MLC 60 will use the combined rating, while a combined MLC less than MLC 60 will use 90% of the value of the combined rating [5].

Specialty vehicles are also given specific guidelines to follow for classification. For vehicles, including those with trailers, with a mass less than 3 t, MLC rating is optional. For hybrid tracked/wheeled vehicles (not considering vehicle trains), the vehicle is considered as having extremely large wheels, with tire ground contact area equivalent to the tracked ground contact area. Vehicles that have classifications higher than MLC 150 are determined by extrapolation of the MLC 120 and MLC 150 curves from the charts indicated in Appendix B, without applying a width correction factor. Similarly, vehicles that have classifications lower than MLC 4 can be determined by extrapolating between the MLC 4 curve and the chart baseline, again without correcting for vehicle width [5].

2.4.2 Classification of Bridges

Due to the plethora of options available to a design engineer, bridges worldwide can have enormous variation in complexity, construction, and material composition. As such, classification of existing bridges can be a sufficiently complex process. To facilitate classification by military engineers with an understanding of bridge mechanics ranging from basic to extensive, various methods of analysis have been outlined in military guidelines.

2.4.2.1 Classification Methods

Five methods of classifying bridges are outlined: hasty, rapid field, correlation-curve, analytical, and load-test classifications. Each type can be selected to inform a commander as to the feasibility of crossing based on the operational tempo and time available for assessment. Similar to vehicle classification, separate ratings for wheeled and tracked vehicle traffic must be completed, and both posted where appropriate [6], [7].

The hasty method is by definition the quickest to complete, and is used only in emergencies. Observation of civilian traffic crossing the bridge is conducted, and assumptions made that military vehicles of similar weight and axle configuration would also be able to cross the bridge safely. MLC of bridges calculated using this method of classification are considered temporary, and should not have postings erected. It is likely that in depth analysis will yield a higher MLC than determined using the hasty classification process [6], [7].

Traffic correlation classification is completed based on the correlation between known civilian design loads and equivalent standard hypothetical vehicle load effects. Correlation curves can be developed that show this relationship for a variety of spans from 1 m to 100 m. Factors can be applied to represent the effective distribution and capacity that may be allowed for a single vehicle crossing a wide, two-lane bridge. Bridges located in back-country or third world areas should not be classified by the traffic correlation method, as the adherence to established design and construction code requirements could be suspect. Again, this classification is temporary in nature [6], [7].

Rapid field classification is based on appropriate analytical theory, with certain assumptions and simplifications applied to generate a conservative MLC value. Basic measurements are required, along with knowledge or assumption of material properties (which could be based on the date range of construction, for example). Rapid field classifications are considered temporary and shall not be posted [6].

The above techniques assume that the bridge is in good condition; for bridges where degradation is evident, no firm rules are in place to downgrade MLC, but a “rule of thumb” loosely followed for steel structures downgrades the classification by a factor equivalent to the amount of cross-sectional area loss.

Deliberate analytical classification methods are the most comprehensive, and are the only ones that generate a permanent MLC rating that can be posted. Qualified engineers should be the only ones making these classifications. Details of the structure must be known, such as the structural layout, and repairs or modifications completed on the bridge, among others [6], [7].

Finally, load-test classification is completed using continually increasing test vehicle masses to determine the maximum appropriate bridge rating. While this method is accurate, it is very time consuming, and is beyond the ability of most engineer units. Additionally, damage incurred by the structure could affect the lifespan of the bridge. This classification is considered temporary [6].

Both correlation and analytical classification can most easily be completed using purpose-designed software. A current Microsoft Windows software suite [48] is available to NATO nations to estimate the MLC of vehicles and bridges. This suite allows for the calculation of bridge MLC values through the application of the traffic correlation method [49], as well as rapid [50] and deliberate [51] analytical assessment methods outlined above.

Secondary classification checks must be completed. These include checks for roadway width and, in the case of timber structures, deck thickness. For roadway width, reference to Table 2.6 [6] should be made. For instances where the roadway width generates the governing (lowest) MLC, the MLC of the bridge is not downgraded but instead a width restriction posting or notice is assigned to the structure [5], [6].

Table 2.6 - MLC classification based on roadway width [6]

Roadway Width (m)	**MLC (One Traffic Lane)**	**MLC (Two Traffic Lanes)**
2.75 – 3.34	12	0
3.35 – 3.99	30	0
4.00 – 4.49	70	0
4.50 – 4.99	100	0
5.00 – 5.40	150	0
5.50 – 7.20	150	30
7.30 – 8.10	150	70
8.20 – 9.70	150	100
> 9.80	150	150

When classifying a timber deck, knowledge of whether or not the deck is single-layer plank, multi-layer plank, or laminated is required. For single-layer planked decks, Figure 2.9 [6] is referenced to determine MLC rating. For multi-layer planked decking, the thickness of the deck, less 50 mm, is used in conjunction with Figure 2.9. Laminated plank decks use Equation 2.19 [6] in conjunction

with Figure 2.9. As with roadway width classification, if deck thickness classification generates the governing MLC rating, this value will be used for the entire bridge [6].

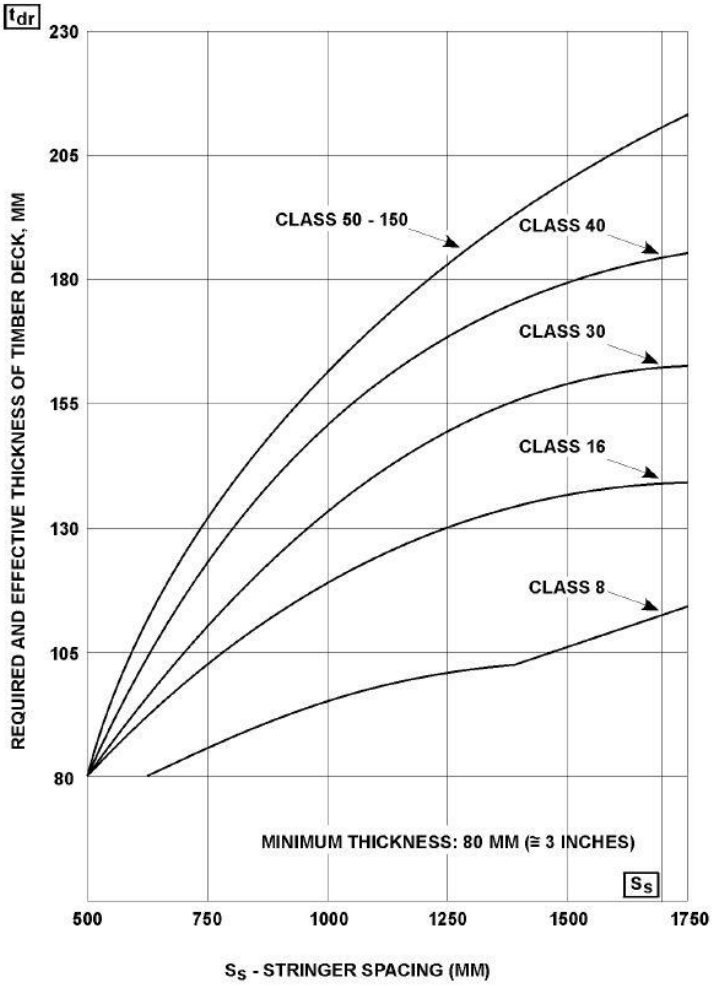

Figure 2.9 - Required and effective timber deck thickness [6]

$$t_{dr} = t_d \times p_{lam} \times 0.75 \times S_s \qquad 2.19$$

where t_{dr} is the required and effective thickness of the timber deck in millimetres;
t_d is the deck thickness;
p_{lam} is the percentage of lamination expressed as a decimal; and
S_s is the stringer spacing in millimetres.

While these classification checks are appropriate for use on simply supported spans, it is likely that military engineers will need to classify continuous-span bridges. To do so, application of a

continuity coefficient will provide adequate estimations, usually within 10%, of bending moment magnitudes. These factors are derived through the application of a UDL over the entire span length to simulate dead load, along with two point loads 6 m apart to simulate vehicle axle loading. Representative of the span length between points of inflection (where bending moment is equal to zero), the continuity coefficients are applied to decrease the continuous span length to an equivalent simple span to allow for classification with one of the methods described above. Figure 2.10 outlines continuity coefficients determined for various common configurations of multi-span bridges [6]. Applicability of these coefficients decreases as span length increases past 30 m, if the bridge has variable-cross-section main members, or if there are very large differences in span lengths across the entire bridge [6], [7].

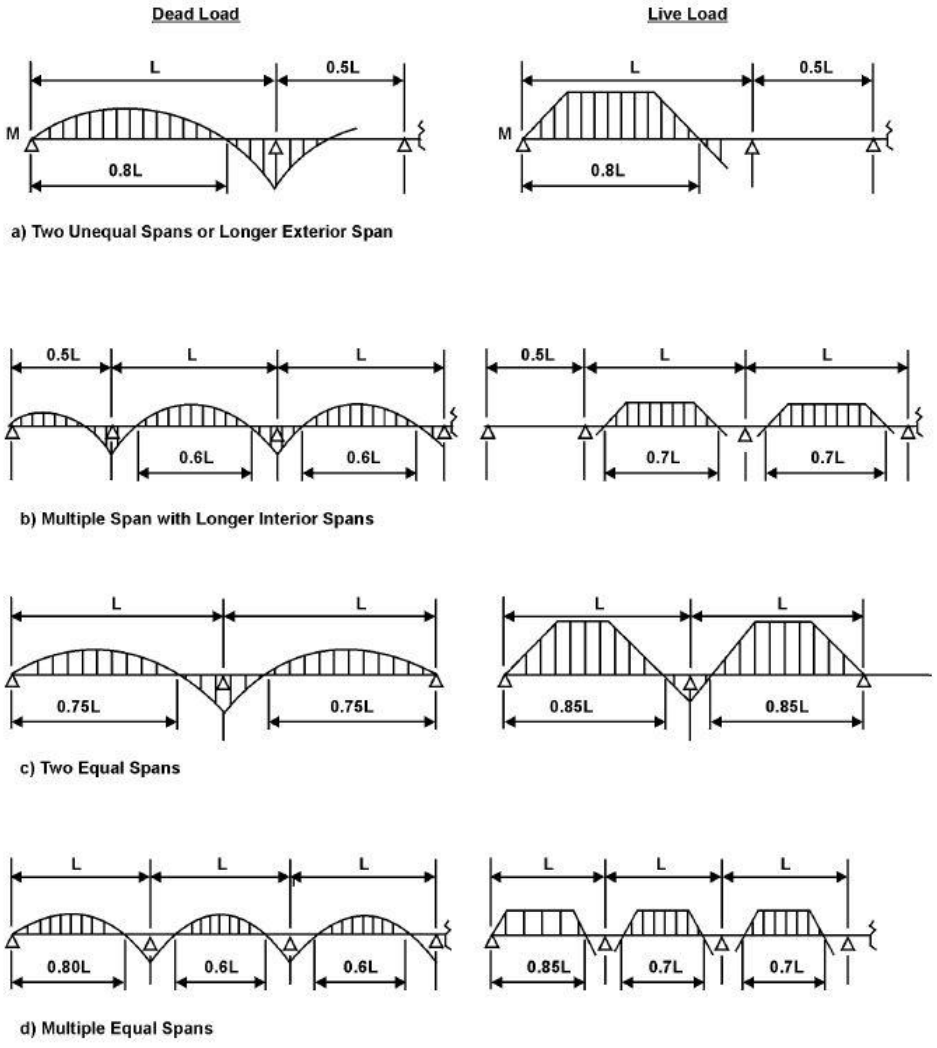

Figure 2.10 - Continuity coefficients [6]

While other nations' bridge manuals indicate alternate methods of calculating continuity coefficients [7], those displayed in Figure 2.10 are more detailed and apply to a more specific range of common bridge configurations. Since rating of the entire bridge occurs using the critical span length (often the longest span), the remaining spans will possess varying levels of conservatism for the specified classification. Rapid classification uses 0.8 as a default continuity coefficient [52].

It should be noted that distinct classification procedures exist within the MLC system for arch-type bridges. These processes will not be examined in this document, as they lie outside of the topics of relevance to this investigation.

2.4.2.2 Application of Factors

NATO AEP-3.12.1.5 (STANAG 2021) does not specify load factors, including DLA, required for calculation of MLC, but rather relies on the assumption that military engineers will apply factors that are appropriate to their national bridge codes [47]. However, application of civilian load factors to the military context presents a number of issues.

Firstly, most civilian load models are described using time-variant loads, which allow engineers to more accurately define current and future loading scenarios. While this is good practice for making current designs efficient and tailored to realistic traffic expectations, it does not correlate well with military loading models. The MLC system, based on hypothetical vehicles, is time-invariant; future (heavier) vehicles will still fall under the MLC definition limits, and so loading designations do not need to change [47].

Secondly, civilian loading models use more comprehensive dynamic loading definitions to apply appropriate DLAs to the traffic being considered. Currently the MLC system does not indicate anything more than the fact that dynamic effects should be taken into account [5], [47]. To fill this gap, Canadian and American military bridge manuals indicate that, when computing structural resistance for normal crossings using the analytical bridge classification process described previously, a DLA of 0.15 shall be taken for all bridge types and spans, the only exception being timber bridges, which have no dynamic load amplification due to the inherent damping properties of the material [6], [7]. As previously indicated, it could be appropriate to increase the DLA to 0.30 for extremely adverse road conditions, and further increase to 0.40 for these adverse conditions for very short elements being loaded by a single axle at a time [6].

The globally-applicable DLA value defined in North American military manuals is a crude method of accounting for dynamic loading; a more refined model should at the very least account for the significantly different vehicle configurations present in modern military vehicle fleets [52]. Documentation generated by the German Federal Ministry of Traffic, Construction and City Development recommend equations defining unique DLA values based on vehicle type, with limits outlined at 0.25 for wheeled vehicles and 0.10 for tracked vehicles [53].

Thirdly, the load value for civilian traffic models often correspond to a large return period (for example, 1000 years in accordance with European code); with the standard hypothetical vehicle list, the MLC method is set up to account for mean traffic load values [47].

Finally, the scale at which civilian and military authorities are interested in bridge life is very different. Civil authorities typically focus on the 50 to 100 year design life when it comes to bridges; military commanders are normally interested in days or weeks of required structural life [47]. Naturally there are some instances where military interest on main supply routes could be measured in years, but such action is not common enough to warrant the drastic modification to bridge classification methods currently used by NATO military engineers.

This comparison highlights some of the rationale behind stating that military traffic-specific factors should be determined and applied to the MLC system. An appropriate first step is the identification of vehicle categories, to which specific reliability indices, representing risk, can be calibrated independently.

As indicated previously, tracked and wheeled military vehicles exhibit significantly different load distribution mechanics. The MLC system already accounts for this difference with the application of separate ratings for each vehicle type. Parallel to this fact, previous research on vehicle weight distribution, a key parameter in calculating load effects, has indicated that there is a notable difference in payload weight fractions across military fleets. These payload weight fractions, defined as the total payload capacity divided by the gross vehicle weight, give an indication as to the variability in the load that can be expected for certain vehicle types, and is mainly governed by the intended purpose of the vehicle in question as opposed to proper load control. It has been found that, using a sample of Canadian Army vehicles, fighting vehicles see payload weight fractions in the range of 0.02 to 0.25, while transport vehicles see payload weight fractions between 0.35 and 0.60. Lower payload weight fractions can be associated with lower vehicle weight variability [52].

Fighting and transport vehicle definition is appropriate in this context. The role of fighting vehicles is to deliver combat capability, whether that be a weapon system such as a MBT main armament or a platoon of infantry soldiers, to a contested area. Transport vehicles, on the other hand, have as their primary purpose the movement and delivery of stores (such as weapons, equipment, ammunition, food, or water) to locations of need. From this definition, it can be seen how the fighting vehicles, with their very specific purpose, have significantly lower payload weight fractions than transport vehicles, which have potential to carry such variable loads that their payload weight fraction is understandably larger.

From this research, it has been recommended that military vehicle fleets be classified using four categories: wheeled-transport, wheeled-fighting, tracked-transport, and tracked-fighting [52]. This would allow for a more accurate definition of vehicle load effects on bridges over the current MLC system. To this end, using a target reliability index of 3.75 and a traffic load of 1000 vehicles per year, the partial load factors outlined in Table 2.7 are recommended for application to the four

categories mentioned previously [52]. While analysis of additional vehicle chassis would be beneficial in expanding the baseline number of vehicles to which these partial factors apply, these values will be considered appropriate for this research. For bridge assessments made within the context of military operations where higher levels of risk are often deemed acceptable, it may be prudent to use a lower reliability index and live load factor combination. Additionally, within the framework of updates made to DLA values used in assessment, it may be pertinent to apply adjustments to the factors in Table 2.7.

Table 2.7 - Partial load factors for proposed military vehicle categories [52]

Proposed Vehicle Category	Partial Load Factor
Wheeled-transport	1.77
Wheeled-fighting	1.48
Tracked-transport	1.77
Tracked-fighting	1.33

Previous research has indicated that tracked vehicles typically have less severe dynamic effects on bridges when compared to wheeled vehicles [8], [52], which can be used as further justification to allocate unique load factors to more specific vehicle categories within a military context.

Current Canadian military guidelines indicate a live load factor of 1.30 should be applied along with a dead load factor of 1.25 when conducting detailed analysis, in all cases. These values are substantiated based on the fact that military loading is much more controlled than civilian loading, especially when considering convoy spacing and speed variation, and the fact that military bridge life requirements are lower compared to their equivalent civil counterparts [6].

2.4.2.3 Types of Crossings

When transiting over established bridges, military commanders have the option of using one of three crossing types based on the operational scenario: normal, caution, and risk. Load factors and assessment techniques previously defined all apply to normal crossings; unrestricted use of civilian bridges is authorized, with normal restrictions to be followed for military bridges for all vehicles operating under standard convoy rules (regarding speed and spacing) [5], [6].

Caution crossings are introduced to allow commanders to have increased flexibility in trafficking heavier vehicles across a span, or cross over a longer span that would normally not be available for use for a normal crossing type. While maintaining the same level of safety, control measures are emplaced to ensure vehicles transit across the bridge at the centreline of the road surface, under control of a guide, while maintaining speeds up to 5 km/h at maximum. Braking, accelerating, shifting gears, and transit of more than one vehicle across an independent span are not authorized. There are no dynamic loading considerations for caution crossings. Commanders at appropriate levels must accept the risks that come with authorizing this crossing type [5], [6].

Risk crossings maintain all control measures defined for caution crossings, but reduce bridge safety factors to allow for even heavier vehicles to traffic a bridge, or use an even longer span. Safety factors are reduced to minimally acceptable values (in conjunction with the assessing engineer's civil code requirements); for example, the live load factor could be reduced to 1.00, since the effects of military vehicle loading are fairly well known. A military commander at an appropriate level of authority must give authorization to use risk crossings, and they must be aware of the increased probability of bridge failure or permanent damage being inflicted upon the bridge due to traffic. Similar to caution crossings, no dynamic load effects are considered. Monitoring of bridge behaviour during vehicle crossings is crucial [5], [6].

The lack of dynamic load effect consideration for caution and risk crossings is logical. With speeds between 5 km/h and 15 km/h producing quasi-static load effects, dynamic loading is often considered immaterial in these cases [47].

2.5 Experimental Testing

Dynamic testing of bridges is conducted for very specific reasons: either to determine dynamic characteristics of the bridge itself, or to determine an estimate of the DA value to be used for bridge assessment [54]. To generate an experimental testing programme suitable to produce appropriate data, various considerations must be made. Failure to properly understand and apply these theories could result in inadequate data capture for a stated goal.

2.5.1 Types of Testing

Generally speaking, there are two main types of dynamic testing. Ambient vibration testing is conducted without control over input forces on the structure in question, which could result in estimated dynamic properties being erroneous due to the lack of knowledge regarding excitation effects on the structure. Forced vibration testing, on the other hand, gives an investigator the ability to study the effects a certain load could have on the dynamic response of the bridge [55].

More specifically, dynamic bridge testing can be divided into five categories: behaviour tests, proof tests, ultimate load tests, stress or load history tests, or diagnostic tests. Behaviour tests are used to validate the results of analytical bridge assessments, in addition to determining characteristics of the bridge and how it responds to and distributes an applied load [41], [54]. For bridges with non-linear load carrying capacity, this information is not adequate to define the global load-carrying capacity of the structure [54].

Proof tests can establish safe load-carrying limits, in addition to outlining load distribution properties. Ultimate load tests have the self-named goal of identifying the ultimate load-carrying capacity of the structure. Stress or load history testing can be used to establish stress distribution characteristics of a structure prone to fatigue, and by extension, be used to establish the fatigue life of the bridge. Finally, diagnostic tests are used to locate the origin to damage on a structure [41],

[54]. Behaviour, diagnostic tests, and stress history testing can be conducted statically and dynamically; proof and ultimate load tests are only static in nature [41].

With road surface roughness having significant impact on dynamic loading of bridges, it is prudent to consider such testing be included in a thorough testing regime. It has been shown that vehicles, while travelling over very rough surfaces, have the potential to experience excitations that are close to their own natural frequency. This quasi-resonance effect could result in very large dynamic forces imparted on the bridge [17]. To simulate this degradation in road surface roughness, is it common to have vehicles pass over wood planks of adequate height to produce the desired irregularity [14], [18], [54]. While not justifiable for well-maintained bridges, this testing may be appropriate for those structures that have unpaved approaches or expansion joints between the road surface and approaches that are not level [14]. Indeed, when considering military scenarios in which obstacles are placed on the bridge or in conditions where infrastructure maintenance routines have been severely interrupted, this type of testing may be quite relevant [8].

2.5.2 Selection of Loads

When considering loading options, various factors should be taken into account. Generally, loads placed on bridges should have the following characteristics: they should be representative of actual vehicle loads, be adjustable, be easily manoeuvrable, be able to repeat weight distribution across axles with the loads stabilizing quickly, be able to transport the loading system with ease, and, in the case of high-risk tests, be able to remotely control the load [54].

When determination of a DA value is required, two types of loads need to be considered: static and dynamic. Static loading could be through the application of something like concrete blocks of known weight, or use of a vehicle that has known axle loads and axle spacing. Concrete blocks are advantageous in that they are scalable in size and mass, but are difficult to remove quickly if required. Vehicle loading is preferable, especially when it is representative of the heavy loads that the bridge would likely encounter [54].

When determining static effects on the bridge, it is possible to take a quasi-static approach and measure bridge response while a test vehicle moves across the span at crawl speeds [14], [16], [17] in addition to completing stationary testing with a vehicle remaining in place on the bridge over a specified timeframe [14].

The most reliable way to generate DA values is to conduct full-scale dynamic testing, preferably with controlled and normal traffic used as the dynamic load [12], [16]. The use of the test vehicle is the more popular method of load application, although uncontrolled traffic does generate more meaningful data [54]. There are some differing views with respect to the type of traffic that should be used for optimal data generation; some research has indicated that use of specific test vehicles cannot be regarded as representative of actual traffic, and instead only provides measured insight into dynamic loading issues. In this case, calculation of accurate DA is recommended to be completed using normal traffic loading, over larger periods of time [14]. In the context of this

research, this will not be an issue. The vehicles selected as representative traffic, although specifically chosen for their load distribution differences, represent normally controlled military traffic, and thus are appropriate for use in determination of a militarily applicable DA value. If generating testing programmes that aim to use a single test vehicle, it should be noted that DA calculation will likely result in a value that is smaller than realistic. In this case, the single test vehicle should have characteristics that would result in an upper-bound DA value [54].

Dynamic testing should be conducted with iterations of testing at multiple speeds when possible, as the maximum dynamic loading effects are determined when speed variation is introduced. As previously indicated, with vehicle speed being a key factor in dynamic loading, conducting testing at multiple speeds allows for an investigating engineer to attempt to clarify the relationship between speed and dynamic impact [12], [16], [18], [21], [54]. There is limited disagreement on the effect speed-variable testing has in literature, although recommendations to conduct this testing are still endorsed [17]. There is indication that direction of travel does not affect the calculation of dynamic structural response, up to approximately 54 km/h [36].

When considering test vehicles to be used to represent traffic loads, uncontrolled dynamic loading should be avoided. Typically, unsecured cargo is one such factor that could influence the dynamic relationship during a test [13]. With the rigidity with which military vehicles are outfitted with cargo, there is limited worry that loads inside a vehicle will be unsecured, thereby limiting any effects associated with this phenomenon. Similarly, the effects of steering corrections, acceleration, or braking could have an impact on the force applied to the bridge by the vehicle [36]; these changes should be avoided while conducting experimental testing as much as possible. Additionally, it should be noted that the positioning of a test vehicle within a driving lane is of importance when conducting experimental testing. Inconsistencies in this transverse vehicle placement along the length of a bridge being tested have been found to have significant impact on bridge response [42].

Dynamic loading mechanisms other than traffic loads are possible. These include the sudden release of deflection, application of a sinusoidal exciter or other energy input methods, or braking vehicles on the bridge. While some dynamic loading options are useful in determining DA values, some are more appropriate for determining other response characteristics of the bridge [12], [54]. Knowledgeable selection of the loading mechanism based on the information desired is important.

2.5.3 Instrumentation

When conducting dynamic testing, various parameters are often of interest. Measured while the bridge is in free vibration after a load has ceased to act on the structure, these factors include the natural frequency, mode shapes, and damping factors of the bridge. Typically quantification of these parameters are made through strain, deflection, or acceleration measurements [54]. Each sensor type has specific properties that are more appropriate to determination of specific parameters.

If measuring natural frequencies, damping, or mode shapes, accelerometer instrumentation of the bridge at mid-span and quarter-span locations (for simply supported bridges) is most appropriate. Calculation of DA in a bridge can use accelerometers, strain gauges, or displacement transducers, although agreement on the best sensor to use is not unanimous in literature. It seems common that, while accelerometer data may be used, displacement and strain effects are more effective for DA calculation [54]. Other research has indicated that displacement data should be used, and substituted with strain data only when acquisition of displacement readings is too difficult. Demonstrations of DA calculation using both instrument types has shown that displacement-derived values are consistently higher than strain-based calculated values [14], [25], and recommendations have been made to use strain-based measurement due to increased levels of reliability [13], [14]. Most research is supportive of using strain measurement to determine accurate DA values [13], [14], [17], [25], [41].

2.5.4 Data Manipulation

When analyzing data, it is imperative that manipulation is applied where and when appropriate. Based on the nature of the experimental programme, this manipulation could manifest itself in a number of ways. For example, the application of a data filter could be required to remove erroneous results, noise, or alternate signals, or the correction of raw data may be required to compensate for errors or uncertainties associated with the data collection system. Details pertaining to data manipulation in the context of dynamic load testing can be found in Appendix C – Data Manipulation.

2.6 Summary

This literature review aimed to impart upon readers adequate knowledge of the concepts employed throughout this investigation. Internationally, dynamic effects are considered using a small number of similar methods, with specific nomenclature varying notably. Generally, the methods followed to calculate the dynamic response of moving traffic loads across various research efforts are the same, with small variations considered based on the experimental setup, and subsequently the data required for specific analysis.

NATO member countries are held to a standardization process to ensure vehicle and bridge ratings are completed to a level that allows for effective consideration of loading effects in almost any scenario. While this MLC system uses similar load factors to those found in civil codes, distinct differences exist between military and civilian approaches that indicate unique military factor values should be applied to military traffic.

To execute experimental dynamic bridge testing, identification of an appropriate type of test must be conducted. Selection of realistic loads, in conjunction with use of appropriate instruments, will enable gathering of useful data for analysis. Strain and displacement measurement can be used for reliable determination of dynamic load factors for the testing outlined above.

CHAPTER 3 MANUSCRIPT 1: TESTING PROCEDURES FOR EXPERIMENTAL ASSESSMENT OF A MODULAR TRUSS BRIDGE SUBJECTED TO MILITARY TRAFFIC

This manuscript has been submitted for possible publishing in the American Society of Civil Engineers (ASCE) Journal of Bridge Engineering.

3.1 Abstract

Experimental bridge testing often produces large datasets that may have applicability to many analysis goals within bridge engineering. To ensure persistence of these records for future analysis, it is essential to properly collect, organize, and define data. A field-testing programme was developed to capture the dynamic loading response of a simply supported, modular-construction bridge to medium and very heavy military vehicle loads that included detailed instrumentation layout and nomenclature assignments, deck surface condition simulators, and iterative tracked and wheeled vehicle testing plans. The result was a complete dataset that includes adequate information to achieve various analysis objectives. This data, and the process through which it was gathered, have the potential to increase the knowledge base relating to dynamic bridge effects in a combined civilian-military context, and generate results that could drastically improve mobility for select military vehicle types.

3.2 Introduction

For some field testing, particularly in austere environments, experimental data collection is completed over a strictly defined timeframe; repetition of a testing programme may not be possible over a prolonged period. In such instances, it is imperative that an appropriate data-gathering programme is generated to allow an investigator to avoid inconclusive results that originate in data of inadequate quality or insufficient quantity.

Collection and sharing of instrumented bridge data enables innumerable studies, analyses, and reports to be generated across the globe. To date, the majority of these data collection and assessment endeavours have largely considered typical wheeled traffic loading. Assessment of loading effects due to alternate vehicle types, such as tracked vehicles, is much less common. Recent research into dynamic load effects of wheeled and tracked vehicle types has indicated that the load response varies significantly between the two [8], a fact to which there is little reference in multiple national and international bridge design codes. It would appear that the German Federal Ministry of Traffic, Construction and City Development was perhaps one of the only government bodies to have acknowledged the dynamic loading effect differences between tracked and wheeled vehicles with their recommended maxima for Dynamic Load Allowance (DLA) of each vehicle type [53].

The DLA is a value that accounts for the increased bridge response due to the passage of a load. The complete reaction of a bridge to loading is a combination of static and dynamic responses; the static effect is caused by the weight of the load, and the dynamic effect caused by the inertia of the moving load [3]. To account for the dynamic effect in design and analysis, a load allowance, or DLA, is applied, which is quantified as a portion of the static load effect [4].

3.2.1 Aim of Experimental Testing

In the context of this field-testing programme, data was collected to allow for the determination of an appropriate DLA value from experimental data of a bridge subjected to both tracked and wheeled military vehicle traffic. While the primary focus was aimed at determining the maximum appropriate DLA from loading effects on a smooth bridge deck, the secondary focus was to determine the dynamic load increases due to loads passing over a simulated rough surface.

3.2.2 Scope

To accomplish the stated goals, a comprehensive experimental programme was developed, based on established research. This programme considered bridge component nomenclature and instrumentation, limited vehicle instrumentation, and a schedule of testing that allowed for the gathering of data across a multitude of speed and deck condition combinations. Simplified numerical modelling was conducted to confirm validity of data, and to ensure that the future manipulation of records could be conducted with confidence consistent with the quality of the original information.

3.3 Background

3.3.1 Dynamic Amplification

To ensure appropriate data is collected to allow for the determination of a DLA, an understanding of how this value is calculated is prudent. First, the Dynamic Amplification (DA) value, which is an experimental value defining the amplification of load effects for a specific test iteration, is quantified. Equation 3.1 is applied using experimental data gathered from static and dynamic tests [3], [13], [14], [16], [33], [41], [42]:

$$DA = \frac{R_{dyn} - R_{sta}}{R_{sta}} \tag{3.1}$$

where R_{dyn} is the maximum dynamic bridge response; and
R_{sta} is the maximum static bridge response.

It is important to note that DLA is a statistically relevant estimation of the increase in load effects, while DA is pertinent to a single test iteration. Therefore, the DA cannot be used to directly describe the dynamic load effect for anything outside of the experiment in question. To generate a DLA

applicable to a range of loading scenarios, DA values calculated for multiple independent test iterations must be aggregated, and the result applied to statistically pertinent factors. This can be done through the application of Equation 3.2 [14], [18], [31]:

$$DLA = \frac{\overline{DA}(1 + vs\beta)}{\alpha_L} \tag{3.2}$$

where $\overline{DA}$ is the average value of the calculated DA terms acquired through testing;
v is the coefficient of variation of the measured quantity;
s is the separation factor for dynamic loading (0.57 [14], [18]);
β is the reliability index; and
α_L is the live load factor.

From this, it can be seen that the dynamic response of the bridge to loading is the main data point that must be captured through testing. Quantification of dynamic responses such as natural frequency, mode shapes, and damping typically occurs through the measurement of acceleration, displacement, or strain. Although all three measurements can be used to determine DA, recommendations appear common to focus on displacement and strain data [54]. While there is some disagreement in the literature between which of these two measurements is most accurate, the majority of research indicates that strain data is more appropriate for determination of accurate DA, and by extension, DLA [13], [14], [17], [25], [41]. Appropriate installation techniques must be followed to mitigate potential sources of error contaminating the data [56]–[58].

3.3.2 Experimental Testing

When developing an experimental testing programme in the context of dynamic bridge analysis, an investigator must first decide which type of testing is most appropriate to gather the information required for the stated aim. These can include behaviour, proof, ultimate load, stress or load history, and diagnostic tests. Behaviour tests are used as to determine the dynamic characteristics of a bridge, as well as validate analytic bridge assessments [41], [54]. Proof tests can be used to identify safe load limits and indicate load distribution characteristics, while ultimate load tests are used to determine the structure's maximum load carrying capacity. Fatigue life and stress distribution properties of a bridge can be determined through an analysis of stress or load history testing. Finally, identification of the origins of existing damage could be accomplished through a diagnostic test [41]. With an understanding of the aim and type of test desired, an investigator can proceed to determine the specific details related to the load to be applied.

Two types of load tests are possible when considering dynamic bridge assessment. Ambient vibration testing is conducted without control over the input forces on a bridge; these unknown effects of excitation have the potential to produce inaccurate estimates of structural dynamic properties [55], but in some cases may be more representative of normal loading [54]. Forced

vibration testing allows for load application control, facilitating the analysis of dynamic bridge response to the specific excitation applied [55].

Bridge loads should have some generic characteristics to mitigate the effects of unknown load influences on the dynamic response of the structure [13]. Vehicle load characteristics include being similar to actual traffic loading, be adjustable and easily manoeuvrable, able to distribute weight across axles with a load stabilizing rapidly, and should be able to be transported without difficulty. In scenarios where high-risk testing is required, it may be prudent to have remote control over the load transportation across the bridge to mitigate risk to personnel [54].

If the stated goal of experimental testing is to determine an appropriate DLA, the conduct of full-scale dynamic testing is most appropriate, with the use of both normal and controlled traffic desirable [12], [16]. While the use of a specific test vehicle is more common when conducting these types of tests, it should be understood that uncontrolled traffic often produces data that are more meaningful. If use of a single test vehicle is unavoidable, effort should be made to ensure the vehicle can produce upper-bound dynamic results [54]. Considering this experimental testing programme, this is not an issue, as the vehicles used to load the bridge represent normally controlled military traffic. Vehicle spacing is a parameter that could impact the response of the bridge in a scenario where multiple vehicles closely spaced load the structure at once; the strict NATO military vehicle spacing requirement of 30.5 m between the trailing axle of one vehicle and the leading axle of a following vehicle attempts to mitigate increased load effects due to vehicle spacing [5].

If conducting full-scale dynamic experimentation, it may be prudent to conduct some testing with a simulated irregular surface to verify possible dynamic effect increases with surface condition degradation. This can be achieved through the installation of timber planks across the lane [14], [18], [54]; this is appropriate for bridges where approaches are unpaved, or if there are significant expansion joints between deck and approach surfaces that are not level [14]. In a military context, obstacle placement on a bridge is a likely scenario; in this case, understanding irregular-surface dynamic effects may be of significant interest to an investigator [8].

In addition to this understanding, it is prudent for an investigator to place constraints on the application of the load where possible. As dynamic bridge responses have been shown to vary with speed, iterative testing conducted at multiple controlled speeds is appropriate [12], [16], [18], [21], [54]. Acceleration, deceleration, and direction change should be avoided, as irregularities in data collected would otherwise be introduced [36].

With an established aim, an understanding of the type of test desired, and an outline of what constitutes an appropriate load, including constraints on load application, the investigator can proceed to develop a detailed testing programme that will allow for the generation and capture of quality data.

3.4 Testing Programme

3.4.1 Bridge Component Terminology

The bridge used for this testing, named the Battle Bridge, was an ACROW 700XS segmental panel design currently in use at 3rd Canadian Division Support Base (3 CDSB) Wainwright. Spanning 39.62 m across the Battle River, this bridge is used principally for military traffic on an unpaved road. The steel bridge has a timber deck, and is made up of thirteen panel bays, with each bay consisting of nine stringers supported on either end by transoms which transferred load to eight modular trusses.

In preparation for instrumentation, naming conventions were generated to identify the specific location that sensors would be placed. These consisted of a triple-identifier alphanumeric approach: the primary term would indicate on which panel bay the sensor would reside, numbered B1 through B7; the secondary term would indicate on which truss or stringer the sensor could be found, numbered T1 to T8, or S1 to S9, respectively; and, the tertiary identifier would indicate the specific location where the instrument would be affixed, or, in the case of linear string potentiometers used to measure displacement, would bear the identifier SP. Tertiary identification codes used are outlined in Table 3.1. Panel bays increased in number starting from the west-most panel; trusses and stringers respectively increased in number starting from the northern side of the bridge. A schematic of the bridge, including panel bay, truss, and stringer nomenclature can be found in Figure 3.1 (after [59]).

Table 3.1 - Tertiary instrument location identifiers

Tertiary Location	Tertiary Location Code
Top of top chord	TTC
Bottom of top chord	BTC
Top of bottom chord	TBC
Side of bridge support (on steel above bearing pad)	SBS
String potentiometer	SP
Bottom of top flange	BTF
Bottom of bottom flange	BBF
Web rosette, horizontal	WH
Web rosette, 45° angle to horizontal	WA
Web rosette, vertical	WV

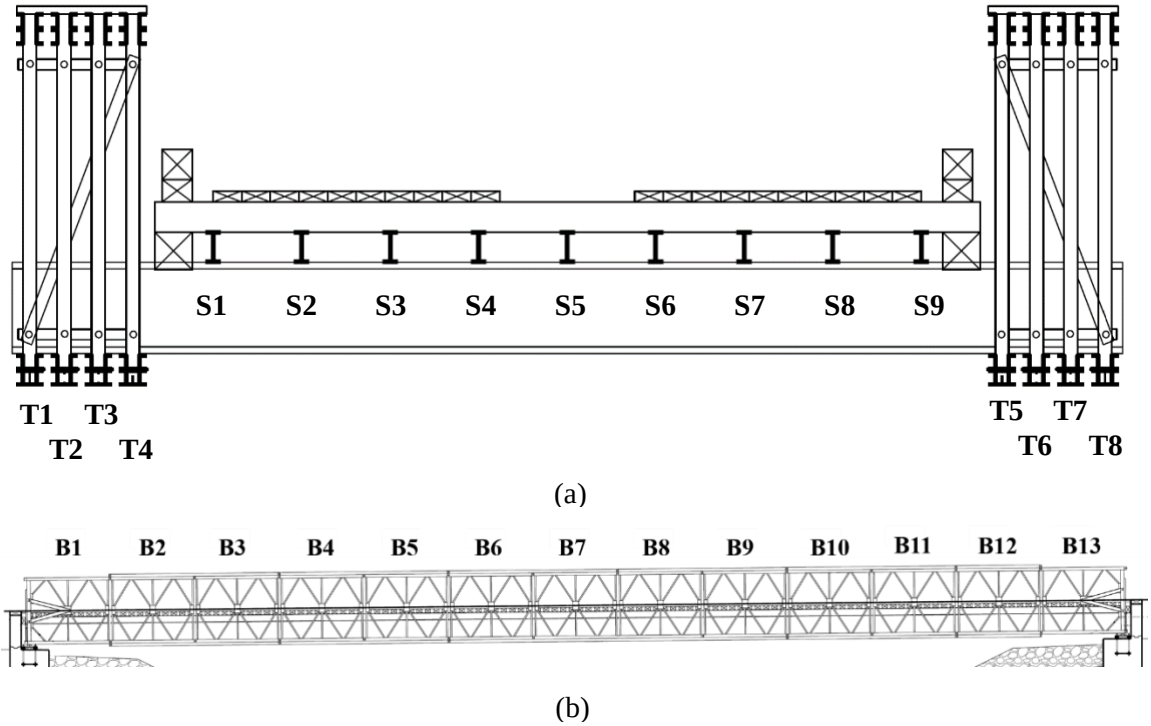

Figure 3.1 - Battle Bridge component terminology showing (a) cross-section as seen from the west, and (b) south elevation (after [59])

3.4.2 Instrumentation Plan

To gather strain data from the bridge, Kyowa N11-FA-5-120-11 strain gauges were used, having a 5 mm gauge length and a resistance of 120 Ω. Displacement data was captured through Celesco SP2-12 compact incremental string potentiometers, having a full stroke range of 317 mm.

To gather data related to maximum bridge response to loading (the primary aim of experimentation), panel B7 was identified for primary instrumentation because it was the mid-span panel. The desired data to be collected from this location included displacement measurements, as well as strain readings for the top and bottom chords, where maximum axial loads in the truss elements were expected. To achieve this, two string potentiometers were installed on the bottom chord of truss T1 and T8, with the extending cable connected to a line secured to a weight resting on the riverbed. Sixteen strain gauges were installed on truss chords; one each on the top surface of the bottom chord, the bottom surface of the top chord, and the top face of the top chord for trusses T3, T4, T5 and T6, while trusses T1 and T8 each had strain gauges on the top face of the bottom chord and top face of the top chord. Instrument locations at the mid-span cross-section are shown in Figure 3.2. Panel B4 was instrumented with two string potentiometers installed on trusses T1 and T8.

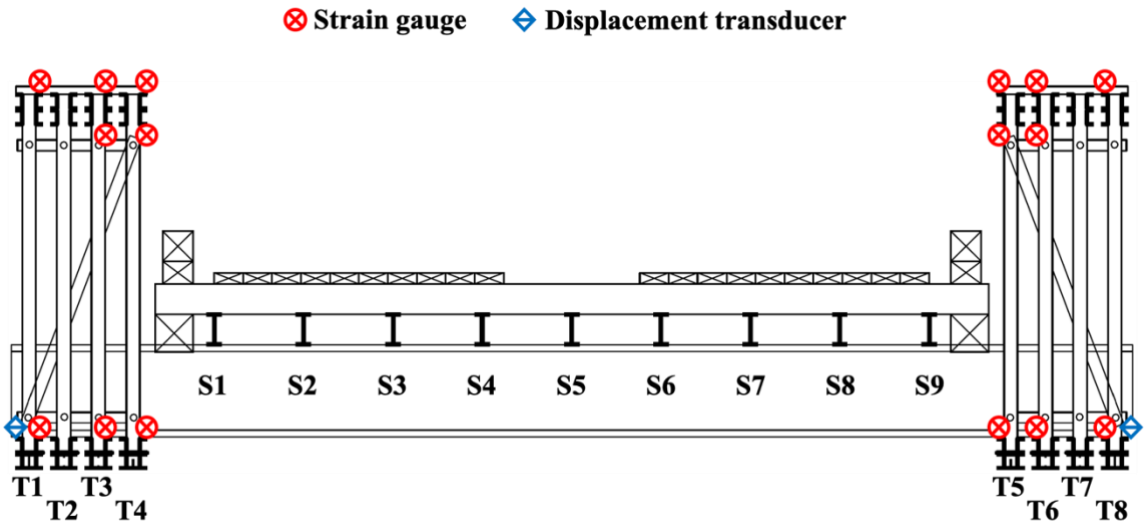

Figure 3.2 - Sensor placement at mid-span (B7) cross-section

Additional data was gathered from panel B1. At this location, it was desired to determine how the structural response to loading affected the DLA calculated from multiple measurements; these included the mid-point along the panel (the mid-span of the stringers), as close to the end of the bridge as possible on the stringers, and at the superstructure supports above the bearings. To gather sufficient data for this aim, twenty-four strain gauges were installed. As given in Figure 3.3, stringers S1, S2, S3, S5 and S9 all had gauges at their mid-span on the bottom of the top flange and the bottom of the bottom flange, while stringer S4 had a single gauge installed on the underside of the bottom flange. Stringers S1, S3 and S5 had triaxial strain gauge rosettes fixed to their respective webs at the end of their length, above the abutment. Finally, strain gauges were installed on the accessible vertical side faces of supports under trusses T1, T4, T5 and T8 to measure the effect of vehicle loading immediately above the superstructure bearings.

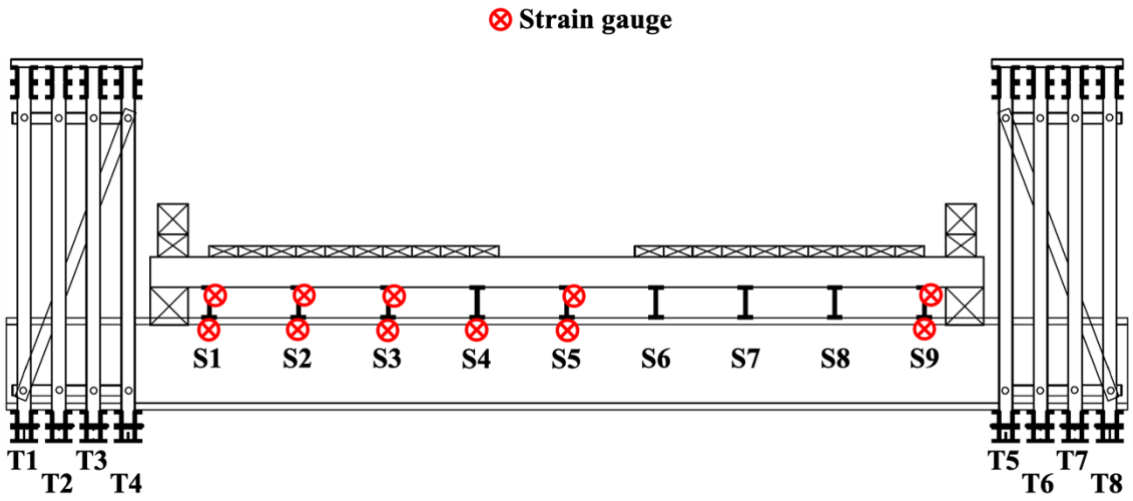

Figure 3.3 - Instrument location at mid-span of B1 stringers

Implementation of this instrumentation plan required that each location where a strain gauge was installed had the steel galvanization ground away, followed by a thorough cleaning prior to gauge installation. Once the gauge was adhered to the structure, leads were connected to previously-run wires which were secured in a manner to minimize any inadvertent pulling on the gauge leads themselves during final cable organization. The final step in instrument install focussed on covering gauges with a foil-putty measuring point protection layer; this helped isolate the sensor from erroneous electromagnetic influence, in addition to humidity effects. Figure 3.4 shows a strain gauge with a cable secured to the chord, as well the same gauge after protective layer application.

(a) (b)

Figure 3.4 - Strain gauge B7-T5-TTC with secured cable (a) before and (b) after protective layer application

All instrumentation was connected to data acquisition units by means of Deca 73-313 shielded multiconductor cable to minimize interference caused by the minimal ambient electromagnetic transmissions in the area. Four data acquisition units were used from the HBM QuantumX family:

one MX440A model, one MX840B model, and two MX1615B models. All data acquisition units liaised with and were controlled by one computer terminal running HBM's catman®AP management software, version 4.1.2.7.

Frequent clearing of debris flowing in the river was required for string potentiometers at mid-span. Review of data gathered by all displacement sensors indicate that some damage may have been induced on the instruments due to full-stroke extension at some point during testing or installation. Prior to instrument tare, readings from sensor B4-T5-SP2 at quarter-span and sensor B7-T5-SP4 at mid-span indicated that they were unable to return to zero displacement; data gathered from these instruments is therefore suspect in their quality.

A complete list of gauge identifiers and the associated data acquisition channels can be found in Appendix D – Instrumentation Identifiers and Associated Data Acquisition Channels.

Two cameras were used to capture video footage of each vehicle crossing; one looking down the longitudinal axis of the structure from the western end, and the other capturing the test run either from the north, perpendicular to the length of the bridge, or looking down the longitudinal axis of the bridge from the eastern end. This was done to confirm records in the case where an issue might be noted during data review. For example, a dataset indicating significantly larger responses of sensors on one side of the bridge compared to the other could be confirmed as the result of eccentric load placement at that sensor location as opposed to faulty gauge readings by examining video references.

While no changes were made to the installation of sensors between smooth and rough surface tests, wooden boards (2 x 10-inch nominal dimensions, or 38 mm x 225 mm) were affixed to the bridge deck to simulate a heavily damaged bridge wearing layer. Five boards were installed along each wheel path at a spacing of 3 m, centred at the bridge mid-span. Figure 3.5 shows the bridge with the simulated irregular surface installed. Obstacle dimensions and spacing are similar to previous research [8], [30], [60].

Reliable power was provided to sensors from a battery bank that was in turn fed by a small portable generator. This setup allowed for isolation of any potential power fluctuations caused by the generator, limiting impacts to sensitive data collection components.

Figure 3.5 - Bridge deck with rough surface simulated by installed boards

3.4.3 Vehicles

Due to the low volume of normal traffic using the bridge, it was determined to be more appropriate to conduct forced vibration testing to gather the necessary data. In keeping with the desired load characteristics for dynamic testing, these vehicles were similar, and indeed identical, to actual bridge traffic, were easily manoeuvrable, and stabilized their load rapidly. The recommendation to have adjustable loads was achieved by using multiple different vehicles, each having different mass and load distribution properties.

Two wheeled and two tracked military vehicles were used to load the bridge, with some general properties of each listed below. All vehicle weights are indicated in metric tonnes. Detailed properties for each vehicle can be found in Appendix E – Vehicle Properties. Note that this appendix contains RESTRICTED information, and therefore may not be found in all copies of this document.

The first tracked vehicle used for testing was the Leopard 2 Armoured Engineer Vehicle (AEV), as seen in Figure 3.6. This vehicle disperses a mass of 69.5 t (681.5 kN) over fourteen road wheels (seven per side) onto a track having ground contact dimensions of 0.64 m by 4.95 m [61]–[63].

Figure 3.6 - Leopard 2 Armoured Engineer Vehicle (AEV)

The second tracked vehicle used was the Leopard 2A4M main battle tank (MBT), as seen in Figure 3.7. This tank distributes its 60.5 t mass (593.3 kN) across fourteen road wheels onto a track with a ground contact area of 0.64 m by 4.95 m [64].

Figure 3.7 - Leopard 2A4M main battle tank (MBT)

The first wheeled vehicle used for loading was the Medium Support Vehicle System (MSVS) Load Handling System (LHS) variant, as indicated in Figure 3.8. This truck distributed its 25.9 t mass (254.2 kN) over four axles.

Figure 3.8 - Medium Support Vehicle System (MSVS) Load Handling System (LHS) variant

Finally, the second wheeled vehicle used to load the bridge was the Tactical Armoured Patrol Vehicle (TAPV), shown in Figure 3.9. This two-axle vehicle had a mass of 16.3 t (159.4 kN), and was the lightest vehicle used.

Figure 3.9 - Tactical Armoured Patrol Vehicle (TAPV)

To ensure adequate data was gathered for the stated experimental analysis, as well as other potential analysis options (modelling), an accelerometer was installed on the TAPV. This data was gathered to allow for analysis of the vehicle dynamic effects specifically. Figure 3.10 indicates the (a) general location and (b) close-up of the sensor on the roof of the TAPV.

(a) (b)

Figure 3.10 - TAPV accelerometer placement showing (a) general and (b) specific placement

3.4.4 Iterative Testing Plan

To gather adequate data to facilitate the required analysis, iterative load testing was required from each vehicle to determine the dynamic effects at different crossing speeds. To this end, an iterative testing plan was developed in which tests were assigned progressive serial numbers. Two tests were conducted at each crossing speed: one in the east-west direction, followed by a separate test in the west-east direction. Constant speed was maintained for each individual crossing to ensure the tenets of proper dynamic bridge testing were being followed. Sensor readings were tared prior to the beginning of each iteration.

Starting with static load testing, each vehicle crawled onto the bridge, stopped at mid-span, and, after waiting a short period for bridge responses to settle, continued crawling off the bridge. These tests were denoted as “stationary” tests. Quasi-static testing followed, in which vehicles crawled continuously across the entire span. These tests were denoted as “crawl” tests.

Dynamic crossings over the smooth bridge deck were then completed. Each vehicle, with the exception of the MBT, varied the crossing speed at each iteration from 10 km/h to 50 km/h in increments of 10 km/h. Finally, dynamic overpasses with the simulated rough bridge deck were completed, using the same speed increments. Due to technical vehicle issues, the Leopard 2 MBT iteration speeds ranged from 10 km/h to 35 km/h, and irregular surface testing was not completed.

Terminology of the independent tests followed the following format: serial-vehicle-direction-speed-surface. Accelerometer data are denoted with the inclusion of “accelerometer” at the end of the file name. As an example, a test, given the arbitrary serial number 03, where the AEV crosses over the irregular surface at 30 km/h from west to east would be named “Ser03 AEV W-E 30k Irregular.” Appendix F – Iterative Testing Plan outlines the complete load-testing schedule followed during field data capture. A total of eighty-six tests were completed.

3.5 Experimental Data

3.5.1 Data Collection and Organization

Three types of instrument data were collected: bridge strain readings, bridge displacement readings, and vehicle accelerometer readings. Following the testing plan outlined in Appendix F, tests were completed in sequential order by serial. Each independent serial gathered data in a separate file that contained all bridge instrument readings. For serials where accelerometer data was also recorded, a standalone file containing only these data points was generated.

In each file, data are organized by data acquisition unit used to gather the data: MX1615B (strain data gathered at bay B7), followed by MX1615B (strain data from bay B1), then MX440A (displacement data gathered from bays B4 and B7), and finally MX840B (strain data from bay B1). Data channels are sequentially listed, as outlined in Appendix C.

Each data file lists metadata associated with the given instrument channel: date and time of data collection, collection frequency, sensor and transducer type, unit of measure, anti-aliasing filter properties, tare value, and gauge factor, among others.

3.5.2 Data Post-Processing

During data capture, one channel was set to sample data at 4800 Hz in error, instead of the 1200 Hz used for all other channels. To rectify this, the affected channel data for each testing iteration was reduced to correspond with the proper 1200 Hz sample rate. This channel has metadata noted in each data file indicating that reduction of the dataset was completed to bring the dataset down to the new sample rate.

3.5.3 Modelling

Although the data collected could be used for various analyses, such as dynamic response modelling, focus was aimed at determining the dynamic loading effects on the bridge; to this end, strain and displacement effects were identified as key to completing the assessment. Therefore, the bridge was modelled using the SAP2000 software platform and validated using raw static data.

The simply supported model, seen in Figure 3.11, consisted of a single two-dimensional truss built from bar elements, each assigned material and geometric properties appropriate for their true-life counterparts. Panels were constructed with ideal pinned connections between them, and connections between panel chords and the reinforcing chords on the bridge were modelled with constrained displacement and rotations at locations of bolting. Static loading was achieved through virtual placement of the AEV at mid-span, with appropriate forces transferred to nodes at pinned connections between panels; this simulates the force of the vehicle on the transoms, which transfer load to the pinned connection between panels. Since only one of eight trusses was modelled, the load applied to the model was also reduced to one eighth of the full vehicle weight.

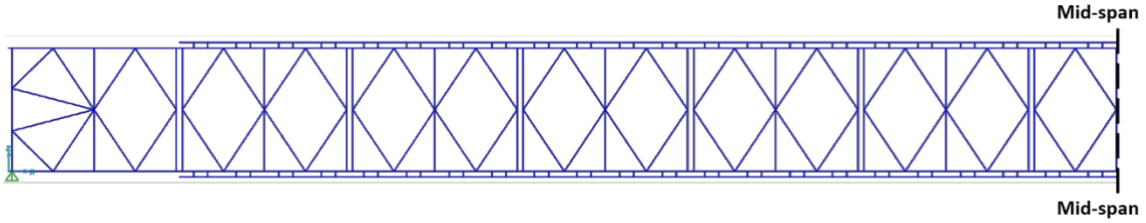

Figure 3.11 - Two-dimensional single truss validation model built in SAP2000 (mirrored at mid-span)

Due to the use of idealized pinned connections in the model that were not perfect representations of the tightly-installed panel pins on the actual bridge, in addition to the fact that panel elements welded to steel plates at mid-height were not included in the model, and the idealization of the support characteristics, it was expected that some difference was to be found in modelled and collected data. To this end, model strain data was found to have a percentage difference of 2% with raw data; model displacement at mid-span had a percentage difference with experimental values of 22%, and a percentage difference of 14% at quarter-span. A breakdown of validation calculations can be found in Appendix G – Model Validation.

3.6 Practical Applications

Understanding bridge response due to vehicular loading is paramount to allow for the safe and efficient design and analysis of these structures. The data gathered during this experimental testing can be used to determine the dynamic load factors that are appropriate for the vehicles used.

Minimal work has been completed to determine scientifically the dynamic load effects of military traffic on bridges. As a result, there is limited data available to compare the effects of military vehicles and their civilian counterparts. The data gathered during this testing provides a unique bridge type, span, and vehicle loading combination from which accurate load factors can be determined for use in general infrastructure codes relating to bridges. As an aside, this information can be used for more than strictly military applications; for example, the MSVS outlined above is very similar to a civilian truck load, as it is, at its core, a conversion from a commercially available vehicle.

Scientifically based DLA values due to military vehicle loading would allow for comparisons to be made between typical martial and civilian DLA factors. With this understanding, civilian and military authorities would be better equipped to determine the effects of vehicle loading on existing and planned bridge infrastructure, and would be better placed to identify and mitigate risks associated with these loads.

Various recommendations can be made for future work to be completed using this dataset. One area is the determination of appropriate DLA factors for tracked and wheeled military vehicles; this analysis of gathered data is part of a larger investigation that aims to achieve this goal. The independent data from the two vehicle types used (tracked and wheeled) also allows for the

determination of DLA based on vehicle classification, and subsequently for the identification of vehicle load distribution effects on bridge response.

Another use of this data could be to generate a complete and viable model for the simulation of load effects from any type of vehicle loading. While strain and displacement data are important in refining this model, the data gathered from the accelerometer placed on one of the vehicles could be used to represent that vehicle's specific loading characteristics acting on the bridge in this context. Modelling of the vehicle dynamic loading and bridge dynamic response could be completed.

Finally, comparison of the results of a DLA analysis using this data can be made with previous work completed by others (see [8]) to determine the validity of conclusions drawn. This, in turn, could give guidance on future experimental testing endeavours to confirm or broaden the knowledge of this specific field.

3.7 Conclusion

An experimental program was conducted to gather data for use in the determination of vehicular dynamic loading effects for a modular truss bridge. Four different vehicles were used: two provided load distribution via wheels, and two distributed loads through tracks. One wheeled vehicle was outfitted with an accelerometer to allow for the possibility of determining dynamic vehicle characteristics. Testing included vehicle crossings over a smooth deck, followed by passages across a simulated rough surface. Bridge data collected consisted of strain readings along truss panel chords, on stringers supporting the deck, and at superstructure supports, in addition to displacement readings at mid- and quarter-span locations. Data was gathered for multiple testing iterations in which vehicles crossed at prescribed speeds and in specific directions across the span.

All remaining data was determined to be adequate for use achieving various analysis goals, such as determination of DLA due to specific vehicle loading, and comparison of dynamic effects with existing research and codes. The dataset presented herein [65] has multiple practical applications, from modelling of dynamic bridge response, to comparison of DLA between codified and experimental values, as well as comparison of load effects due to civilian and military vehicle classes.

3.8 Data Availability Statement

Some or all data, models, or code generated or used during the study are available in a repository or online in accordance with funder data retention policies. For additional information, see B. Pinkney, "Experimental Data for Assessment of a Modular Truss Bridge." Harvard Dataverse, 2020, doi: 10.7910/DVN/APACSE.

3.9 Acknowledgements

This research would not have been possible without the funding provided by the Department of National Defence, and specific cooperation and support from multiple Canadian Armed Forces establishments: Director Combat Support Equipment Management, 1 Combat Engineer Regiment, Lord Strathcona's Horse (Royal Canadians), and Real Property Operations Detachment Wainwright.

3.10 References

[3] H. Hawk and A. Ghali, "Dynamic response of bridges to multiple truck loading," *Can. J. Civ. Eng.*, vol. 8, no. 3, pp. 392–401, Sep. 1981.

[4] CSA Group, C*ommentary on CAN/CSA S6-14, Canadian Highway Bridge Design Code*. CSA Group, 2014.

[5] North Atlantic Treaty Organization, *AEP-3.12.1.5 Military Load Classification of Bridges, Ferries, Rafts and Vehicles*, Ed. A, V1. NATO Standardization Office, 2017.

[8] A. Everitt, "Dynamic Load Effects of Tracked and Wheeled Military Vehicles From Bridge Load Testing," Royal Military College of Canada, 2019.

[12] P. Paultre, J. Proulx, and M. Talbot, "Dynamic Testing Procedures for Highway Bridges Using Traffic Loads," *J. Struct. Eng.*, vol. 121, no. 2, pp. 362–376, 1995.

[13] J. W. Wekezer, P. Szurgott, L. Kwasniewski, and E. Taft, "Dynamic response of reinforced concrete bridges due to heavy vehicles," *Adv. Transp. Stud.*, vol. 28, no. 28, pp. 35–50, 2012.

[14] B. Bakht and S. G. Pinjarkar, "Dynamic Testing of Highway Bridges - A Review," *Transp. Res. Rec.*, no. 1223, pp. 93–100, 1989.

[16] P. Paultre, O. Chaallal, and J. Proulx, "Bridge dynamics and dynamic amplification factors - a review of analytical and experimental findings," *Can. J. Civ. Eng.*, vol. 19, no. 2, pp. 260–278, 1992.

[17] Y. Zhou, Z. J. Ma, Y. Zhao, X. Shi, and S. He, "Improved definition of dynamic load allowance factor for highway bridges," *Struct. Eng. Mech.*, vol. 54, no. 3, pp. 561–577, 2015.

[18] R. Cantieni, "Dynamic load tests on highway bridges in Switzerland - 60 years of experience of EMPA," 1983.

[21] L. Deng, Y. Yu, Q. Zou, and C. S. Cai, "State-of-the-Art Review of Dynamic Impact Factors of Highway Bridges," *J. Bridg. Eng.*, vol. 20, no. 5, pp. 1–14, 2014.

[25] Q. Gao, Z. Wang, C. G. Koh, and C. Chen, “Dynamic load allowances corresponding to different responses in various sections of highway bridges to moving vehicular loads,” *Adv. Struct. Eng.*, vol. 18, no. 10, pp. 1685–1701, 2015.

[31] J. R. Billing, “Dynamic loading and testing of bridges in Ontario,” *Can. J. Civ. Eng.*, vol. 11, no. 4, pp. 833–843, 1984.

[33] M. F. Green and D. Cebon, “Dynamic tests on two highway bridges,” in *Proceedings of the Third International Symposium on Heavy Vehicle Weights and Dimensions*, 1992, pp. 1–8.

[36] R. Green, “Dynamic response of bridge superstructures - Ontario observations,” 1977.

[41] J. R. Billing and A. C. Agarwal, “The Art and Science of Dynamic Testing of Highway Bridges,” in *Developments in Short and Medium Span Bridge Engineering*, 1990, pp. 531–544.

[42] R. Cantieni, “Dynamic Behaviour of Highway Bridges Under the Passage of Heavy Vehicles,” *EMPA Report No. 220*, Dübendorf, p. 249, 1992.

[53] Bundesministerium für Verkehr Bau und Stadtentwicklung Abteilung Straßenbau, “Hinweise zur Anwendung des Eurocode 1, Teil 2: „Verkehrslasten auf Brücken“ sowie zu den Teilen 1-1 und 1-3 bis 1-7,” 2012.

[54] B. Bakht and P. F. Csagoly, “Bridge Testing,” Downsview, Ontario, 1979.

[55] O. S. Salawu and C. Williams, “Review of full-scale dynamic testing of bridge structures,” *Eng. Struct.*, vol. 17, no. 2, pp. 113–121, 1995.

[56] J. Arpin-Pont, M. Gagnon, A. S. Tahan, A. Coutu, and D. Thibault, “Methodology for estimating strain gauge measurement biases and uncertainties on isotropic materials,” *J. Strain Anal. Eng. Des.*, vol. 50, no. 1, pp. 40–50, Jan. 2015.

[57] J. Pople, “Errors and Uncertainties in Strain Measurement,” in *Strain Gauge Technology*, A. L. Window and G. Holister, Eds. New York: Elsevier Science Publishing, 1989, pp. 209–264.

[58] H. K. P. Neubert, *Strain Gauges: Kinds and Uses*. Toronto: MacMillan & Co., 1967.

[59] WSP Group, “L-W5-0707-601 Battle Bridge Upgrade.” Government of Canada, Edmonton, 2017.

[60] I. Paeglite and A. Paeglitis, “The dynamic amplification factor of the bridges in Latvia,” *Procedia Eng.*, vol. 57, pp. 851–858, 2013.

[61] FFG Canada, *Operator Training: WISENT 2 AEV CAN*. 2016.

[62] FFG Canada, *Operating Manual for Training AEV WISENT 2 CAN*. 2016.

[63] FFG Canada, *C-30-B66-000/MA-000 Specific Data Summary Wisent 2 AEV Can*. 2018.

[65] B. Pinkney, “Experimental Data for Assessment of a Modular Truss Bridge.” Harvard Dataverse, 2020.

CHAPTER 4 MANUSCRIPT 2: DYNAMIC LOAD TESTING OF A MODULAR TRUSS BRIDGE USING MILITARY VEHICLES

This manuscript has been submitted for possible publishing in the American Society of Civil Engineers (ASCE) Journal of Bridge Engineering.

4.1 Abstract

Determination of appropriate load factors ensures bridge assessments completed using limit states design are applicable for all potential loading scenarios. Extremely limited research has been completed to determine accurate Dynamic Load Allowance (DLA) values for military vehicle loading of bridges, specifically independent values for tracked and wheeled vehicle types. An experimental testing programme was used to assess the dynamic load effects caused by these vehicle categories by subjecting a bridge to loading from multiple different vehicle types at different speeds, while controlling deck surface condition. It was found that tracked vehicles generate approximately half the dynamic bridge response of wheeled vehicles. Using this knowledge, tracked vehicle DLA value recommendations are made for use in the North Atlantic Treaty Organization (NATO) Military Load Classification (MLC) system, and in the Canadian Highway Bridge Design Code (CHBDC) and American Association of State Highway and Transportation Officials (AASHTO) bridge code, which could lead to strategic increases in tracked vehicle mobility.

4.2 Introduction

Determination of load effects acting on structures is a critical component to quantifying the maximum load carrying capacity of bridges. Following limit states philosophy, the Ultimate Limit State (ULS) analysis process allows for the comparison of factored load effects to factored structural resistance, with the aim of ensuring factored resistance is greater than factored load effects [2], [10]. One such load factor applied through ULS analysis is the Dynamic Load Allowance (DLA), which is a fractional increase of the design live load to account for the influence of inertia from transitory loads on bridges [3], [17].

4.2.1 Aim

The aim of this research was to validate the difference in dynamic bridge response to tracked and wheeled vehicle loading, determine independent DLA values for each vehicle category, and to examine the effects of a rough deck surface on bridge response. To achieve this goal, experimental testing was completed using both of these vehicle types by varying speed and deck condition during transit across a modular truss bridge. Comparison with previous research and existing code

recommendations sought to confirm the validity of results, and provide rationalization for recommendations.

4.2.2 Background

Engineering design often incorporates factors to increase loading effects and decrease structural resistance with an aim of maintaining a certain level of conservatism, and therefore safety. Generally, structures are considered to have an acceptable design when the factored resistance is greater than the factored load [2], [10]. One such element that applies to vehicle live loads is the DLA. To determine an appropriate value for this allowance, dynamic assessment of a bridge is necessary. To this end, the bridge response to dynamic loading must be examined, understanding the complete response is comprised of two parts: the static response, and the dynamic response [3]. Due to the complexity of the response, it is common to approximate dynamic effects as a portion of the static load effects acting on a bridge [12], [13]. To achieve this, a Dynamic Amplification (DA) term is introduced to relate these two responses through Equation 4.1 [3], [12], [14], [15]:

$$R_{dyn} = R_{sta}(1 + DA) \tag{4.1}$$

where R_{dyn} is the maximum dynamic response of the bridge;
R_{sta} is the maximum static response of the bridge; and
DA (Dynamic Amplification) is a ratio of dynamic response to static response [16].

Rearrangement of Equation 4.1 allows for the quantification of DA through experimental testing. It should be noted that the maximum dynamic and static responses of the bridge are compared to each other, even if the data originates in sensors at different locations on the bridge, through the rearranged Equation 4.2 [3], [13], [14], [16], [31], [33], [41], [42]:

$$DA = \frac{R_{dyn} - R_{sta}}{R_{sta}} \tag{4.2}$$

where R_{dyn} is the maximum dynamic bridge response; and
R_{sta} is the maximum static bridge response.

DA is an experimentally-applicable definition of dynamic bridge response to a specific loading case, and should not be confused with the codified DLA values that are applied to a broad range of loading scenarios. To determine a DLA value that is statistically relevant to define the bridge response, conversion of DA to DLA is required. This can be accomplished using limit states philosophy; among other limit states, Ultimate Limit State calculations take account of risk of structural failure through the application of a reliability index, and the variability of transitory loads through the use of a live load factor. Applying these values in addition to the average DA value from many iterative test serials, DLA can be calculated using Equation 4.3 [14], [18], [31]:

$$DLA = \frac{\overline{DA}(1 + \nu s\beta)}{\alpha_L} \quad 4.3$$

where $\overline{DA}$ is the average value of the calculated DA terms acquired through testing;
ν is the coefficient of variation of the measured quantity, in this case DA;
s is the separation factor for dynamic loading;
β is the reliability index; and
α_L is the live load factor.

The coefficient of variation of the data is commonly defined as the ratio of mean value to the standard deviation of the dataset [4], [14]. Considering the separation factor, also known as the sensitivity factor, a value of 0.57 has been shown to be appropriate [14], [18].

The majority of modern bridge codes around the globe use metrics such as loading scenarios, span length or first flexural frequency of a bridge to define DLA [2], [20]–[22], [41], [44]. In a North Atlantic Treaty Organization (NATO) context, the Military Load Classification (MLC) system is used to analyze bridges. This system, outlined in NATO AEP-3.12.1.5 (Standardization Agreement (STANAG) 2021), relates vehicle loading effects with bridge, raft, or ferry capacities through numeric identifiers, and differentiates between tracked and wheeled vehicles to account for the notable differences in load distribution characteristics between the two vehicle categories. For vehicle classification, it is important to understand that this numeric identifier is a number only, and does not represent the mass of the vehicle being classified [5].

The MLC system allows for more accurate classification of both bridges and vehicles. However, despite the acceptance of unique vehicle sets for classification, this system does not indicate that separate DLA values should be used for each; rather, the recommendation for military engineers to follow their own national guidelines is made [5]. In a Canadian and American military context, this manifests itself as a universally-applicable prescribed DLA value of 0.15 [6], [7]. This generalization poses various issues, mainly that vehicles with distinctly different load distribution characteristics are not considered independently when analyzing bridge response.

When aiming to determine appropriate dynamic characteristics of a bridge, full-scale dynamic testing using regular and controlled traffic is preferable [12], [16]. Iterations completed at multiple speeds is recommended, as this variation will assist with clarifying the relationship between dynamic bridge response and speed [12], [16], [18], [21], [54]. Care must be taken to limit uncontrolled dynamic loading, such as loose cargo in a test vehicle, as well as accelerating, braking, or making steering corrections along the span [13], [36]. Of similar importance is the fact that vehicles must maintain consistent course along the traffic lane while transiting across the bridge; failure to do so has been found to impact bridge response, and therefore the reliability of data gathered [42].

While multiple transits made at speed are needed for determination of DLA, Equations 4.1 and 4.2 indicate that quantification of static load effects on the bridge are also required. For this, it is possible to gather bridge response either from static load tests ("stationary" tests) in which a vehicle stops at a predetermined location along the bridge, or through quasi-static loading ("crawl" tests) created by a vehicle crawling steadily across the entire span [14], [16], [17].

Consensus on which types of instrumentation to use for dynamic testing is not unanimous in literature. When considering sensors on the bridge, it is possible to use accelerometers, displacement transducers, or strain gauges to monitor dynamic response. While both displacement and strain data are more appropriate for determination of DLA, the majority of research has indicated that strain measurements are more reliable [13], [14], [17], [25], [41].

4.3 Experimental Testing

4.3.1 Bridge

The bridge used for experimental testing, named Battle Bridge after the river over which it crosses, was an ACROW 700XS modular panel structure, as seen in Figure 4.1. Located at 3rd Canadian Division Support Base (CDSB) Wainwright, it has a span of 39.62 m, and transfers load from the timber decking to 3 m-long stringers mounted on transoms at each panel intersection, and from the transoms into the truss panels. Eight adjacent trusses, four on each side of the deck, form the primary load distribution members of the structure.

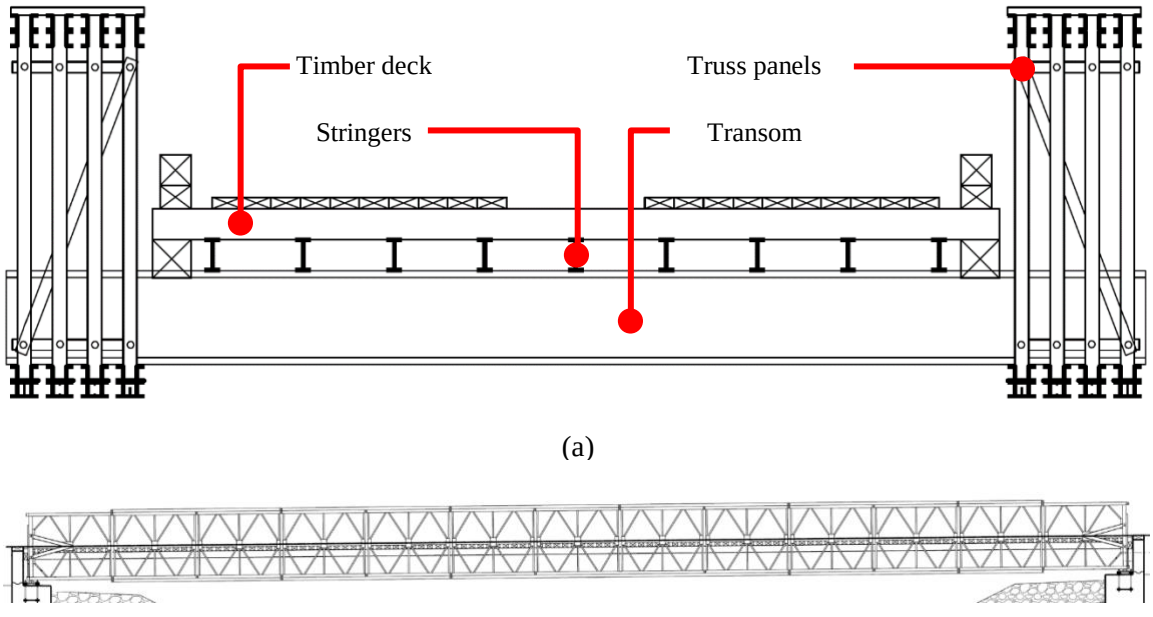

Figure 4.1 - Battle Bridge structural components showing (a) cross-section and (b) south elevation (after [59])

Two types of deck surfaces were used for testing. The first was the smooth unmodified deck surface of the existing structure; the second was a simulated irregular deck. A common method of simulating degraded deck surfaces is the addition of timber planks across the driving lane [14], [18], [54]; this was achieved through the placement of five 2 x 10-inch boards (nominal dimensions, or 35 mm x 228 mm) at the bridge mid-span, with a spacing of 3 m between successive planks.

4.3.2 Instrumentation

The bridge was instrumented with strain gauges and displacement sensors. Sixteen strain gauges were installed at mid-span along top and bottom truss chords. Nineteen strain gauges provided data on bridge response at the western-most panel bay; ten of these were placed to provide strain readings at mid-span of the stringers at this location, five indicated strain at the end of the stringer above the abutment, and four gauges measured strains immediately above superstructure bearings. Displacement was recorded at mid- and quarter-span locations. Two linear string potentiometers were installed at each location, one on each external truss.

For a complete description of bridge instrumentation, including details of the sensors used, instrumentation priority, and specific gauge placement, refer to Section 3.4.2.

4.3.3 Vehicles

Four vehicles were used during experimental testing. These consisted of two wheeled military vehicles, and two tracked vehicles. Due to the nature of vehicles that normally use this bridge, the military vehicles outlined below are considered normal traffic. Following the guidance set out by the MLC system, military traffic maintains convoy spacing of 30.5 m between vehicles [5], [6]; therefore, simultaneous loading of multiple vehicles on this bridge was not considered.

The first tracked vehicle used in testing was the Leopard 2 Armoured Engineer Vehicle (AEV), as given in Figure 4.2. This fighting vehicle, massing 69.5 t (681.5 kN), distributes load across fourteen road wheels onto a track with ground contact area dimensions of 0.64 m by 4.95 m [61], [62], [64].

Figure 4.2 - Leopard 2 Armoured Engineer Vehicle (AEV)

The second tracked testing vehicle was the Leopard 2A4M main battle tank (MBT). Shown in Figure 4.3, this tank distributes a 60.5 t mass (593.3 kN) over over fourteen road wheels onto a track that has a ground contact area of 0.64 m by 4.95 m [64].

Figure 4.3 - Leopard 2A4M main battle tank (MBT)

Wheeled vehicles consisted of the Medium Support Vehicle System (MSVS) Load Handling System (LHS) variant, and the Tactical Armoured Patrol Vehicle (TAPV). Massing 25.9 t (254.2 kN) on testing day, the MSVS was a transport vehicle that boasts four axles, as given in Figure 4.4. The TAPV was the lightest vehicle used for testing. At 16.3 t (159.4 kN) on testing day, this fighting vehicle distributed its mass across two axles, as seen in Figure 4.5.

Figure 4.4 - Medium Support Vehicle System (MSVS) Load Handling System (LHS) variant

Figure 4.5 - Tactical Armoured Patrol Vehicle (TAPV)

4.4 Analysis

4.4.1 Modelling

To allow for the potential of bridge response assessment to alternate vehicle loads, simplified numerical modelling was conducted using SAP2000 software and validated using collected data [65]. The model consisted of a single two-dimensional truss, with appropriately scaled static loads placed along the structure to simulate a vehicle resting at mid-span. One-half of the model (from one support to mid-span) can be seen in Figure 4.6.

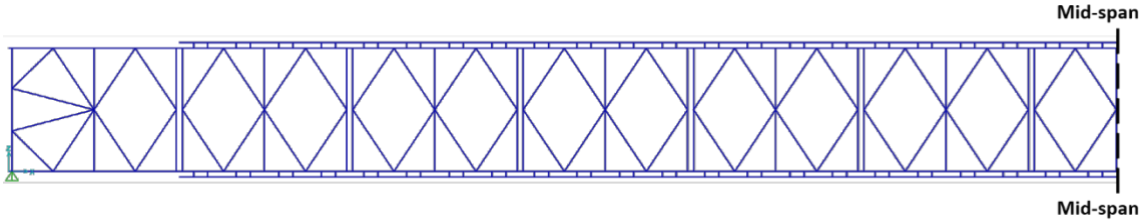

Figure 4.6 - Two-dimensional SAP2000 validation model (mirrored at mid-span)

Aside from simplifying the model to a single truss, additional simplifications were made. Adjacent truss panel connections were modelled as idealized pins, instead of attempting to quantify the physical properties of the tightly installed pins that connected the real structure. Plates welded at mid-height on individual panels were also not included, and superstructure support characteristics were idealized as a perfect pin-roller combination. Model strain results were consistent with raw data, having been found to have 2% difference with raw data. Model displacement effects were compared with experimental data at mid- and quarter-span locations, with modelled values being within 22% of experimental values at mid-span, and 14% at quarter-span. Complete model validation calculations can be found in Appendix G – Model Validation.

4.4.2 Uncertainty

To ensure accuracy of results, it is imperative to understand how error affects all components in a data collection system. Once these errors are taken into account, an uncertainty with respect to the final result can be stated; this uncertainty is given as a range of values within which one would expect the true value of a measurement to lie [56], [57], [66]. To account for errors in this experimental investigation, the law of propagation of uncertainties was used to compile the effects of multiple sources of error to determine a single appropriate quantification of uncertainty in the calculated DLA [66].

The errors that combined to generate stated measurement uncertainties included the following: carrier frequency, circuit excitation, and bridge linearity errors of data acquisition systems; resistance, and, in the case of strain gauges, gauge factor errors of sensors; and average voltage drop in cables connecting instruments to the data acquisition systems. For strain gauge readings, an average uncertainty among the three data acquisition systems connected to these sensors was ± 5.16%; displacement sensor data had a calculated uncertainty of ± 11.18%. With knowledge of the uncertainty associated with each reading, the global uncertainty in a calculated DLA value can then be generated using the same law of propagation of uncertainties, as given in Equation 4.4 [66]:

$$u^2(y) = \sum_{i=1}^{N} \left(\frac{\partial f}{\partial x_i}\right)^2 u^2(x_i) + 2 \sum_{i=1}^{N-1} \sum_{j=i+1}^{N} \frac{\partial f}{\partial x_i} \frac{\partial f}{\partial x_j} u(x_i, x_j) \qquad 4.4$$

where $u(y)$ is the combined uncertainty of the measurement y;
y, the measured result, is a function of the input variables such that $y = f(x_1, x_2, \ldots, x_n)$;
$u(x_i)$ is the standard uncertainty for an input variable;
x_i is an input variable;
x_j is an input variable correlated to input variable x_i;
$u(x_i, x_j)$ is the covariance of x_i and x_j; and
N is the number of input variables.

Understanding of error propagation is best accomplished through an example; to this end, uncertainty associated with a strain measurement will be made. An input variable (x_i) is selected, in this case the resistance of the strain gauge, and its standard uncertainty ($u(x_i)$, or ± 0.3%) is used to determine the overall impact on strain measurement uncertainty. Similarly, the standard uncertainties associated with the following input variables are considered: gauge factor (± 1%), bridge linearity error (± 0.02%), circuit excitation (± 5%), carrier frequency (± 0.17%), and cable voltage drop (in the case of one data acquisition unit, ± 0.35%). Summation in quadrature indicates the global uncertainty of these input variable errors acting on a strain gauge reading made through the specific data acquisition unit (± 5.12%).

4.4.3 Dynamic Load Allowance

Determination of iteration-specific DA values required the comparison of both static and dynamic response readings. As outlined previously, static or quasi-static testing can be completed to determine an appropriate static bridge response. Analysis of raw data indicated the presence of dynamic oscillations throughout static test data, but more notably at points where the vehicle stopped or began moving after being stopped. These short-duration dynamic influences were not as prominent in the quasi-static tests, but were still present, possibly the result of vehicle engine vibration. To isolate the static bridge response from these small dynamic influences, a filter was applied to the data.

To maintain data integrity in the time domain, a low-pass Bessel filter was used [67]. Various cut-off frequencies, from 2 Hz down to 0.25 Hz, were compared to determine the effects on the dataset; a convergence test showed that using a cut-off frequency of 1 Hz allowed for the maximum retention of data while reducing the dynamic oscillations, as given in Appendix H – Data Filter Convergence Test Results. Figure 4.7 indicates a sample isolation of static readings from raw data at peak response during quasi-static loading of the bridge by the AEV. The maximum filtered bridge response during quasi-static testing was used for the calculation of iteration DA, as dynamic influences were found to still be present in static testing data, even after the application of a low-pass filter; the use of a lower cut-off frequency was required to eliminate these peak influences, which had a negative effect on the remainder of the static response dataset.

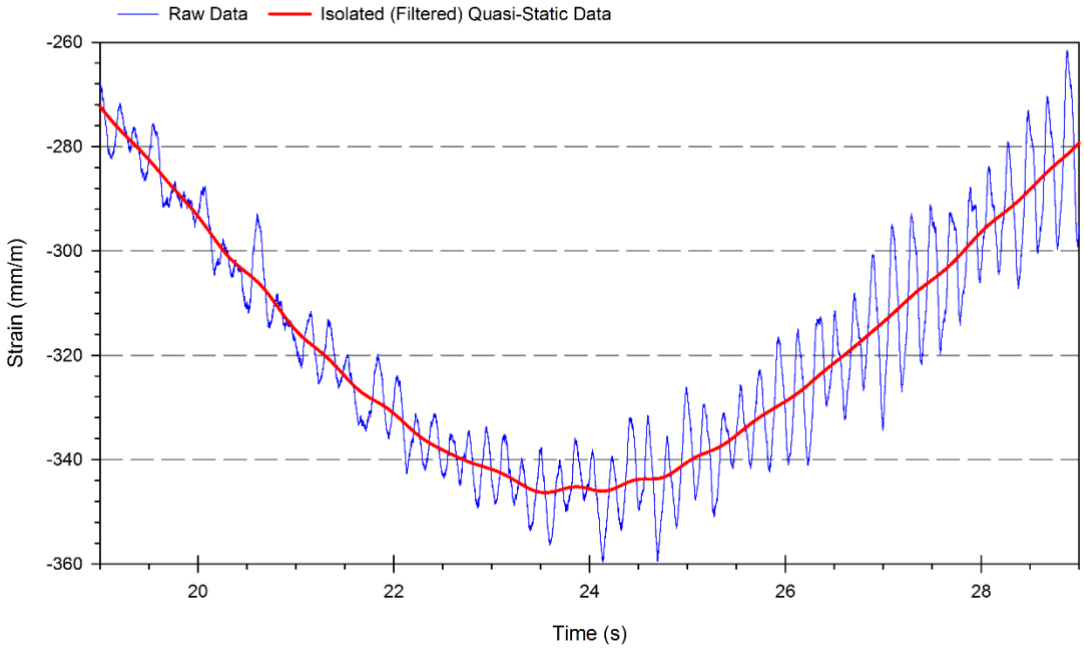

Figure 4.7 - Isolated (filtered) quasi-static load effects of an AEV compared with raw data

With the isolation of static bridge response readings, determination of DA values for each testing iteration of each vehicle was completed using Equation 4.2. Using the DA values from smooth-surface testing, a comprehensive DLA was generated for each vehicle. With the aim of this analysis being the determination of DLA values appropriate for application in a military context, live load and target reliability index values are those previously recommended by draft CAF doctrine [68]: namely 1.35 and 3.75, respectively. DLA was only calculated for smooth-surface testing to facilitate comparison with bridge codes.

4.5 Results

Analysis of smooth-surface results indicates there is a general trend of increasing DA value with speed for all vehicles. Due to their improved ability to distribute weight and suspension optimized for cross-country travel, tracked vehicles exhibit a decreased dynamic response when compared to wheeled vehicles. Figure 4.8 presents a comparison of smooth-surface DA with respect to speed for each vehicle used in this investigation. As concluded by previous research in the field [16], [21], [35], it can be seen that speed does have an impact on the response of the bridge to dynamic loading.

A detailed analysis of results outlined in Figure 4.8(a) indicates select points of interest. First is the fact that tracked vehicles do not see an appreciable increase in DA until vehicle speeds exceed 20 km/h. Above this speed, both tracked vehicles exhibit what appears to be steady increase in DA up to the maximum testing speed used. Two MBT results can be noted as exceptional; the first at

10 km/h, and the second at 30 km/h, both of which saw the vehicle completing notable course correction pivots while crossing the span. Increased dynamic load was introduced into the structure in both instances, resulting in DA values in excess of other calculated values for these crossing speeds. This data was still used in computation of appropriate DLA values, as it is possible that, during a real crossing with limited or no control measures in place, vehicle operators could complete course corrections that affect the bridge in the manner seen during these tests. Due to technical issues, the MBT completed crossings up to a maximum speed of 35 km/h, substituting higher-speed iterations with crossings made at additional intermediate speeds. The AEV was able to complete tests at all speeds with relatively low DA values observed at all speeds.

A focus on Figure 4.8(b) shows wheeled vehicles cause notable dynamic effects in the bridge at all speeds. In almost all cases, the TAPV generates increased dynamic response of the bridge compared to the MSVS. This is to be expected, as previous research has indicated that lighter vehicles tend to create larger DA values compared to their heavier counterparts [14], [21], [31].

The same analysis steps were followed to determine the effects of the rough deck on DA. Vehicle crossings over an irregular surface at low speeds can generate excitation frequencies close to the natural frequency of the vehicle, possibly resulting in increased excitation forces on the bridge [29]. As expected, calculated DA values were notably larger due to the effects of the simulated surface degradation, as given in Figure 4.9. Similar to smooth-surface testing, wheeled vehicles can still be seen to cause a larger dynamic response in the bridge.

Analysis of tracked vehicle results in Figure 4.9(a) indicate similar trends to smooth-surface tracked vehicle effects. Minimal dynamic responses are found at 20 km/h, while speeds in excess of this seem to cause a steady increase in dynamic bridge response. Due to technical issues, the MBT was unable to complete rough surface testing.

Figure 4.9(b) seems to indicate that wheeled vehicles have a larger range of dynamic load effects than tracked vehicles, similar to smooth-surface testing. Of interest is the fact that wheeled vehicles tend to have the largest dynamic effect during rough-surface crossings at low speeds, followed by a decrease in DA at higher speeds. This could be due to the fact that board spacing on the bridge was very similar to axle spacing, resulting in all vehicle axles loading on the bridge deck simultaneously after clearing the obstacles, instead of each axle loading the deck out of phase with other axles. It is likely that wheeled vehicle suspensions were able to absorb some force from crossing over obstacles at higher speeds, resulting in the lower DA in the bridge at these speeds.

Understanding the effect of sub-optimal deck condition on load response is crucial in a military context. With potential for damage to bridges significantly higher during times of conflict, and the need to continue trafficking military vehicles across bridges that may have been damaged, NATO has outlined increased-risk crossing scenarios that require additional traffic controls over normal crossings. Named caution and risk crossings, these crossing categories impose additional limitations on vehicles; among others, these include speed restrictions limiting movement to a

maximum of 5 km/h across the span, and restrictions on acceleration, braking, and abrupt course corrections while crossing [5]. Indications given in Figure 4.9 point towards the fact that bridges have notable response to vehicles crossing over a degraded deck even at 10 km/h, emphasizing the need for these strict caution and risk crossing controls.

The error bars indicated in Figure 4.8 and Figure 4.9 pertain to the uncertainties associated with data collection for each test iteration completed. As outlined in Section 4.4.2, uncertainty associated with data acquisition systems, sensors themselves, and cabling were assessed to determine the overall uncertainty associated with calculated DA values. Expressed as a percentage of the DA, the final uncertainty range for each experimental iteration increases as the DA value rises.

Statistical parameters related to the data used to calculate the DLA are given in Table 4.1. It should be noted that these parameters refer to smooth-surface testing; since codified DLA values typically indicate effects due to vehicle loading on a wearing surface in good condition, inclusion of simulated rough-surface tests was not deemed appropriate. Eight test iterations were used for the determination of each vehicle's DLA, with crossings made at 20 km/h up to 50 km/h. Crossings at 10 km/h were neglected from these calculations, as this speed is significantly lower than typical traffic expected for this bridge.

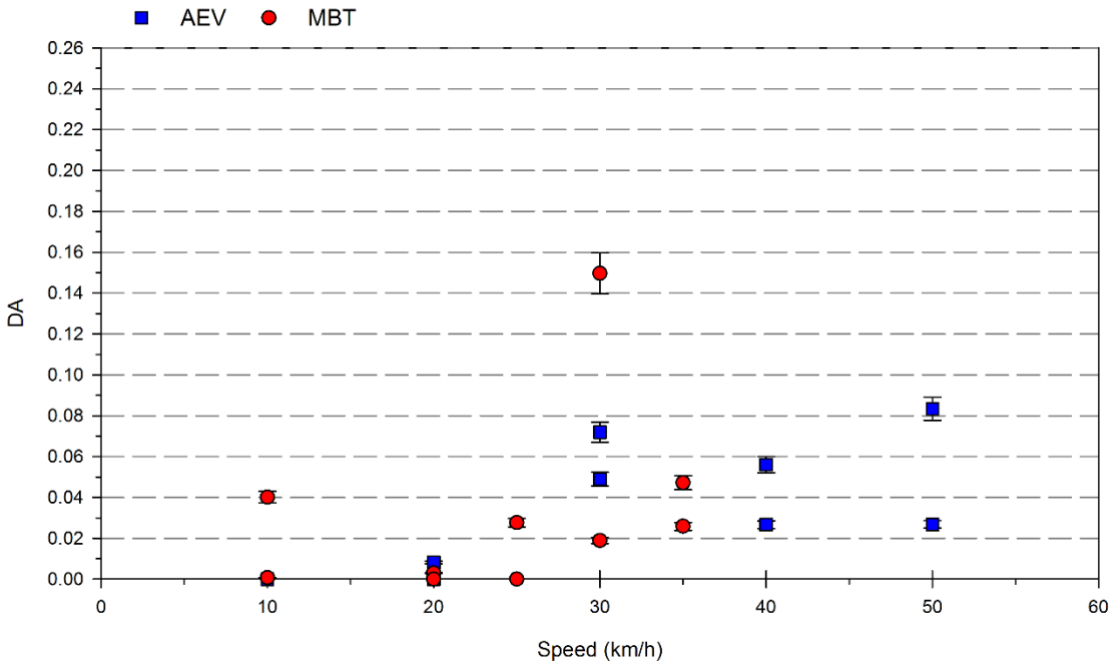

(a)

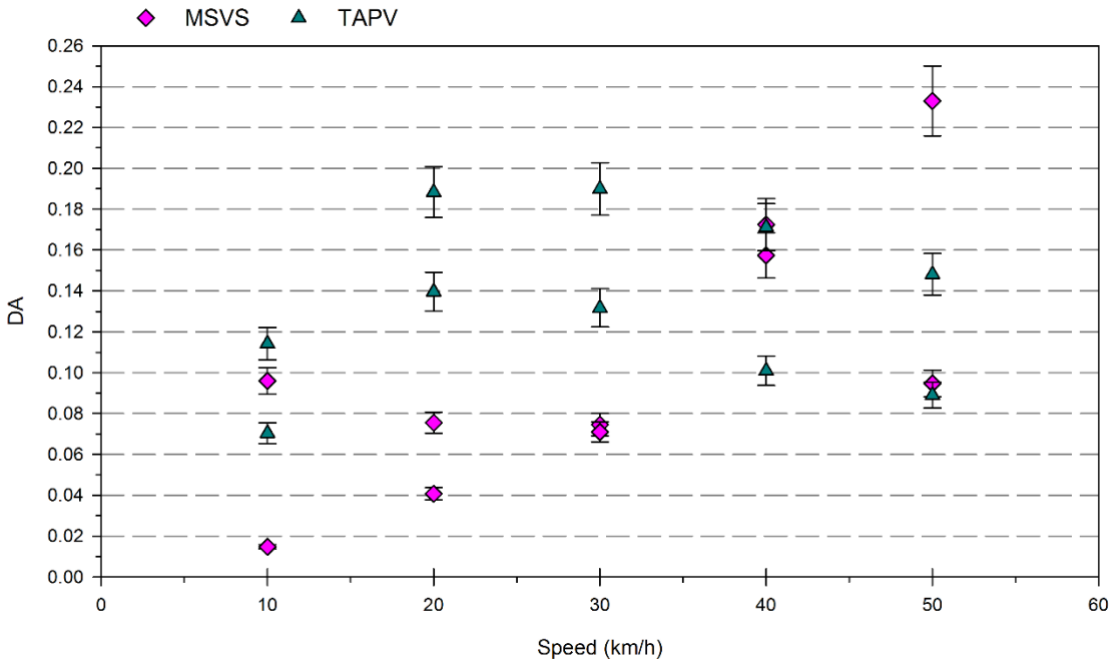

(b)

Figure 4.8 - Smooth surface DA of (a) tracked and (b) wheeled vehicles at various speeds

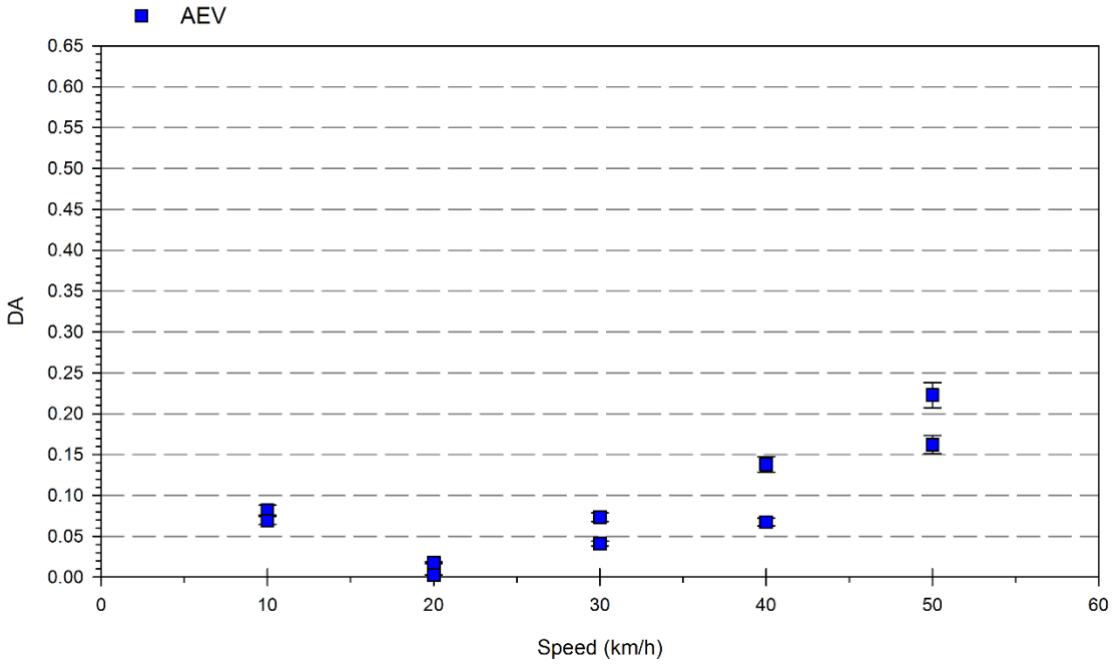

(a)

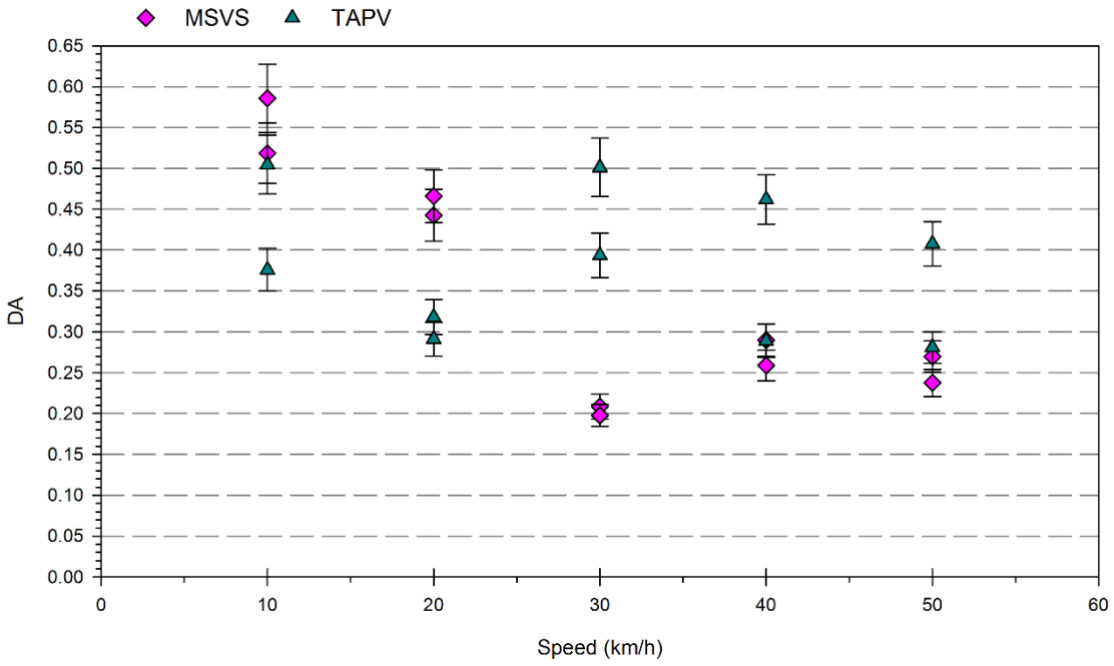

(b)

Figure 4.9 - Simulated rough surface DA of (a) tracked and (b) wheeled vehicles at various speeds

Table 4.1 - Statistical parameters related to DLA calculation

Vehicle	Mean DA	σ	Test Iterations
AEV	0.04	0.03	8
MBT	0.03	0.05	8
MSVS	0.11	0.06	8
TAPV	0.14	0.04	8
All Tracked	0.04	0.04	16
All Wheeled	0.13	0.05	16

DLA values calculated from independent DA test results for each vehicle are given in Table 4.2; also presented is the average DLA values with associated uncertainty based on vehicle type (either tracked or wheeled). Due to the method through which each vehicle class distributes load, there was found to be significant difference in the dynamic response of the bridge to the vehicle type; wheeled vehicles caused approximately twice the effects of tracked vehicles. Application of a reduced tracked DLA would have strategic impacts on the mobility of this vehicle class, as an increase would very likely occur in the number of existing bridges that could safely cross tanks.

Table 4.2 - DLA of test vehicles

Vehicle	DLA
AEV	0.07 ± 3.2%
MBT	0.10 ± 4.4%
MSVS	0.18 ± 2.9%
TAPV	0.16 ± 2.7%
All Tracked	0.09 ± 2.6%
All Wheeled	0.18 ± 2.0%

4.6 Dynamic Load Allowance Comparison

Using the data gathered through experimental testing, DLA comparison can be made based on the source of target reliability index and live load factor values. There are three broad source categories for factors presented, including military-related sources, code-based origins (both Canadian and American), and factor values recommended in literature; this comparison is given in Table 4.3.

Analysis indicates that DLA values for tracked and wheeled vehicles do not vary significantly between factor sources. Military-sourced factors indicate that appropriate DLA values for tracked and wheeled vehicles could be 0.09 and 0.18, respectively. Canadian code live load factor and reliability index values designate potential DLA values as 0.07 for tracked vehicles, and 0.14 for

wheeled vehicles. American Load and Resistance Factor Design (LRFD) factor values generate a possible tracked DLA of 0.07, and a possible wheeled DLA of 0.15. Literature factor-based DLA values can be seen in Table 4.3.

A comparison of all factor combinations indicates that DLA values for tracked vehicles are consistently between 45-50% of those recommended for wheeled vehicles. Therefore, the relationship between DLA of the two vehicle categories outlined in Section 4.5 is maintained for all factor sources indicated in Table 4.3.

To verify that the range of DLA values for this experimental testing is accurate, a comparison can be made of the DLA for the bridge itself based on various countries' national bridge codes and military bridge manuals, as given in Appendix I – Bridge Dynamic Load Allowance Comparison. It should be noted that this comparison is made for wheeled vehicles only. The DLA of a bridge can be described as a function of span length, first natural frequency, or traffic loading models [12], [16], [17], [21], [24], [28], [40], [43]. To determine an estimation of the first natural frequency of the bridge, Equation 4.5 can be applied [18], [27]:

$$f = 95.4\, L^{-0.933} \qquad 4.5$$

where f is the bridge fundamental frequency in Hertz; and
L is the bridge span in metres.

Using the bridge span of 39.62 m, and estimated first natural frequency of 3.08 Hz, the DLA of the bridge was calculated based on the guidelines from multiple codes; it was determined that maximum and minimum DLA values for the bridge were 0.40 and 0.15, respectively, with a mean value of 0.25. For tracked vehicle traffic, it may be appropriate to reduce these calculated DLA values by up to one-half, as outlined in Section 4.5. Based on this analysis, it can be seen that the experimentally derived DLA values given in Table 4.3 for wheeled vehicles fall within these provisions.

The German Federal Ministry of Traffic, Construction and City Development was the sole literature source that indicated different DLA application based on the vehicle categories presented. This guidance indicated the use of a maximum DLA of 0.10 for tracked vehicles, and 0.25 for wheeled vehicles [53]. Based on experimental testing, the dynamic factor limit for tracked vehicle traffic was found to be acceptable. Despite the prescribed value of DLA for wheeled vehicles being larger than experimental values, the recommended maximum is also determined to be appropriate, given the variability in wheeled vehicle mass and load distribution combinations possible.

Table 4.3 - DLA comparison

Source	β	α_L	DLA					
			AEV	**MBT**	**MSVS**	**TAPV**	**All Tracked**	**All Wheeled**
NATO AEP-3.12.1.5 [5]	3.30	1.35	0.07	0.09	0.17	0.16	0.08	0.17
CAF Bridge Manual [6]	3.75	1.30	0.08	0.10	0.19	0.17	0.09	0.19
CAF Bridge Manual (Draft) [68]	3.75	1.35	0.07	0.10	0.18	0.16	0.09	0.18
CHBDC Table 14.8 (normal traffic, all spans) [2]	2.50	1.35	0.06	0.07	0.15	0.14	0.07	0.15
	2.75	1.42	0.06	0.08	0.15	0.14	0.07	0.15
	3.00	1.49	0.06	0.08	0.15	0.14	0.07	0.15
	3.25	1.56	0.06	0.08	0.15	0.13	0.07	0.15
	3.50	1.63	0.06	0.08	0.15	0.13	0.07	0.14
	3.75	1.70	0.06	0.08	0.14	0.13	0.07	0.14
	4.00	1.77	0.06	0.08	0.14	0.13	0.07	0.14
CHBDC Table 14.10 (PA traffic, simplified, short span) [2]	2.50	1.48	0.05	0.07	0.14	0.13	0.06	0.14
	2.75	1.55	0.05	0.07	0.14	0.13	0.06	0.14
	3.00	1.62	0.05	0.07	0.14	0.13	0.06	0.14
	3.25	1.70	0.05	0.07	0.13	0.12	0.06	0.13
	3.50	1.78	0.05	0.07	0.13	0.12	0.06	0.13
	3.75	1.87	0.05	0.07	0.13	0.12	0.06	0.13
	4.00	1.96	0.05	0.07	0.13	0.11	0.06	0.13
CHBDC Table 14.10 (PA traffic, simplified, other span) [2]	2.50	1.28	0.06	0.08	0.16	0.15	0.07	0.16
	2.75	1.34	0.06	0.08	0.16	0.15	0.07	0.16
	3.00	1.40	0.06	0.08	0.16	0.15	0.07	0.16
	3.25	1.47	0.06	0.08	0.16	0.14	0.07	0.15
	3.50	1.53	0.06	0.08	0.16	0.14	0.07	0.15
	3.75	1.60	0.06	0.08	0.15	0.14	0.07	0.15
	4.00	1.67	0.06	0.08	0.15	0.13	0.07	0.15
AASHTO LRFD Strength I [15]	3.50	1.75	0.05	0.07	0.14	0.12	0.06	0.13
AASHTO LRFD Strength II [15]	3.50	1.35	0.07	0.09	0.18	0.16	0.08	0.17
Billing, Bakht and Pinjarkar, Cantieni [14], [18], [31]	3.50	1.40	0.07	0.09	0.17	0.15	0.08	0.17
MacDonald [52]	3.75	1.77	-	-	0.14	-	-	-
	3.75	1.48	-	-	-	0.15	-	-
	3.75	1.33	0.08	0.10	-	-	0.09	-

4.7 Conclusion

Experimental testing was conducted with the aim of determining appropriate DLA values for both wheeled and tracked military vehicles by incorporating variable-speed bridge crossings with smooth and simulated rough surface decking. Using strain data and accounting for instrumentation system uncertainties, DLA values were determined for each vehicle used during testing, as well as the tracked and wheeled vehicle classifications. These values were then compared with multiple national bridge codes and military bridge manuals, and were found to be within expected ranges. Key results are given as follows:

1. Tracked vehicles exhibit notably reduced dynamic effects when compared to wheeled vehicles. Therefore, application of a separate, reduced DLA for tracked vehicles should be considered where appropriate;

2. For inclusion into future revisions of NATO AEP-3.12.1.5 (STANAG 2021), which does not specify exact values of DLA, it may be appropriate to indicate that tracked vehicle DLA values could be set as low as half the value of national code-specified wheeled vehicle DLA values;

3. Appropriate DLA values in both a Canadian and American military context could be 0.09 for tracked vehicles, and 0.18 for wheeled vehicles;

4. An appropriate DLA for tracked vehicles could be 0.07 for bridge components excluding deck joints in both the CHBDC and AASHTO LRFD Bridge Design Specification contexts;

5. Considering existing bridge infrastructure, application of separate, reduced tracked DLA values would see strategic mobility increases for tracked vehicles;

6. Rough bridge surfaces have a notable effect on increasing dynamic effects within a bridge; the dynamic loading effects of the tracked military vehicles associated with a rough deck surface are less than wheeled vehicles; and

7. Additional research should be conducted to support the recommendation for reduced DLA values for tracked vehicles; use of other vehicle chassis and variants on different bridge types should be included to expand the breadth of data available.

4.8 Data Availability Statement

Some or all data, models, or code generated or used during the study are available in a repository or online in accordance with funder data retention policies. For additional information, see B. Pinkney, “Experimental Data for Assessment of a Modular Truss Bridge.” Harvard Dataverse, 2020, doi: 10.7910/DVN/APACSE.

4.9 Acknowledgements

This research would not have been possible without the funding provided by the Department of National Defence, and specific cooperation and support from multiple Canadian Armed Forces establishments: Director Combat Support Equipment Management, 1 Combat Engineer Regiment, Lord Strathcona's Horse (Royal Canadians), and Real Property Operations Detachment Wainwright.

4.10 References

[2] CSA Group, *Canadian Highway Bridge Design Code*. CSA Group, 2014.

[3] H. Hawk and A. Ghali, "Dynamic response of bridges to multiple truck loading," *Can. J. Civ. Eng.*, vol. 8, no. 3, pp. 392–401, Sep. 1981.

[4] CSA Group, *Commentary on CAN/CSA S6-14, Canadian Highway Bridge Design Code*. Mississauga: CSA Group, 2014.

[5] North Atlantic Treaty Organization, *AEP-3.12.1.5 Military Load Classification of Bridges, Ferries, Rafts and Vehicles*, Ed. A, V1. NATO Standardization Office, 2017.

[6] Department of National Defence, *B-GL-361-014/FP-001 Manual for Military Nonstandard Fixed Bridges*. Ottawa, 2007.

[7] US Department of the Army, *FM 3-34.343 Military Nonstandard Fixed Bridging*. Washington, DC, 2002.

[10] P. F. Csagoly and R. A. Dorton, "The Development of the Ontario Highway Bridge Design Code," in *Transportation Research Record*, 1978, vol. 2, no. 655, pp. 1–12.

[12] P. Paultre, J. Proulx, and M. Talbot, "Dynamic Testing Procedures for Highway Bridges Using Traffic Loads," *J. Struct. Eng.*, vol. 121, no. 2, pp. 362–376, 1995.

[13] J. W. Wekezer, P. Szurgott, L. Kwasniewski, and E. Taft, "Dynamic response of reinforced concrete bridges due to heavy vehicles," *Adv. Transp. Stud.*, vol. 28, no. 28, pp. 35–50, 2012.

[14] B. Bakht and S. G. Pinjarkar, "Dynamic Testing of Highway Bridges - A Review," *Transp. Res. Rec.*, no. 1223, pp. 93–100, 1989.

[15] M. A. Grubb, K. E. Wilson, C. D. White, and W. N. Nickas, *Load and Resistance Factor Design (LRFD) for Highway Bridge Superstructures - Reference Manual*. US Department of Transportation, 2015.

[16] P. Paultre, O. Chaallal, and J. Proulx, "Bridge dynamics and dynamic amplification factors - a review of analytical and experimental findings," *Can. J. Civ. Eng.*, vol. 19, no. 2, pp. 260–278, 1992.

[17] Y. Zhou, Z. J. Ma, Y. Zhao, X. Shi, and S. He, "Improved definition of dynamic load allowance factor for highway bridges," *Struct. Eng. Mech.*, vol. 54, no. 3, pp. 561–577, 2015.

[18] R. Cantieni, "Dynamic load tests on highway bridges in Switzerland - 60 years of experience of EMPA," 1983.

[20] American Association of State Highway and Transportation Officials, *Standard Specifications for Highway Bridges*, Eleventh E. 1973.

[21] L. Deng, Y. Yu, Q. Zou, and C. S. Cai, "State-of-the-Art Review of Dynamic Impact Factors of Highway Bridges," *J. Bridg. Eng.*, vol. 20, no. 5, pp. 1–14, 2014.

[22] New Zealand Transportation Agency, *Bridge manual (SP/M/022)*, Third Ed. 2018.

[24] J. R. Billings and R. Green, "Design Provisions for Dynamic Loading of Highway Bridges," *Second Bridg. Eng. Conf.*, vol. 1, no. 950, pp. 94–103, 1984.

[25] Q. Gao, Z. Wang, C. G. Koh, and C. Chen, "Dynamic load allowances corresponding to different responses in various sections of highway bridges to moving vehicular loads," *Adv. Struct. Eng.*, vol. 18, no. 10, pp. 1685–1701, 2015.

[27] E. S. Hwang and A. S. Nowak, "Dynamic analysis of girder bridges," *Transp. Res. Rec.*, vol. 4, no. 1223, pp. 85–92, 1989.

[28] R. A. Imbsen, W. D. Lui, R. A. Schamber, and R. V. Nutt, "Strength evaluation of existing reinforced concrete structures," 1987.

[29] S. S. Law and X. Q. Zhu, "Bridge dynamic responses due to road surface roughness and braking of vehicle," *J. Sound Vib.*, vol. 282, no. 3–5, pp. 805–830, 2005.

[31] J. R. Billing, "Dynamic loading and testing of bridges in Ontario," *Can. J. Civ. Eng.*, vol. 11, no. 4, pp. 833–843, 1984.

[33] M. F. Green and D. Cebon, "Dynamic tests on two highway bridges," in *Proceedings of the Third International Symposium on Heavy Vehicle Weights and Dimensions*, 1992, pp. 1–8.

[35] K. Samanipour and H. Vafai, "Effect of boundary conditions on dynamic behaviour of bridges," *Proc. Inst. Civ. Eng. - Struct. Build.*, vol. 169, no. 2, pp. 121–140, 2016.

[36] R. Green, "Dynamic response of bridge superstructures - Ontario observations," 1977.

[40] M. F. Green, "Discussion: Bridge dynamics and dynamic amplification factors - a review of analytical and experimental findings," *Can. J. Civ. Eng.*, vol. 20, no. 5, pp. 876–877, 1993.

[41] J. R. Billing and A. C. Agarwal, "The Art and Science of Dynamic Testing of Highway Bridges," in *Developments in Short and Medium Span Bridge Engineering*, 1990, pp. 531–544.

[42] R. Cantieni, “Dynamic Behaviour of Highway Bridges Under the Passage of Heavy Vehicles,” *EMPA Report No. 220*, Dübendorf, p. 249, 1992.

[43] B. Bakht and R. A. Dorton, “The Ontario Bridge Code: Second Edition,” in *Second Bridge Engineering Conference*, 1984, vol. 1, pp. 88–93.

[44] D. K. Kirkcaldie and J. H. Wood, “Review of Australian standard AS5100 Bridge design with a view to adoption,” 2008.

[52] A. J. Macdonald, “Applying Probabilistic Methods to the NATO Military Load Classification System for Bridges,” The University of Western Ontario, 2014.

[53] Bundesministerium für Verkehr Bau und Stadtentwicklung Abteilung Straßenbau, “Hinweise zur Anwendung des Eurocode 1, Teil 2: „Verkehrslasten auf Brücken“ sowie zu den Teilen 1-1 und 1-3 bis 1-7,” 2012.

[54] B. Bakht and P. F. Csagoly, “Bridge Testing,” Downsview, Ontario, 1979.

[56] J. Arpin-Pont, M. Gagnon, A. S. Tahan, A. Coutu, and D. Thibault, “Methodology for estimating strain gauge measurement biases and uncertainties on isotropic materials,” *J. Strain Anal. Eng. Des.*, vol. 50, no. 1, pp. 40–50, Jan. 2015.

[57] J. Pople, “Errors and Uncertainties in Strain Measurement,” in *Strain Gauge Technology*, A. L. Window and G. Holister, Eds. New York: Elsevier Science Publishing, 1989, pp. 209–264.

[60] I. Paeglite and A. Paeglitis, “The dynamic amplification factor of the bridges in Latvia,” *Procedia Eng.*, vol. 57, pp. 851–858, 2013.

[61] FFG Canada, *Operator Training: WISENT 2 AEV CAN*. 2016.

[62] FFG Canada, *Operating Manual for Training AEV WISENT 2 CAN*. 2016.

[63] Department of National Defence, *C-30-B66-000/MA-000 Specific Data Summary Wisent 2 AEV Can*. 2018.

[64] Department of National Defence, *TM 2350/089-10 Leopard 2 Technical Manual*. 2007.

[65] B. Pinkney, “Experimental Data for Assessment of a Modular Truss Bridge.” Harvard Dataverse, 2020.

[66] Joint Committee For Guides In Metrology, *Evaluation of measurement data - Guide to the expression of uncertainty in measurement JCGM 100:2008*, First Ed. 2008.

[67] B. Carter, “Filters for Data Transmission,” 2001.

[68] Department of National Defence, *B-GL-361-014/FP-001 Manual for Military Nonstandard Fixed Bridges (Draft)*. 2019.

CHAPTER 5 CONCLUSIONS AND RECOMMENDATIONS

5.1 General

This research focussed on confirming the difference in dynamic loading effects of tracked and wheeled vehicles and determining separate DLA values for each vehicle type. The effects of speed and surface condition variation on dynamic bridge response were investigated through the conduct of a comprehensive field-testing programme.

This plan saw the crossing of four different vehicles across an ACROW modular pony truss bridge during eighty-six independent iterations, with each test gathering strain and displacement data from the bridge at a sample rate of 1200 Hz over thirty-nine channels. Both static and quasi-static tests were conducted to quantify static bridge response, which was then compared with dynamic vehicle crossing effects to determine appropriate DLA values for the vehicles used. Testing speeds were controlled in all cases, and ranged from 10 km/h to 50 km/h in 10 km/h increments. Introduction of wooden boards on the deck surface simulated rough deck conditions, and the associated dynamic bridge responses were compared with smooth-surface effects. Vehicles used for testing included the Leopard 2 AEV and the Leopard 2 MBT, both of which are tracked vehicles, and the MSVS LHS variant and TAPV wheeled vehicles.

The comparison of dynamic effects due to vehicle loading on a smooth deck surface was made with the intent of determining if reduced factors should be applied to tracked vehicles to account for the differences in dynamic loading between tracked and wheeled vehicle types. Application of separate DLA values for these vehicle categories, in concert with the use of appropriate live load factors, has the potential to increase tracked vehicle mobility on existing bridge infrastructure at a strategic scale.

5.2 Conclusions

Analysis of experimental strain results indicated clear dynamic loading effects. A simple numerical model was created and validated using collected data, with the aim of facilitating future load effect analysis. Accounting for sources of error within the monitoring system used to gather data, DLA values were determined for each of the four vehicles used in the established testing programme, as well as for the tracked and wheeled vehicle categories. These values were compared with bridge codes from multiple nations, in addition to various military bridge manuals, resulting in a validation of the calculated values. Key results from this research are summarized as follows:

1. Tracked vehicles generate significantly reduced dynamic effects compared to wheeled vehicles. Application of a DLA value for tracked vehicles that is independent and reduced from the value used for wheeled vehicles should be considered where appropriate to account for this difference;

2. While recent versions of NATO AEP-3.12.1.5 (STANAG 2021) do not indicate precise values of DLA to be used by member military forces, it may be suitable to indicate that the DLA values used for tracked vehicles could be set as low as half the value of the DLA given in national codes for wheeled vehicles;

3. Appropriate values of DLA for application in Canadian and American military bridge guides could be 0.09 for tracked vehicles, and 0.18 for wheeled vehicles;

4. In the context of Canadian and American national bridge codes, a suitable DLA used for tracked vehicle traffic could be 0.07 for bridge components excluding deck joints;

5. Considering the bridging infrastructure currently in place globally, application of a distinct tracked vehicle DLA value would see mobility increases for these vehicles at a strategic scale; and

6. Degraded deck conditions significantly increase the dynamic response of bridges to loading. The dynamic loading effects created by tracked military vehicles are less than those caused by wheeled military vehicles.

5.3 Recommendations

Based on the research conducted, recommendations are made to further the knowledge base related to dynamic effects of military vehicles on bridges. These include the following:

1. Supplementary research should be performed to support the findings related to use of a reduced DLA value for tracked vehicles compared to the DLA value used for wheeled vehicles. Future testing should focus on the application of other vehicle variants and chassis loads on alternate bridge types to increase the extent of existing information on the subject of military vehicle dynamic effects on bridges;

2. Generation of more accurate models should be made to allow for the determination of load effects caused by a multitude of other vehicles that may not be available at the time of experimental testing;

3. Additional research should be completed to determine live load factor values that are more applicable to tracked and wheeled military vehicle loading; it is expected that these factors, in conjunction with DLA values applicable to each vehicle type, would have notable impact on the total assessed loads on bridges, which in particular could see further notable increases in military tracked vehicle mobility; and

4. Further examination of bridge deck condition on dynamic vehicle loading should be made, through analysis of effects caused by alternate degradation sources such as potholes or gaps in the decking, or the application of common obstacles expected in military operations.

CHAPTER 6 REFERENCES

[1] Statistics Canada, "Canada's Core Public Infrastructure Survey: Roads, bridges and tunnels, 2016," 2018.

[2] CSA Group, *Canadian Highway Bridge Design Code*. CSA Group, 2014.

[3] H. Hawk and A. Ghali, "Dynamic response of bridges to multiple truck loading," *Can. J. Civ. Eng.*, vol. 8, no. 3, pp. 392–401, Sep. 1981.

[4] CSA Group, *Commentary on CAN/CSA S6-14, Canadian Highway Bridge Design Code*. CSA Group, 2014.

[5] North Atlantic Treaty Organization, *AEP-3.12.1.5 Military Load Classification of Bridges, Ferries, Rafts and Vehicles*, Ed. A, V1. NATO Standardization Office, 2017.

[6] Department of National Defence, *B-GL-361-014/FP-001 Manual for Military Nonstandard Fixed Bridges*. 2007.

[7] US Department of the Army, *FM 3-34.343 Military Nonstandard Fixed Bridging*. Washington, DC, 2002.

[8] A. Everitt, "Dynamic Load Effects of Tracked and Wheeled Military Vehicles From Bridge Load Testing," Royal Military College of Canada, 2019.

[9] Royal Military College of Canada, *Thesis Preparation Guidelines*. Kingston, 2015.

[10] P. F. Csagoly and R. A. Dorton, "The Development of the Ontario Highway Bridge Design Code," in *Transportation Research Record*, 1978, vol. 2, no. 655, pp. 1–12.

[11] D. E. Allen, "Canadian highway bridge evaluation: reliability index," *Can. J. Civ. Eng.*, vol. 19, pp. 987–991, 1992.

[12] P. Paultre, J. Proulx, and M. Talbot, "Dynamic Testing Procedures for Highway Bridges Using Traffic Loads," *J. Struct. Eng.*, vol. 121, no. 2, pp. 362–376, 1995.

[13] J. W. Wekezer, P. Szurgott, L. Kwasniewski, and E. Taft, "Dynamic response of reinforced concrete bridges due to heavy vehicles," *Adv. Transp. Stud.*, vol. 28, no. 28, pp. 35–50, 2012.

[14] B. Bakht and S. G. Pinjarkar, "Dynamic Testing of Highway Bridges - A Review," *Transp. Res. Rec.*, no. 1223, pp. 93–100, 1989.

[15] M. A. Grubb, K. E. Wilson, C. D. White, and W. N. Nickas, *Load and Resistance Factor Design (LRFD) for Highway Bridge Superstructures - Reference Manual*. US Department of Transportation, 2015.

[16] P. Paultre, O. Chaallal, and J. Proulx, “Bridge dynamics and dynamic amplification factors - a review of analytical and experimental findings,” *Can. J. Civ. Eng.*, vol. 19, no. 2, pp. 260–278, 1992.

[17] Y. Zhou, Z. J. Ma, Y. Zhao, X. Shi, and S. He, “Improved definition of dynamic load allowance factor for highway bridges,” *Struct. Eng. Mech.*, vol. 54, no. 3, pp. 561–577, 2015.

[18] R. Cantieni, “Dynamic load tests on highway bridges in Switzerland - 60 years of experience of EMPA,” 1983.

[19] European Committee for Standardization, *Eurocode 1: Actions on structures - Part 2: Traffic loads on bridges*. Brussels, 2003.

[20] American Association of State Highway and Transportation Officials, *Standard Specifications for Highway Bridges*, Eleventh E. 1973.

[21] L. Deng, Y. Yu, Q. Zou, and C. S. Cai, “State-of-the-Art Review of Dynamic Impact Factors of Highway Bridges,” *J. Bridg. Eng.*, vol. 20, no. 5, pp. 1–14, 2014.

[22] New Zealand Transportation Agency, *Bridge manual (SP/M/022)*, Third Ed. 2018.

[23] M. F. Green and D. Cebon, “Dynamic Response of Highway Bridges to Heavy Vehicle Loads: Theory and Experimental Validation,” *J. Sound Vib.*, vol. 170, no. 1, pp. 51–78, Feb. 1994.

[24] J. R. Billings and R. Green, “Design Provisions for Dynamic Loading of Highway Bridges,” *Second Bridg. Eng. Conf.*, vol. 1, no. 950, pp. 94–103, 1984.

[25] Q. Gao, Z. Wang, C. G. Koh, and C. Chen, “Dynamic load allowances corresponding to different responses in various sections of highway bridges to moving vehicular loads,” *Adv. Struct. Eng.*, vol. 18, no. 10, pp. 1685–1701, 2015.

[26] M. Paz and Y. H. Kim, *Structural Dynamics*, Sixth Ed. Cham: Springer International Publishing, 2019.

[27] E. S. Hwang and A. S. Nowak, “Dynamic analysis of girder bridges,” *Transp. Res. Rec.*, vol. 4, no. 1223, pp. 85–92, 1989.

[28] R. A. Imbsen, W. D. Lui, R. A. Schamber, and R. V. Nutt, “Strength evaluation of existing reinforced concrete structures,” 1987.

[29] S. S. Law and X. Q. Zhu, “Bridge dynamic responses due to road surface roughness and braking of vehicle,” *J. Sound Vib.*, vol. 282, no. 3–5, pp. 805–830, 2005.

[30] J. Page, “Dynamic wheel load measurements on motorway bridges,” 1976.

[31] J. R. Billing, “Dynamic loading and testing of bridges in Ontario,” *Can. J. Civ. Eng.*, vol. 11, no. 4, pp. 833–843, 1984.

[32] M. F. Green, D. Cebon, and D. J. Cole, “Effects of vehicle suspension design on dynamics of highway bridges,” *J. Struct. Eng.*, vol. 121, no. 2, pp. 272–282, 1995.

[33] M. F. Green and D. Cebon, “Dynamic tests on two highway bridges,” in *Proceedings of the Third International Symposium on Heavy Vehicle Weights and Dimensions*, 1992, pp. 1–8.

[34] M. F. Green and D. Cebon, “Dynamic interaction between heavy vehicles and highway bridges,” *Comput. Struct.*, vol. 62, no. 2, pp. 253–264, 1997.

[35] K. Samanipour and H. Vafai, “Effect of boundary conditions on dynamic behaviour of bridges,” *Proc. Inst. Civ. Eng. - Struct. Build.*, vol. 169, no. 2, pp. 121–140, 2016.

[36] R. Green, “Dynamic response of bridge superstructures - Ontario observations,” 1977.

[37] O. Mohammed, A. González, and D. Cantero, “Dynamic impact of heavy long vehicles with equally spaced axles on short-span highway bridges,” *Balt. J. Road Bridg. Eng.*, vol. 13, no. 1, pp. 1–13, 2018.

[38] G. P. Tilly, “Damping of Highway Bridges: A Review,” 1977.

[39] R. Shepherd and R. Aves, “Impact factors for simple concrete bridges,” *Proc. Inst. Civ. Eng.*, vol. 55, no. 1, pp. 191–210, Mar. 1973.

[40] M. F. Green, “Discussion: Bridge dynamics and dynamic amplification factors - a review of analytical and experimental findings,” *Can. J. Civ. Eng.*, vol. 20, no. 5, pp. 876–877, 1993.

[41] J. R. Billing and A. C. Agarwal, “The Art and Science of Dynamic Testing of Highway Bridges,” in *Developments in Short and Medium Span Bridge Engineering*, 1990, pp. 531–544.

[42] R. Cantieni, “Dynamic Behaviour of Highway Bridges Under the Passage of Heavy Vehicles,” *EMPA Report No. 220*, Dübendorf, p. 249, 1992.

[43] B. Bakht and R. A. Dorton, “The Ontario Bridge Code: Second Edition,” in *Second Bridge Engineering Conference*, 1984, vol. 1, pp. 88–93.

[44] D. K. Kirkcaldie and J. H. Wood, “Review of Australian standard AS5100 Bridge design with a view to adoption,” 2008.

[45] Steel and Concrete Bridges Standards Committee, *BS 5400-2 Steel, concrete and composite bridges - Part 2: Specification for loads*. London: British Standards Institute, 1978.

[46] B. J. Sia, E. Townsend, and A. Rudow, *Trilateral Design And Test Code Gap-Crossing Equipment*. 2019.

[47] R. Lenner, “Safety Concept and Partial Factors for Military Assessment of Existing Concrete Bridges,” Universität der Bundeswehr München, 2014.

[48] R. Tanovic, S. Penstone, J. O'Reilly, and G. Wight, "MLC Suite Launcher." Royal Military College of Canada (Department of National Defence), 2020.

[49] R. Tanovic, S. Penstone, J. O'Reilly, and G. Wight, "Correlation Vehicle Military Load Classification (CORVMLC)." Royal Military College of Canada (Department of National Defence), 2020.

[50] R. Tanovic, S. Penstone, J. O'Reilly, and G. Wight, "Rapid Field Bridge Military Load Classification (RFBMLC)." Royal Military College of Canada (Department of National Defence), 2020.

[51] R. Tanovic, S. Penstone, J. O'Reilly, and G. Wight, "Canadian Bridge Military Load Classification (CABMLC)." Royal Military College of Canada (Department of National Defence), 2020.

[52] A. J. Macdonald, "Applying Probabilistic Methods to the NATO Military Load Classification System for Bridges," The University of Western Ontario, 2014.

[53] Bundesministerium für Verkehr Bau und Stadtentwicklung Abteilung Straßenbau, "Hinweise zur Anwendung des Eurocode 1, Teil 2: „Verkehrslasten auf Brücken" sowie zu den Teilen 1-1 und 1-3 bis 1-7," 2012.

[54] B. Bakht and P. F. Csagoly, "Bridge Testing," Downsview, Ontario, 1979.

[55] O. S. Salawu and C. Williams, "Review of full-scale dynamic testing of bridge structures," *Eng. Struct.*, vol. 17, no. 2, pp. 113–121, 1995.

[56] J. Arpin-Pont, M. Gagnon, A. S. Tahan, A. Coutu, and D. Thibault, "Methodology for estimating strain gauge measurement biases and uncertainties on isotropic materials," *J. Strain Anal. Eng. Des.*, vol. 50, no. 1, pp. 40–50, Jan. 2015.

[57] J. Pople, "Errors and Uncertainties in Strain Measurement," in *Strain Gauge Technology*, A. L. Window and G. Holister, Eds. New York: Elsevier Science Publishing, 1989, pp. 209–264.

[58] H. K. P. Neubert, *Strain Gauges: Kinds and Uses*. Toronto: MacMillan & Co., 1967.

[59] WSP Group, "L-W5-0707-601 Battle Bridge Upgrade." Government of Canada, Edmonton, 2017.

[60] I. Paeglite and A. Paeglitis, "The dynamic amplification factor of the bridges in Latvia," *Procedia Eng.*, vol. 57, pp. 851–858, 2013.

[61] FFG Canada, *Operator Training: WISENT 2 AEV CAN*. 2016.

[62] FFG Canada, *Operating Manual for Training AEV WISENT 2 CAN*. 2016.

[63] Department of National Defence, *C-30-B66-000/MA-000 Specific Data Summary Wisent 2 AEV Can*. 2018.

[64] Department of National Defence, *TM 2350/089-10 Leopard 2 Technical Manual*. 2007.

[65] B. Pinkney, “Experimental Data for Assessment of a Modular Truss Bridge.” Harvard Dataverse, 2020.

[66] Joint Committee For Guides In Metrology, *Evaluation of measurement data - Guide to the expression of uncertainty in measurement JCGM 100:2008*, First Ed. 2008.

[67] B. Carter, “Filters for Data Transmission,” 2001.

[68] Department of National Defence, *B-GL-361-014/FP-001 Manual for Military Nonstandard Fixed Bridges (Draft)*. 2019.

[69] T. Masters, *Neural, Novel & Hybrid Algorithms for Time Series Prediction*. Toronto: John Wiley & Sons, 1995.

[70] J. Sebek, “Elements of Passive Filter Design.” pp. 1–21, 2001.

[71] W. Montero, R. Farag, V. Díaz, M. Ramirez, and B. L. Boada, “Uncertainties Associated with Strain-Measuring Systems Using Resistance Strain Gauges,” *J. Strain Anal. Eng. Des.*, vol. 46, no. 1, pp. 1–13, Jan. 2011.

[72] S. G. Rabinovich, *Measurement Errors and Uncertainties: Theory and Practice*, Third Ed. Springer Science and Media, 2005.

[73] Kyowa Electronic Instruments Co., “Method of Obtaining Magnitude and Direction of Principal Stress (Rosette Analysis),” *Technical Memo*. [Online]. Available: https://www.kyowa-ei.com/eng/technical/notes/index.html. [Accessed: 03-Jan-2020].

[74] Micro-Measurements, “TN-515 Strain Gage Rosettes: Selection, Application and Data Reduction.” Vishay Precision Group.

[75] J. W. Dally and W. F. Riley, *Experimental Stress Analysis*, Third Ed. Toronto, 1991.

[76] Department of National Defence, *C-30-K80-000/MB-000 Truck, Load Handling System, 9.5 Ton, 8x8, MSVS SMP*. 2019.

[77] Department of National Defence, *C-30-B87-000/MB-001 Tactical Armoured Patrol Vehicle (TAPV), Wheeled, 4 x 4, Diesel*. 2016.

APPENDIX A CHARACTERISTICS OF MILITARY LOAD CLASSIFICATION HYPOTHETICAL VEHICLES

The following tables outline the physical characteristics that define the hypothetical vehicles of the MLC system. Both the hypothetical wheeled vehicles and their tracked vehicle equivalents are indicated. Where given, units are metric tonnes and metres.

Table A-1 - Hypothetical MLC vehicle characteristics [5]

MLC	Hypothetical Tracked Vehicle	Hypothetical Wheeled Vehicle					
		Axle load (t) and spacing (m)	Maximum single axle load (t)	Tire Load (t)	Tire Ground Contact Width (m)	Tire Ground Contact Length (m)	Wheel Spacing and Nominal Ground Contact Width (m)
4	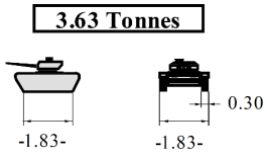	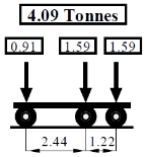	2.27	1.13	0.15	0.15	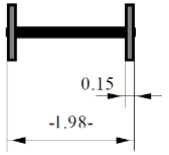
8	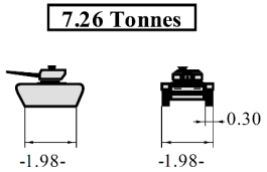	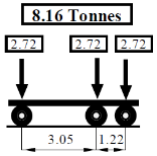	4.99	2.49	0.20	0.20	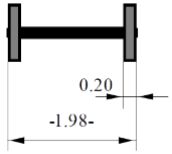
12	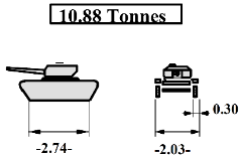	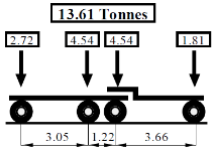	7.26	3.63	0.25	0.25	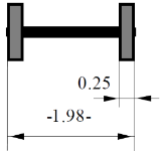
16	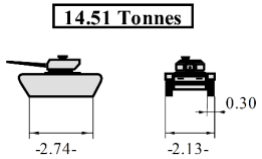	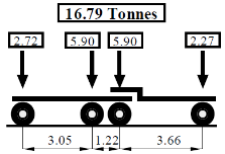	8.62	4.31	0.25	0.25	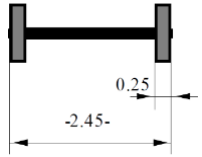

MLC	Hypothetical Tracked Vehicle	Hypothetical Wheeled Vehicle					
		Axle load (t) and spacing (m)	Maximum single axle load (t)	Tire Load (t)	Tire Ground Contact Width (m)	Tire Ground Contact Length (m)	Wheel Spacing and Nominal Ground Contact Width (m)
20	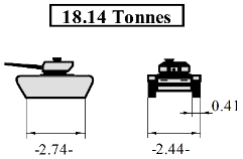	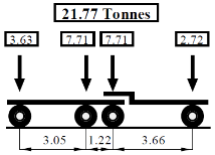	9.98	4.99	0.30	0.25	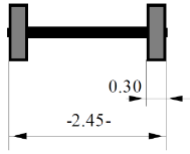
24	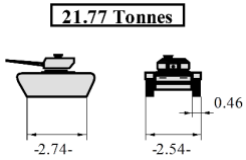	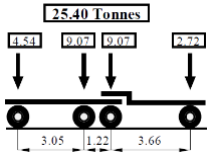	10.89	5.44	0.30	0.25	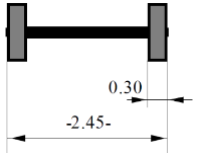
30	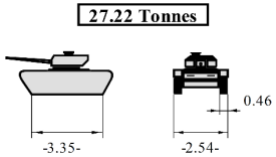	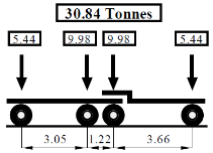	13.15	6.57	0.35	0.30	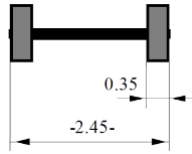
40	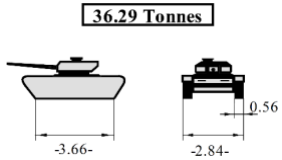	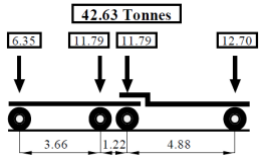	15.42	7.71	0.35	0.30	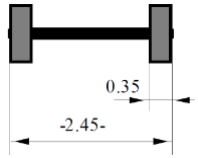
50	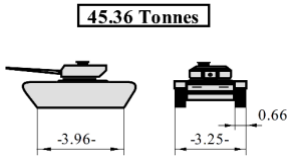	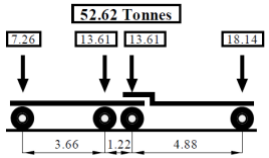	18.14	9.07	0.40	0.30	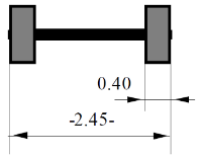

MLC	Hypothetical Tracked Vehicle	Hypothetical Wheeled Vehicle					
		Axle load (t) and spacing (m)	Maximum single axle load (t)	Tire Load (t)	Tire Ground Contact Width (m)	Tire Ground Contact Length (m)	Wheel Spacing and Nominal Ground Contact Width (m)
60	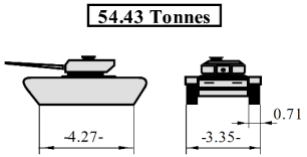	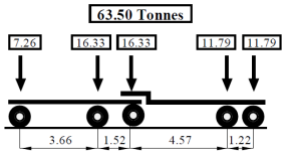	20.86	9.07	0.30	0.35	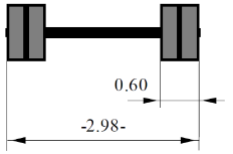
70	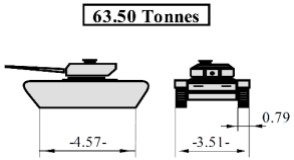	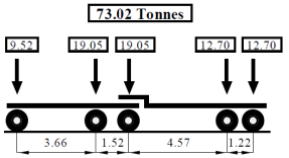	23.13	9.07	0.33	0.35	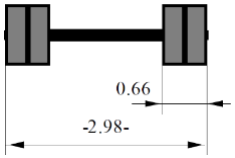
80	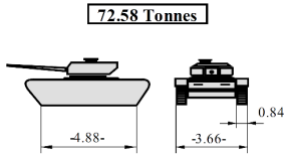	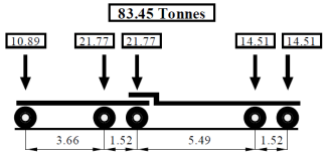	25.40	9.07	0.36	0.40	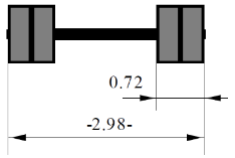
90	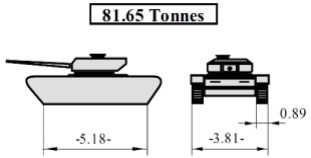	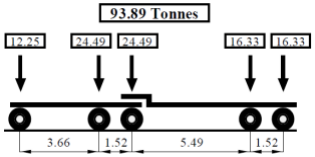	27.21	9.07	0.40	0.40	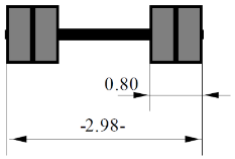
100	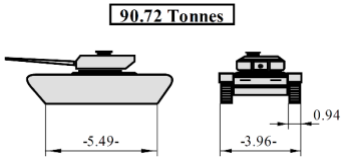	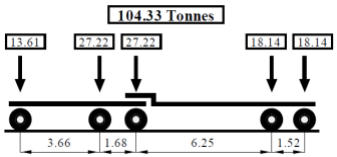	29.03	9.07	0.45	0.40	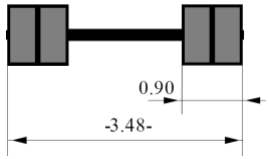

MLC	Hypothetical Tracked Vehicle	Hypothetical Wheeled Vehicle					
		Axle load (t) and spacing (m)	Maximum single axle load (t)	Tire Load (t)	Tire Ground Contact Width (m)	Tire Ground Contact Length (m)	Wheel Spacing and Nominal Ground Contact Width (m)
120	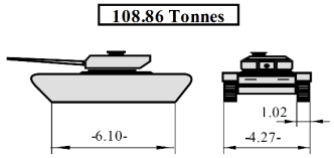	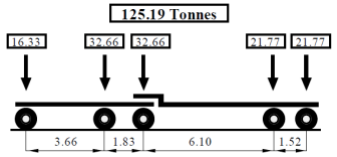	32.66	9.07	0.50	0.40	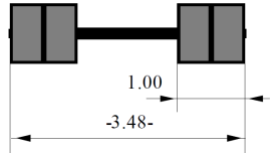
150	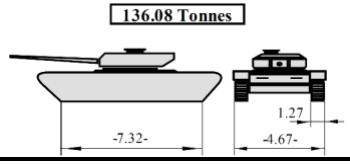	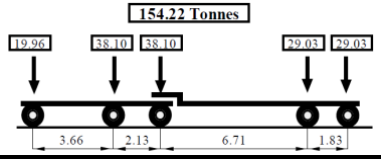	38.10	9.52	0.50	0.40	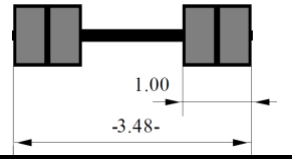

APPENDIX B STANDARD MILITARY LOAD CLASSIFICATION CURVES

The following figures outline bending moment and shear effects associated with indicated MLC classifications. This relationship allows personnel investigating bridges within the MLC system to quantify the live load capacity of an existing bridge for both tracked and wheeled military vehicles. It should be noted that no consideration is made for dynamic loading. Following tenets of the MLC system, vehicle spacing used to generate these graphs is the standard 30.5 m.

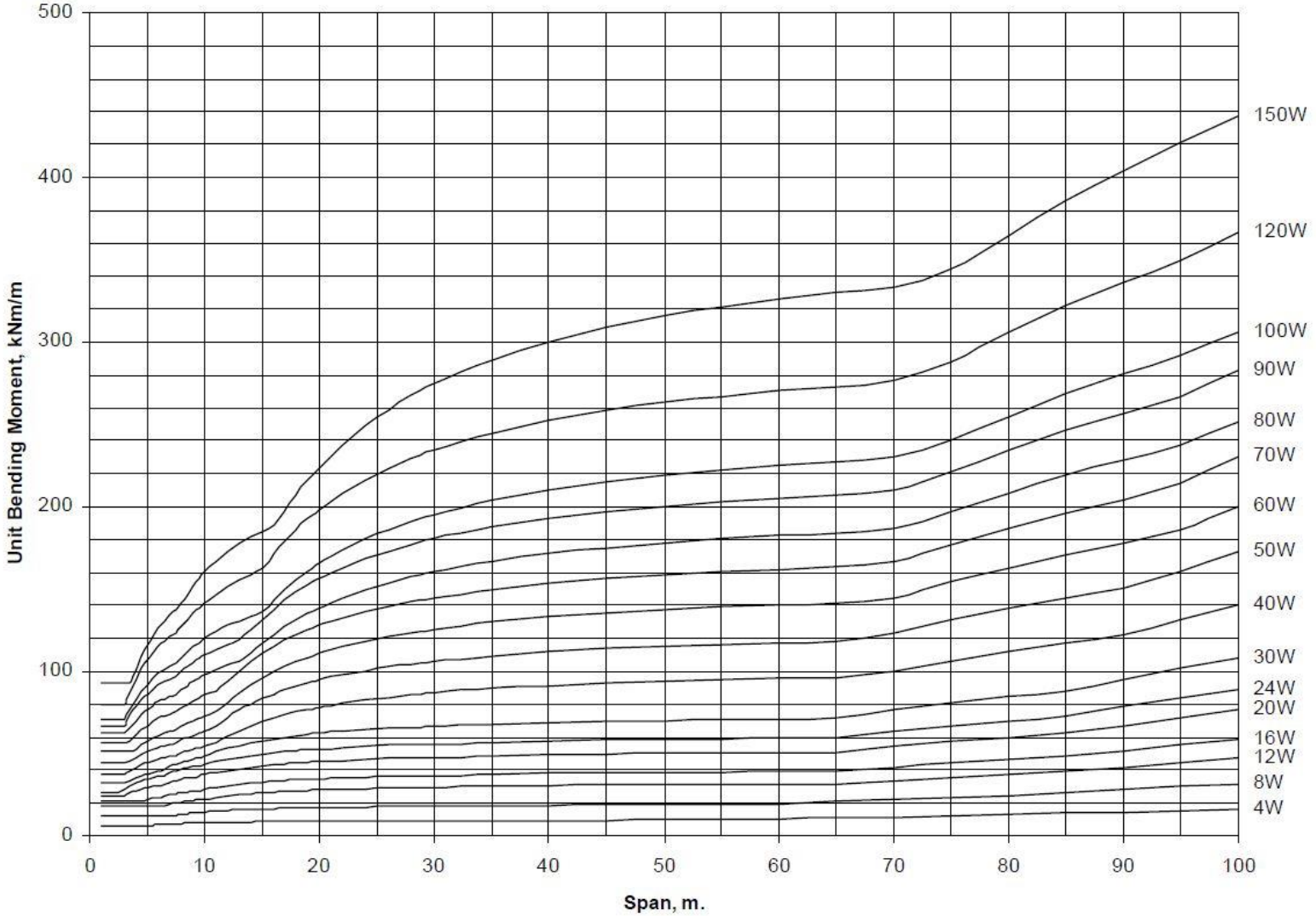

Figure B-1 - Unit bending moments due to theoretical wheeled vehicles for spans from 1 m to 100 m [6]

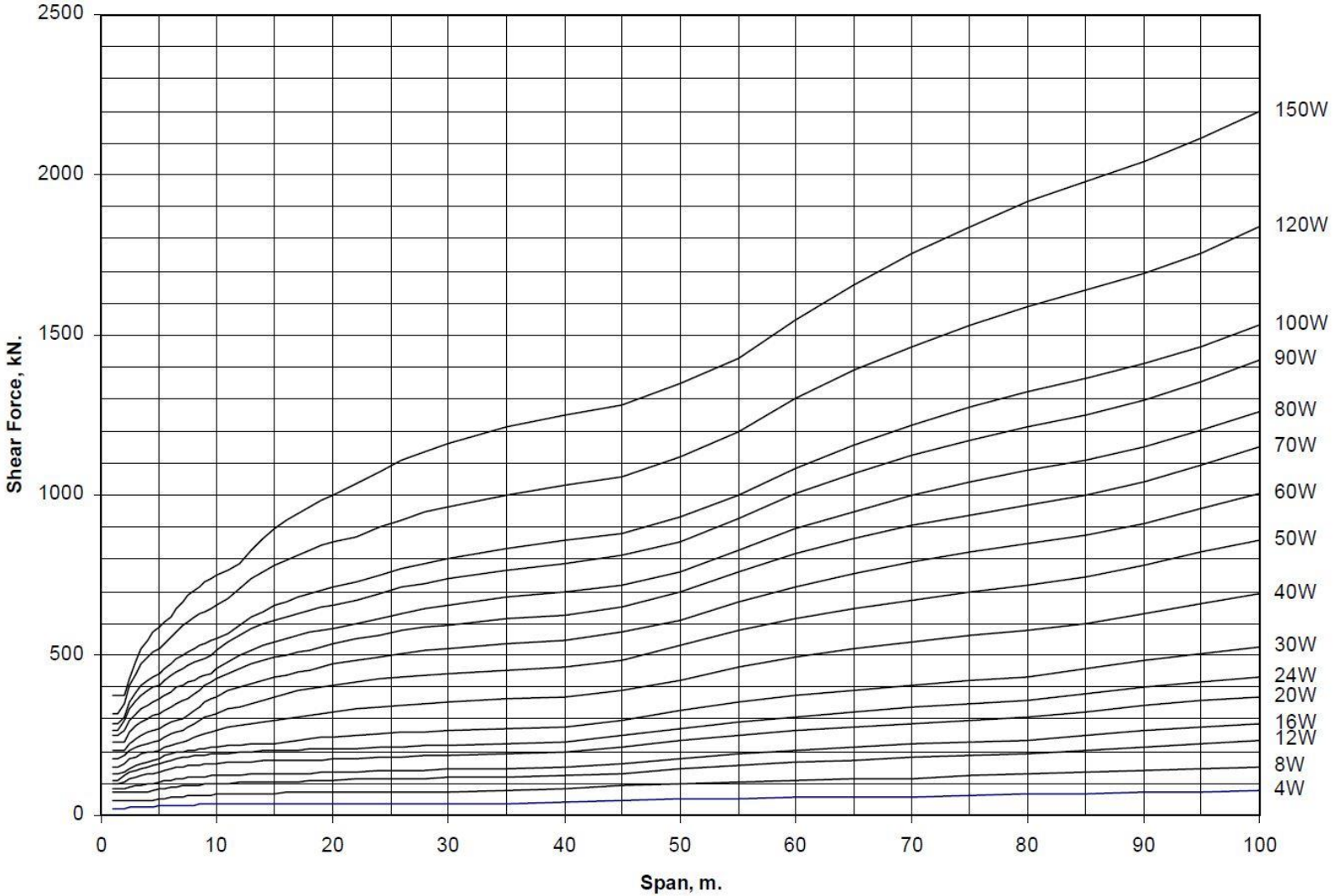

Figure B-2 - Shear due to theoretical wheeled vehicles for spans from 1 m to 100 m [6]

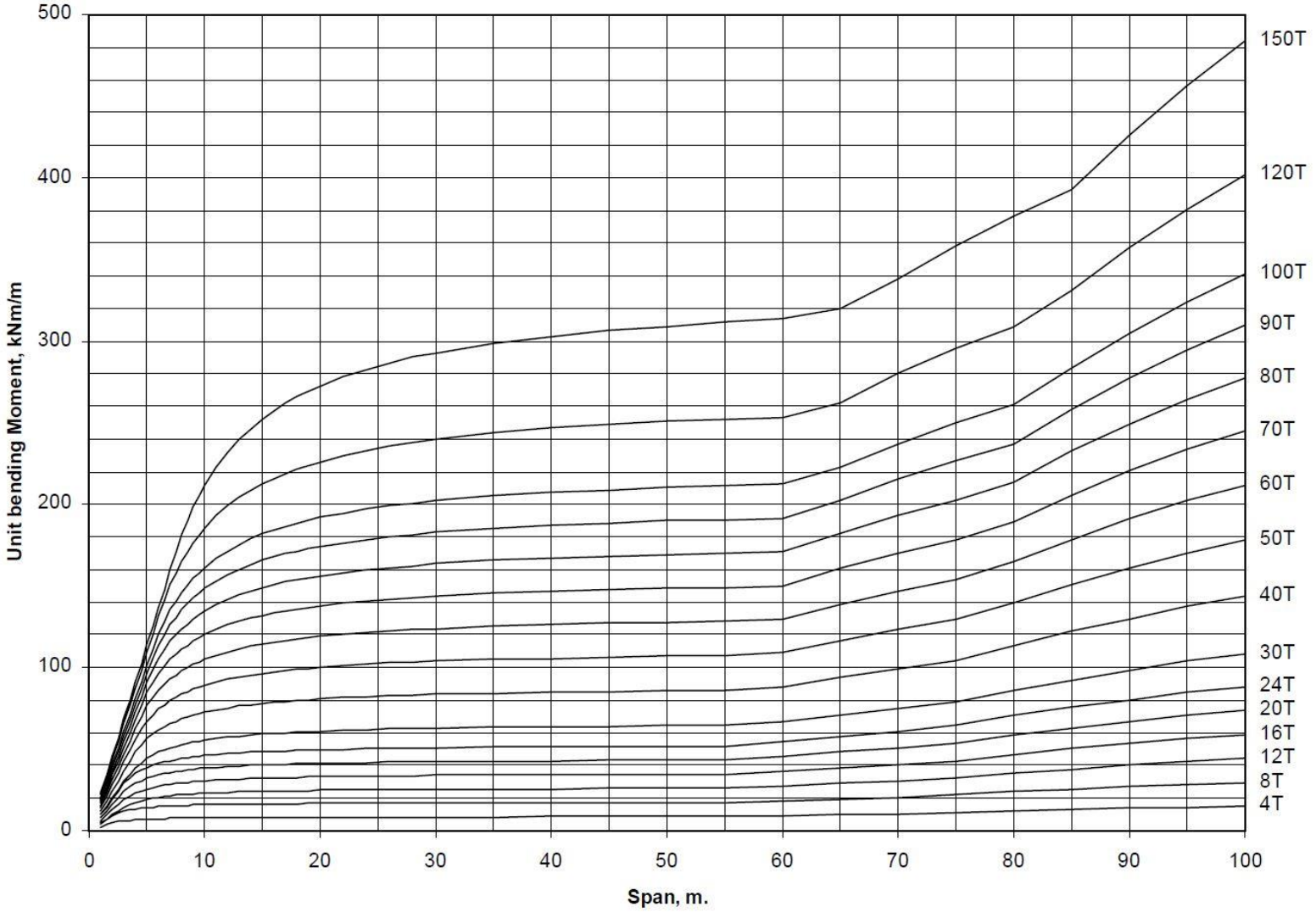

Figure B-3 - Unit bending moments due to theoretical tracked vehicles for spans from 1 m to 100 m [6]

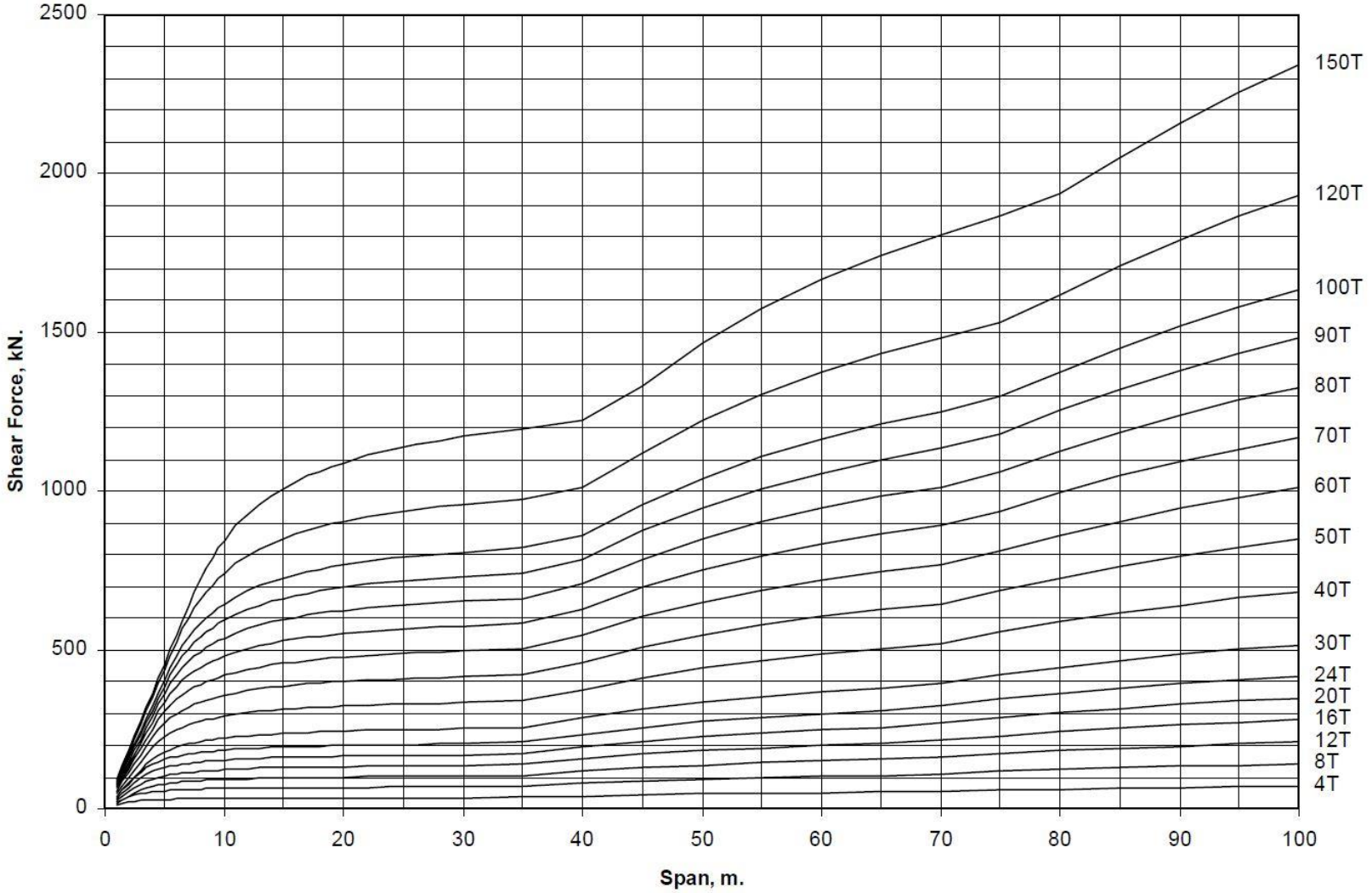

Figure B-4 - Shear due to theoretical wheeled vehicles for spans from 1 m to 100 m [6]

APPENDIX C DATA MANIPULATION

C.1 Data Filters

When analyzing experimental data generated through dynamic load testing, the static response can be estimated by filtering or modifying the median dynamic responses gathered through the instrumentation setup, by analyzing the high and low dynamic responses over the period being assessed [14]. This could be especially useful when analyzing quasi-static data, as perfect static responses are not likely to occur.

In the case of dynamic testing, data gathered will likely be comprised of a static and dynamic response. Differentiating the two is crucial to accurately apply the DA relationship given in Equation 2.15, especially if executed static testing contains any dynamic response influence (quasi-static testing). To this end, application of a low-pass filter is appropriate, which aims to remove rapid variation in data over a specified cut-off frequency caused by dynamic effects to leave only the smoother, slower variations that denote static response of the system [69].

When considering filtering a dataset, the application has significant impact on the type of filter chosen. Butterworth, Chebyshev, and Bessel are commonly used filters, each having their own advantages and disadvantages.

Butterworth filters pass signal pulses reasonably well and have a maximally flat origin; in the context of a low-pass filter, this allows for the passage of all data at the low end of the frequency spectrum. This type of filter can affect signals in either the time or frequency domain [70], but use in the time domain may affect group delay (delay of frequencies with respect to the fundamental frequency of the system) for harmonic signals [67].

Chebyshev low-pass filters also have non-constant group delay, but also have much sharper transition between the passband (the zone of the frequency within which frequencies are allowed to pass and are not stopped) and stopband (the zone of frequency within which frequencies are filtered out of the data) regions. Although there exists a distinct ripple in the passband, this sharper transition zone allows for more distinct differentiation between passed and filtered frequencies in the dataset. The sharper transition zone of a Chebyshev filter often imparts undesirable signal response if used in the time domain.

If preservation of time domain characteristics is desired for analysis, use of a Bessel filter may be appropriate. With this preservation of signal comes a reduction in the rate of attenuation of the signal, increasing the size of the filter's transition zone [70]. Of the list presented here, Bessel responses are the only ones that experience constant group delay response, making this the preferred option if time domain analysis is required [67].

C.2 Error and Uncertainty

When considering data gathered during experimental testing, failure to account for errors inherent in measurement procedures and materials will have negative impact on the accuracy and validity of results. Therefore, it is prudent to understand how error and uncertainty influence experimental testing and the subsequent results, which will be given in the context of an experimental testing procedure applying strain gauges as the main data gathering instrument.

To begin, an understanding of term definitions is appropriate. When conducting testing aimed at collecting data, there is a quantity that is intended to be measured; this is defined as the measurand. Often the measurand is a quantity that is not measured directly, but calculated based on the magnitudes of other readings which are possible [71]. The actual value of the measurand cannot be known, due to inherent imperfections and subsequent errors in the data capture processes [66], [71], [72]. Error, defined as the difference between a true value and a measured value [56], [57], comprises all components that make up a stated uncertainty [72]. To that end, uncertainty can be defined as a value range within which a true value could reasonably be expected to lie [56], [57], [66]. The true value is a corrected measurement that is the best estimate of the measurand [66].

When following the flow of information through an experimental data acquisition setup, there are multiple opportunities for error to be introduced into the system. Additionally, certain measurands are not appraised directly, but calculated based on measurements of other parameters. Therefore, combining uncertainties due to various sources of error is required [71]. Listing individual error quantities when presenting a single result is not a useful nor practical approach to take to indicate the global uncertainty associated with the result itself. An approach such as the law of propagation of uncertainties can be followed to generate a value of uncertainty for an entire measuring system, as given in Equation C.1 [66]:

$$u^2(y) = \sum_{i=1}^{N} \left(\frac{\partial f}{\partial x_i}\right)^2 u^2(x_i) + 2 \sum_{i=1}^{N-1} \sum_{j=i+1}^{N} \frac{\partial f}{\partial x_i} \frac{\partial f}{\partial x_j} u(x_i, x_j) \qquad \text{C.1}$$

where $u(y)$ is the combined uncertainty of the measurement y;
y, the measured result, is a function of the input variables such that $y = f(x_1, x_2, \dots, x_n)$;
$u(x_i)$ is the standard uncertainty for an input variable;
x_i is an input variable;
x_j is an input variable correlated to input variable x_i;
$u(x_i, x_j)$ is the covariance of x_i and x_j; and
N is the number of input variables.

For systems where the input variables are independent, and therefore not correlated, the equation for system uncertainty can be simplified, as outlined in Equation C.2 [66]:

$$u^2(y) = \sum_{i=1}^{N} \left(\frac{\partial f}{\partial x_i}\right)^2 u^2(x_i) \quad \text{C.2}$$

Continuing with the strain gauge-instrumented setup context, identification of the sources of error is now required. Broadly speaking, error can originate within the instrument itself, in the method used to collect the data, the environment, and, most importantly, the user themselves [56], [57].

Location errors deal mostly with the physical installation of the gauge itself. Positioning error is caused by installation of the gauge in a manner in which the centre of the gauge is not the same as the target location. Alignment errors are the result of installation of the gauge with the primary sensing axis being at an angle to the intended target axis [56]. Control over humidity is also key, both during installation as well as throughout the testing programme, as corrosion from moisture infiltration may impact or completely eliminate otherwise viable results [56], [58].

Errors associated with the gauge that are outside of the control of the user are important to consider. Depending on the application of the strain gauge, integration error, or the averaging effect of the strain field underneath the strain gauge grid, may result in a user modifying the instrument selected to provide better spatial result resolution [56]. Simply due to the two-dimensional layout of the sensing grid, transverse sensitivity of a strain gauge may also impact results. The effect of transverse strain readings is significantly more important when that reading is larger than the strain reading in the longitudinal direction of the gauge grid. For cases such as this, it is prudent to utilize bi-axial gauges or a rosette setup. It is not possible to determine the effect of transverse sensitivity on a desired reading if only one uniaxial strain gauge is used [56], [58]. Typically, the gauge factor specified by the manufacturer will take transverse strain effects into account, but the responsibility falls to the end user to ensure the conditions under which the strain gauge is being used is similar to those the manufacturer applied to determine the value of this factor [71].

Temperature plays a significant role in introducing error to an experimental testing programme relying on strain gauge instrumentation [41]. Since thermal variation can produce changes in the sensitivity of a strain gauge of the similar magnitude to strain-induced readings, data could easily become corrupt and of no use [58]. Since material properties change with temperature, consideration must be made to ensure these effects are minimized or counteracted completely. There are a variety of ways this can be accomplished. For example, use of a dummy gauge to isolate the effects of temperature on the system would enable a user to remove these effects from gauges installed on surfaces being tested, or, if appropriate to the type of testing being completed, zero balancing could be completed through the data acquisition system prior to conducting testing iterations to eliminate the effects of thermal fluctuations on the instrumented material [58], [71].

It should be noted that gauge factor mentioned previously is also influenced by temperature. In cases where temperature variation is small, this error is usually of a magnitude that it can be

neglected. Manufacturers often provide gauge factor compensation information for applications where thermal variation may be an issue [71].

If multiple iterations of testing are to be completed, or the testing is to be completed over a longer timeframe, considerations of the effects of hysteresis and creep should be made [56], [58]. Hysteresis will be visible in strain results as a variation of values over repeated tests, independent of time. The use of modern high-quality strain gauges and bonding materials, as well as proper bonds being made during installation, usually cause these effects to be negligible. Creep, mostly affected by temperature variation, can be combatted using bonding materials appropriate for the thermal zone in which testing is to be completed [58].

Compensating for errors is not always straightforward. For example, Wheatstone bridge output level and linearity, temperature errors, and separation of unwanted signals are not always able to have compensation adequately applied to eliminate their effects. Selection of an appropriate Wheatstone bridge before testing will mitigate the effect of output level errors, while bridge linearity could be considered negligible for small strain readings [57], [71], as this generates an error of approximately 0.1% for strain readings of 1000 $\mu\varepsilon$ [57]. Equations are available to quantify the nonlinearity error for select gauge layout options [71]. Temperature errors, as previously outlined, can be quantified and corrected given adequate preparation and use of an appropriate compensation technique. Equations are available to complete the corrections for instances where they are warranted [71]. Finally, separation of unwanted signals is more commonly aimed at separating the effects of bending strain from axial strain, where the separation is required and both effects are felt by the same gauge. Use of multiple gauges arranged in specific layouts along the Wheatstone bridge will assist in mitigating and possibly eliminating these influences [57].

Other errors for which equations of compensation are available include gauge misalignment, transverse sensitivity, and gauge factor corrections for instances where manufacturer-indicated values are not equivalent to those used by data acquisition systems [71].

C.3 Principal Strain

When using strain gauge rosettes to capture strain data along multiple axes, determination of the principal strains and the directions in which they act in the material being monitored is often of interest. To accomplish this, a triaxial strain rosette with gauges offset by 45° is often used, as shown in Figure C-1 (after [73]). The angle at which the principal strains occur, in relation to the axis of one of the gauges, is given by θ_P. Maximum and minimum strain values occur at right angles to each other. It is useful to note that the principal strains can also be calculated for other strain gauge rosette geometry [74].

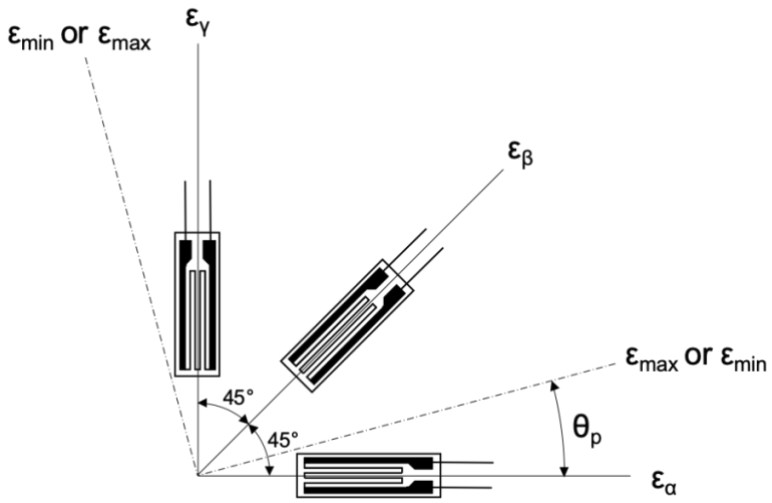

Figure C-1 - Strain gauge rosette showing principal axes (after [73])

Equation C.3 is used to determine the magnitude of principal strains, while Equation C.4 indicates the direction at which the principal strain acts from the reference axis of the rosette [58], [73]–[75]:

$$\varepsilon_{max,min} = \frac{1}{2}\left(\varepsilon_\alpha + \varepsilon_\gamma\right) \pm \frac{1}{2}\sqrt{\left(\varepsilon_\alpha - \varepsilon_\gamma\right)^2 + \left(2\varepsilon_\beta - \varepsilon_\alpha - \varepsilon_\gamma\right)^2} \quad \text{C.3}$$

$$\tan\theta_p = \frac{2\varepsilon_\beta - \varepsilon_\alpha - \varepsilon_\gamma}{\varepsilon_\alpha - \varepsilon_\gamma} \quad \text{C.4}$$

where $\varepsilon_{max,min}$ are the principal strains;
ε_α, ε_β and ε_γ are the strains from the respective gauge locations seen in Figure C-1; and
θ_p is the angle at which the principal strains occur, with respect to the reference axis of the rosette.

APPENDIX D INSTRUMENTATION IDENTIFIERS AND ASSOCIATED DATA ACQUISITION CHANNELS

Table D-1 - Instrument identifiers and associated data acquisition channels

Data Acquisition Unit	Channel Name	Instrument Identifier	Notes
MX1615B (1)	MX1615_B1_CH_1	B1-S1-BBF	1
	MX1615_B1_CH_2	B1-S1-BTF	
	MX1615_B1_CH_3	B1-S1-WA	
	MX1615_B1_CH_4	B1-S1-WH	
	MX1615_B1_CH_5	B1-S1-WV	2
	MX1615_B1_CH_6	B1-S2-BBF	
	MX1615_B1_CH_7	B1-S2-BTF	
	MX1615_B1_CH_8	B1-S3-BBF	2
	MX1615_B1_CH_9	B1-S3-BTF	
	MX1615_B1_CH_10	B1-S3-WA	2
	MX1615_B1_CH_11	B1-S3-WH	2
	MX1615_B1_CH_12	B1-S3-WV	2
	MX1615_B1_CH_13	B1-S4-BBF	
	MX1615_B1_CH_14	B1-S5-WH	
	MX1615_B1_CH_15	B1-S5-WV	
	MX1615_B1_CH_16	B1-S5-WA	
MX1615B (2)	MX1615_B7_CH_1	B7-T3-BTC	
	MX1615_B7_CH_2	B7-T3-TBC	
	MX1615_B7_CH_3	B7-T3-TTC	
	MX1615_B7_CH_4	B7-T4-BTC	
	MX1615_B7_CH_5	B7-T4-TBC	
	MX1615_B7_CH_6	B7-T4-TTC	
	MX1615_B7_CH_7	B7-T5-BTC	
	MX1615_B7_CH_8	B7-T5-TBC	
	MX1615_B7_CH_9	B7-T5-TTC	
	MX1615_B7_CH_10	B7-T6-BTC	
	MX1615_B7_CH_11	B7-T6-TBC	
	MX1615_B7_CH_12	B7-T6-TTC	

Data Acquisition Unit	Channel Name	Instrument Identifier	Notes
	MX1615_B7_CH_13	B7-T1-TTC	
	MX1615_B7_CH_14	B7-T1-TBC	
	MX1615_B7_CH_15	B7-T8-TTC	
	MX1615_B7_CH_16	B7-T8-TBC	
MX440A	MX440A_B4_T4_CH_1	B4-T4-SP1	
	MX440A_B4_T5_CH_2	B4-T5-SP2	
	MX440A_B7_T4_CH_3	B7-T4-SP3	
	MX440A_B7_T5_CH_4	B7-T5-SP4	
MX840B	MX840B_B1_CH_1	B1-S5-BBF	
	MX840B_B1_CH_2	B1-S5-BTF	
	MX840B_B1_CH_3	B1-S9-BBF	
	MX840B_B1_CH_4	B1-S9-BTF	
	MX840B_B1_CH_5	B1-T1-SBS	
	MX840B_B1_CH_6	B1-T4-SBS	
	MX840B_B1_CH_7	B1-T5-SBS	
	MX840B_B1_CH_8	B1-T8-SBS	

Notes:

1. Data gathered at 4800 Hz sampling rate. Post-processing included reduction of dataset using a sampling rate of 1200 Hz to align data with other channels.

2. Data capture failure.

APPENDIX E VEHICLE PROPERTIES

This appendix includes technical specification for each of the vehicles used in this testing programme [61]–[64], [76], [77]. Vehicle variants refer to those employed by the Canadian Armed Forces. The vehicles used include: the Leopard 2 AEV; the Leopard 2A4M MBT; the MSVS LHS variant; and the TAPV.

Note that the full version of this appendix contains RESTRICTED information. Transmission, use, and reproduction of this appendix is therefore restricted to the purposes identified as necessary by the Department of National Defence (DND) and the CAF, including appropriately authorized assignees with the explicit permission of relevant authorities. Transmission to third parties is not permitted.

A complete copy of this thesis is available that includes the information contained in this appendix, if so required.

APPENDIX F ITERATIVE TESTING PLAN

Table F-1 indicates the details pertinent to the iterative testing plan followed. Tests conducted with the Leopard 2 MBT are denoted as "Leo 2."

Table F-1 - Iterative testing plan

Serial	Vehicle	Direction	Speed (km/h)	Surface Condition	Iteration Name
01	Leo 2	E-W	Stationary	Smooth	Ser01 Leo E-W Stationary Smooth
02	AEV	E-W	Stationary	Smooth	Ser02 AEV E-W Stationary Smooth
03	Leo 2	W-E	Stationary	Smooth	Ser03 Leo W-E Stationary Smooth
04	AEV	W-E	Stationary	Smooth	Ser04 AEV W-E Stationary Smooth
05	Leo 2	E-W	Crawl	Smooth	Ser05 Leo E-W Crawl Smooth
06	AEV	E-W	Crawl	Smooth	Ser06 AEV E-W Crawl Smooth
07	Leo 2	W-E	Crawl	Smooth	Ser07 Leo W-E Crawl Smooth
08	AEV	W-E	Crawl	Smooth	Ser08 AEV W-E Crawl Smooth
09	Leo 2	E-W	10	Smooth	Ser09 Leo E-W 10k Smooth
10	AEV	E-W	10	Smooth	Ser10 AEV E-W 10k Smooth
11	Leo 2	W-E	10	Smooth	Ser11 Leo W-E 10k Smooth
12	AEV	W-E	10	Smooth	Ser12 AEV W-E 10k Smooth
13	Leo 2	E-W	20	Smooth	Ser13 Leo E-W 20k Smooth
14	AEV	E-W	20	Smooth	Ser14 AEV E-W 20k Smooth
15	Leo 2	W-E	20	Smooth	Ser15 Leo W-E 20k Smooth
16	AEV	W-E	20	Smooth	Ser16 AEV W-E 20k Smooth
17	Leo 2	E-W	25	Smooth	Ser17 Leo E-W 25k Smooth
18	AEV	E-W	30	Smooth	Ser18 AEV E-W 30k Smooth
19	Leo 2	W-E	25	Smooth	Ser19 Leo W-E 25k Smooth
20	AEV	W-E	30	Smooth	Ser20 AEV W-E 30k Smooth
21	Leo 2	E-W	35	Smooth	Ser21 Leo E-W 35k Smooth
22	AEV	E-W	40	Smooth	Ser22 AEV E-W 40k Smooth
23	Leo 2	W-E	35	Smooth	Ser23 Leo W-E 35k Smooth
24	AEV	W-E	40	Smooth	Ser24 AEV W-E 40k Smooth
25	Leo 2	E-W	30	Smooth	Ser25 Leo E-W 30k Smooth
26	AEV	E-W	50	Smooth	Ser26 AEV E-W 50k Smooth

Serial	Vehicle	Direction	Speed (km/h)	Surface Condition	Iteration Name
27	Leo 2	W-E	30	Smooth	Ser27 Leo W-E 30k Smooth
28	AEV	W-E	50	Smooth	Ser28 AEV W-E 50k Smooth
29	AEV	E-W	10	Irregular	Ser29 AEV E-W 10k Irregular
30	AEV	W-E	20	Irregular	Ser30 AEV W-E 20k Irregular
31	AEV	E-W	30	Irregular	Ser31 AEV E-W 30k Irregular
32	AEV	W-E	40	Irregular	Ser32 AEV W-E 40k Irregular
33	AEV	E-W	50	Irregular	Ser33 AEV E-W 50k Irregular
34	AEV	W-E	10	Irregular	Ser34 AEV W-E 10k Irregular
35	AEV	E-W	20	Irregular	Ser35 AEV E-W 20k Irregular
36	AEV	W-E	30	Irregular	Ser36 AEV W-E 30k Irregular
37	AEV	E-W	40	Irregular	Ser37 AEV E-W 40k Irregular
38	AEV	W-E	50	Irregular	Ser38 AEV W-E 50k Irregular
39	MSVS	E-W	Stationary	Smooth	Ser39 MSVS E-W Stationary Smooth
40	MSVS	W-E	Stationary	Smooth	Ser40 MSVS W-E Stationary Smooth
41	MSVS	E-W	Crawl	Smooth	Ser41 MSVS E-W Crawl Smooth
42	MSVS	W-E	Crawl	Smooth	Ser42 MSVS W-E Crawl Smooth
43	MSVS	E-W	10	Smooth	Ser43 MSVS E-W 10k Smooth
44	MSVS	W-E	10	Smooth	Ser44 MSVS W-E 10k Smooth
45	MSVS	E-W	20	Smooth	Ser45 MSVS E-W 20k Smooth
46	MSVS	W-E	20	Smooth	Ser46 MSVS W-E 20k Smooth
47	MSVS	E-W	30	Smooth	Ser47 MSVS E-W 30k Smooth
48	MSVS	W-E	30	Smooth	Ser48 MSVS W-E 30k Smooth
49	MSVS	E-W	40	Smooth	Ser49 MSVS E-W 40k Smooth
50	MSVS	W-E	40	Smooth	Ser50 MSVS W-E 40k Smooth
51	MSVS	E-W	50	Smooth	Ser51 MSVS E-W 50k Smooth
52	MSVS	W-E	50	Smooth	Ser52 MSVS W-E 50k Smooth
53	MSVS	E-W	10	Irregular	Ser53 MSVS E-W 10k Irregular
54	MSVS	W-E	20	Irregular	Ser54 MSVS W-E 20k Irregular
55	MSVS	E-W	30	Irregular	Ser55 MSVS E-W 30k Irregular
56	MSVS	W-E	40	Irregular	Ser56 MSVS W-E 40k Irregular
57	MSVS	E-W	50	Irregular	Ser57 MSVS E-W 50k Irregular
58	MSVS	W-E	10	Irregular	Ser58 MSVS W-E 10k Irregular

Serial	Vehicle	Direction	Speed (km/h)	Surface Condition	Iteration Name
59	MSVS	E-W	20	Irregular	Ser59 MSVS E-W 20k Irregular
60	MSVS	W-E	30	Irregular	Ser60 MSVS W-E 30k Irregular
61	MSVS	E-W	40	Irregular	Ser61 MSVS E-W 40k Irregular
62	MSVS	W-E	50	Irregular	Ser62 MSVS W-E 50k Irregular
63	TAPV	E-W	Stationary	Smooth	Ser63 TAPV E-W Stationary Smooth
64	TAPV	W-E	Stationary	Smooth	Ser64 TAPV W-E Stationary Smooth
65	TAPV	E-W	Crawl	Smooth	Ser65 TAPV E-W Crawl Smooth
66	TAPV	W-E	Crawl	Smooth	Ser66 TAPV W-E Crawl Smooth
67	TAPV	E-W	10	Smooth	Ser67 TAPV E-W 10k Smooth
68	TAPV	W-E	10	Smooth	Ser68 TAPV W-E 10k Smooth
69	TAPV	E-W	20	Smooth	Ser69 TAPV E-W 20k Smooth
70	TAPV	W-E	20	Smooth	Ser70 TAPV W-E 20k Smooth
71	TAPV	E-W	30	Smooth	Ser71 TAPV E-W 30k Smooth
72	TAPV	W-E	30	Smooth	Ser72 TAPV W-E 30k Smooth
73	TAPV	E-W	40	Smooth	Ser73 TAPV E-W 40k Smooth
74	TAPV	W-E	40	Smooth	Ser74 TAPV W-E 40k Smooth
75	TAPV	E-W	50	Smooth	Ser75 TAPV E-W 50k Smooth
76	TAPV	W-E	50	Smooth	Ser76 TAPV W-E 50k Smooth
77	TAPV	E-W	10	Irregular	Ser77 TAPV E-W 10k Irregular
78	TAPV	W-E	20	Irregular	Ser78 TAPV W-E 20k Irregular
79	TAPV	E-W	30	Irregular	Ser79 TAPV E-W 30k Irregular
80	TAPV	W-E	40	Irregular	Ser80 TAPV W-E 40k Irregular
81	TAPV	E-W	50	Irregular	Ser81 TAPV E-W 50k Irregular
82	TAPV	W-E	10	Irregular	Ser82 TAPV W-E 10k Irregular
83	TAPV	E-W	20	Irregular	Ser83 TAPV E-W 20k Irregular
84	TAPV	W-E	30	Irregular	Ser84 TAPV W-E 30k Irregular
85	TAPV	E-W	40	Irregular	Ser85 TAPV E-W 40k Irregular
86	TAPV	W-E	50	Irregular	Ser86 TAPV W-E 50k Irregular

APPENDIX G MODEL VALIDATION

To confirm the legitimacy of data gathered during experimental testing, validation should be completed. This ensures that the conclusions drawn from analysis that uses this data are appropriate, realistic, and rational in their roots.

To this end, data validation was completed on strain and displacement readings made during experimental testing. Initially strain data validation was completed using simplified hand calculations, as given in Section G.1 below. More accurate validation occurred using a numerical model as given in Section G.2 (also outlined in Section **Error! Reference source not found.**); the strain and displacement values recorded on-site were recorded to the model results in Section G.3 and Section 0, respectively. Section 0 outlines some simplifications that were part of the validation model, with the aim of explaining why identical results are not observed between modelled and real data points.

Validation calculations were made using the MathCAD Prime software platform, version 5.0.0.0.

G.1 Strain Data Validation (Hand Calculations)

G.1.1 Description

Using the simplified truss shown in Figure G-1, determine the strain expected in the top chord at mid-span due to loading by the AEV. Note that, throughout these calculations, "TC" represents "top chord." Assume negligible effect of load transfer through angled members (in comparison with chord).

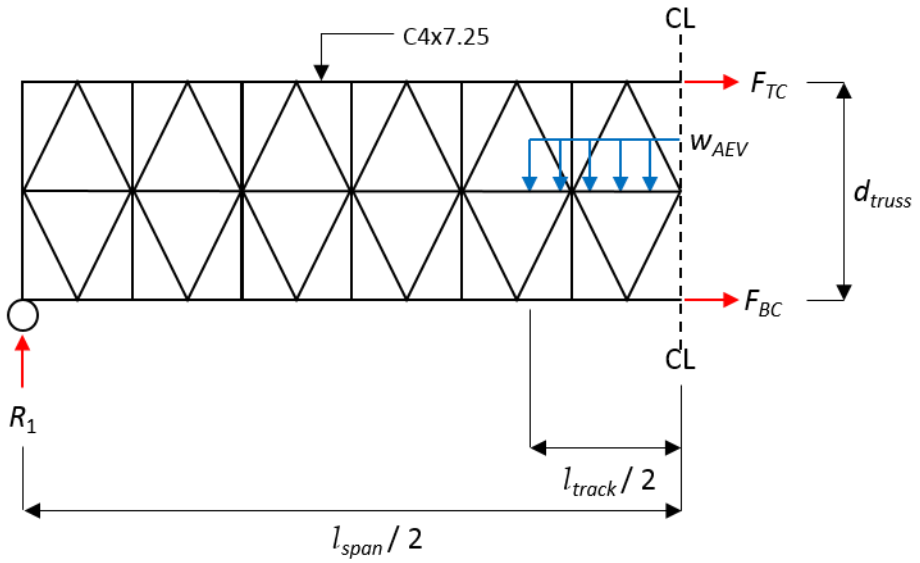

Figure G-1 - Simplified bridge with mid-span AEV loading

Bridge: $d_{truss} := 2184\ mm$ $A_{C4x7.25} := 2.13\ in^2$

$l_{span} := 39.62\ m$ $E_s := 200\ GPa$

AEV: $l_{track} := 4.95\ m$ $m_{AEV} := 69500\ kg$

General: $g = 9.807\ \frac{m}{s^2}$

G.1.2 Determine the magnitude of the AEV's UDL acting on the bridge

$$w_{AEV} := \frac{m_{AEV} \cdot g}{l_{track}} = 138 \ \frac{kN}{m}$$

G.1.3 Determine the magnitude of the support reaction due to the live load

$$\Sigma F_y = 0 = R_1 - w_{AEV} \cdot \frac{l_{track}}{2} \quad ; \qquad R_1 := w_{AEV} \cdot \frac{l_{track}}{2} = 341 \ kN$$

G.1.4 Determine the magnitude of the top chord axial force (summed force for all trusses)

$$\Sigma M_{BC@CL} = 0 = -F_{TC} \cdot d_{truss} + \left(w_{AEV} \cdot \frac{l_{track}}{2} \right) \cdot \frac{l_{track}}{4} - R_1 \cdot \frac{l_{span}}{2}$$

$$F_{TC} := \frac{1}{d_{truss}} \left(\left(w_{AEV} \cdot \frac{l_{track}}{2} \right) \cdot \frac{l_{track}}{4} - R_1 \cdot \frac{l_{span}}{2} \right)$$

$$F_{TC} = -2898 \ kN$$

G.1.5 Determine the axial force for a single truss chord (superstructure comprised of eight trusses)

$$F_{TC\_single} := \frac{F_{TC}}{8} = -362.246 \ kN$$

G.1.6 Determine the strain in a single truss chord (four C4x7.25 channels make up one truss chord)

$$\sigma_{TC} = \frac{F_{TC\_single}}{4 \cdot A_{C4x7.25}} \quad \text{and} \quad \varepsilon_{TC} = \frac{\sigma_{TC}}{E_s} \quad ;$$

$$\varepsilon_{TC\_calculated} := \frac{F_{TC\_single}}{4 \cdot E_s \cdot A_{C4x7.25}} = -330 \ \frac{\mu m}{m}$$

G.1.7 List strain readings gathered during experimental testing

Test serial "AEV E-W Stationary Smooth Ser02" was used for data comparison; readings from instruments in the TTC (top of top chord) and BTC (bottom of top chord) locations are indicated:

TTC instruments:

$$\varepsilon_{B7\_T1} := -351\ \frac{\mu m}{m} \qquad \varepsilon_{B7\_T5} := -325\ \frac{\mu m}{m}$$

$$\varepsilon_{B7\_T3} := -353\ \frac{\mu m}{m} \qquad \varepsilon_{B7\_T6} := -326\ \frac{\mu m}{m}$$

$$\varepsilon_{B7\_T4} := -334\ \frac{\mu m}{m} \qquad \varepsilon_{B7\_T8} := -318\ \frac{\mu m}{m}$$

$$\varepsilon_{TTC\_data} := \text{mean}\left(\varepsilon_{B7\_T1}, \varepsilon_{B7\_T3}, \varepsilon_{B7\_T4}, \varepsilon_{B7\_T5}, \varepsilon_{B7\_T6}, \varepsilon_{B7\_T8}\right) = -335\ \frac{\mu m}{m}$$

BTC instruments:

$$\varepsilon_{B7\_T3} := -282\ \frac{\mu m}{m} \qquad \varepsilon_{B7\_T5} := -244\ \frac{\mu m}{m}$$

$$\varepsilon_{B7\_T4} := -254\ \frac{\mu m}{m} \qquad \varepsilon_{B7\_T6} := -253\ \frac{\mu m}{m}$$

$$\varepsilon_{BTC\_data} := \text{mean}\left(\varepsilon_{B7\_T3}, \varepsilon_{B7\_T4}, \varepsilon_{B7\_T5}, \varepsilon_{B7\_T6}\right) = -258\ \frac{\mu m}{m}$$

All TC instruments:

$$\varepsilon_{TC\_data} := \text{mean}\left(\varepsilon_{TTC\_data}, \varepsilon_{BTC\_data}\right) = -296\ \frac{\mu m}{m}$$

G.1.8 Compare experimental and calculated strain values

$$\varepsilon_{TC\_data} = -296\ \frac{\mu m}{m} \qquad \varepsilon_{TC\_calculated} = -330\ \frac{\mu m}{m}$$

$$difference_{percent} := \frac{\text{abs}\left(\varepsilon_{TC\_data} - \varepsilon_{TC\_calculated}\right)}{\text{mean}\left(\varepsilon_{TC\_data}, \varepsilon_{TC\_calculated}\right)} = -10.6\%$$

G.2 Simple SAP2000 Model

The model built within SAP2000 was made using 2D frame elements, as indicated in Figure G-2. Section properties were customized such that each element in the model had the same geometric and material properties as the corresponding element of the real bridge.

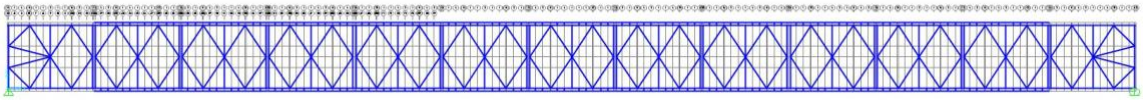

Figure G-2 - Simplified 2D SAP2000 bridge model

A single truss was used in the model. This corresponds to approximately 1/8th of the bridge superstructure that provides load resistance. As such, the load transferred by the vehicle to the superstructure was reduced to 1/8th of its magnitude.

For bays B2 through B12, each panel has top and bottom chord reinforcement that provides increased load resistance across two spans (with a single-bay reinforcing chord added to bay B12). On the actual bridge, these are secured to the panels with four bolts per panel. To model this, a line element with no mass and no geometric properties was used to create nodes at the bolted locations on the top chord and chord reinforcement were constrained to translate and rotate with each other in all six directions. Figure G-3 indicates this linking.

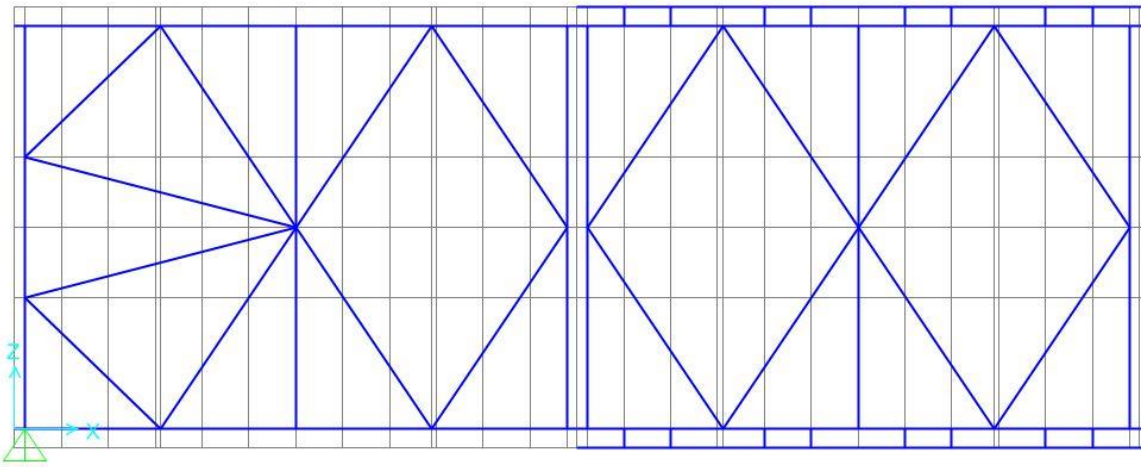

Figure G-3 - Modelled linked chord reinforcement

Loading was modelled by applying appropriate live loads (point loads) at transom locations. The simulated loading scenario saw the AEV stopped at mid-span. Due to the length of the vehicle exceeding the length of a single bay, the vehicle loaded the transoms between bays B5 and B6, B6 and B7, B7 and B8, and B8 and B9.

G.3 Strain Data Validation (Numerical Model)

G.3.1 Convert model axial forces in the top chord to strain

$F_{TC1} := -189.99\ kN$ (force in top chord reinforcement)

$F_{TC2} := -143.62\ kN$ (force in top chord)

$F_{TC\_model} := F_{TC1} + F_{TC2} = -333.61\ kN$

$\sigma_{TC} = \frac{F_{TC\_model}}{4 \cdot A_{C4x7.25}}$ and $\varepsilon_{TC} = \frac{\sigma_{TC}}{E_s}$;

$\varepsilon_{TC\_model} := \frac{F_{TC\_model}}{4 \cdot E_s \cdot A_{C4x7.25}} = -303\ \frac{\mu m}{m}$

G.3.2 List strain readings gathered during experimental testing

Test serial "AEV E-W Stationary Smooth Ser02" was used for data comparison; readings from instruments in the TTC (top of top chord) and BTC (bottom of top chord) locations are indicated:

TTC instruments:

$\varepsilon_{B7\_T1} := -351\ \frac{\mu m}{m}$ $\varepsilon_{B7\_T5} := -325\ \frac{\mu m}{m}$

$\varepsilon_{B7\_T3} := -353\ \frac{\mu m}{m}$ $\varepsilon_{B7\_T6} := -326\ \frac{\mu m}{m}$

$\varepsilon_{B7\_T4} := -334\ \frac{\mu m}{m}$ $\varepsilon_{B7\_T8} := -318\ \frac{\mu m}{m}$

$\varepsilon_{TTC\_data} := \text{mean}\left(\varepsilon_{B7\_T1}, \varepsilon_{B7\_T3}, \varepsilon_{B7\_T4}, \varepsilon_{B7\_T5}, \varepsilon_{B7\_T6}, \varepsilon_{B7\_T8}\right) = -335\ \frac{\mu m}{m}$

BTC instruments:

$$\varepsilon_{B7\_T3} := -282\ \frac{\mu m}{m} \qquad \varepsilon_{B7\_T5} := -244\ \frac{\mu m}{m}$$

$$\varepsilon_{B7\_T4} := -254\ \frac{\mu m}{m} \qquad \varepsilon_{B7\_T6} := -253\ \frac{\mu m}{m}$$

$$\varepsilon_{BTC\_data} := \text{mean}\left(\varepsilon_{B7\_T3}, \varepsilon_{B7\_T4}, \varepsilon_{B7\_T5}, \varepsilon_{B7\_T6}\right) = -258\ \frac{\mu m}{m}$$

All TC instruments:

$$\varepsilon_{TC\_data} := \text{mean}\left(\varepsilon_{TTC\_data}, \varepsilon_{BTC\_data}\right) = -296\ \frac{\mu m}{m}$$

G.3.3 Compare experimental and calculated strain values

$$\varepsilon_{TC\_data} = -296\ \frac{\mu m}{m} \qquad \varepsilon_{TC\_model} = -303\ \frac{\mu m}{m}$$

$$difference_{percent} := \frac{\text{abs}\left(\varepsilon_{TC\_data} - \varepsilon_{TC\_model}\right)}{\text{mean}\left(\varepsilon_{TC\_data}, \varepsilon_{TC\_model}\right)} = -2.4\%$$

G.4 Displacement Data Validation (Numerical Model)

G.4.1 Determine (1/8th) loads on transoms for input into model

Note: transoms denoted "Tr[#1]&[#2]" indicating the transom located between bays "#1" and "#2."

$$l_{bay} := \frac{l_{span}}{13} = 3.048\ m$$

$$l_{overhang} := \frac{l_{track} - l_{bay}}{2} = 0.951\ m$$

(overhang of track into B6 and B8, each, when AEV at mid-span)

Determine loading on transoms due to load across B6:

$$P_{B6@Tr5\&6} := \frac{w_{AEV} \cdot l_{overhang}^{2}}{2 \cdot l_{bay}} = 20.436\ kN$$

$$P_{B6@Tr6\&7} := \frac{w_{AEV} \cdot l_{overhang}}{2 \cdot l_{bay}} \left(2 \cdot l_{bay} - l_{overhang}\right) = 110.528\ kN$$

Determine loading on transoms due to load across B7:

$$P_{B7@Tr6\&7} := \frac{w_{AEV} \cdot l_{bay}}{2} = 209.817\ kN$$

$$P_{B7@Tr6\&7} := \frac{w_{AEV} \cdot l_{bay}}{2} = 209.817\ kN$$

Determine loading on transoms due to load across B8:

$$P_{B8@Tr7\&8} := \frac{w_{AEV} \cdot l_{overhang}}{2 \cdot l_{bay}} \left(2 \cdot l_{bay} - l_{overhang}\right) = 110.528\ kN$$

$$P_{B8@Tr8\&9} := \frac{w_{AEV} \cdot l_{overhang}^{2}}{2 \cdot l_{bay}} = 20.436\ kN$$

Determine loading at each transom acting on a single truss (i.e. 1/8th of the transom load):

$$P_{Tr5@6} := \frac{1}{8}\left(P_{B6@Tr5@6}\right) = 2.555\ kN$$

$$P_{Tr6@7} := \frac{1}{8}\left(P_{B6@Tr6@7} + P_{B7@Tr6@7}\right) = 40.043\ kN$$

$$P_{Tr7@8} := \frac{1}{8}\left(P_{B7@Tr7@8} + P_{B8@Tr7@8}\right) = 40.043\ kN$$

$$P_{Tr8@9} := \frac{1}{8}\left(P_{B8@Tr8@9}\right) = 2.555\ kN$$

G.4.2 List displacement readings gathered from simple SAP2000 model

$\delta_{SAP\_B7} := -47.69\ mm$ (mid-span)

$\delta_{SAP\_B4} := -33.76\ mm$ (quarter-span)

G.4.3 List displacement readings gathered during experimental testing at B7

Readings from string potentiometers are indicated from instrument B7-T4-SP3 (instrument B7-T8-SP4 shows erratic data across test serials and was discounted from analysis). AEV static and quasi-static (crawl) tests were used for data comparison from the following serials: Ser02 AEV E-W Stationary Smooth, Ser04 AEV W-E Stationary Smooth, Ser06 AEV E-W Crawl Smooth, and Ser08 AEV W-E Crawl Smooth.

$\delta_{Ser02\_B7} := -41.51\ mm$ $\delta_{Ser06\_B7} := -38.23\ mm$

$\delta_{Ser04\_B7} := -37.50\ mm$ $\delta_{Ser08\_B7} := -35.66\ mm$

$$\delta_{data\_B7} := \text{mean}\left(\delta_{Ser02\_B7}, \delta_{Ser04\_B7}, \delta_{Ser06\_B7}, \delta_{Ser08\_B7}\right) = -38.23\ mm$$

G.4.4 List displacement readings gathered during experimental testing at B4

Readings from string potentiometers are indicated from instrument B4-T1-SP1 (instrument B4-T8-SP2 shows erratic data across test serials and was discounted from analysis). The same AEV static and quasi-static (crawl) tests were used as above.

$\delta_{Ser02\_B4} := -31.05\ mm$ $\delta_{Ser06\_B4} := -29.86\ mm$

$\delta_{Ser04\_B4} := -28.57\ mm$ $\delta_{Ser08\_B4} := -27.45\ mm$

$\delta_{data\_B4} := \text{mean}\left(\delta_{Ser02\_B4}, \delta_{Ser04\_B4}, \delta_{Ser06\_B4}, \delta_{Ser08\_B4}\right) = -29.23\ mm$

G.4.5 Compare experimental and calculated displacement values

Mid-span (B7):

$\delta_{data\_B7} = -38.23\ mm$

$\delta_{SAP\_B7} = -47.69\ mm$

$difference_{percent} := \frac{\text{abs}\left(\delta_{data\_B7} - \delta_{SAP\_B7}\right)}{\text{mean}\left(\delta_{data\_B7}, \delta_{SAP\_B7}\right)} = -22\%$

Quarter-span (B4):

$\delta_{data\_B4} = -29.23\ mm$

$\delta_{SAP\_B4} = -33.76\ mm$

$difference_{percent} := \frac{\text{abs}\left(\delta_{data\_B4} - \delta_{SAP\_B4}\right)}{\text{mean}\left(\delta_{data\_B4}, \delta_{SAP\_B4}\right)} = -14\%$

G.5 Discussion

Simplifications in the modelling of the bridge have been made. One of the primary simplifications is the idealization of panel connections as pure pinned connections. In reality, the pins that are used to connect adjacent bridge components are not perfectly free-rotating; the pins are tightly installed, such that is it feasible to have some moment transfer and rotational transfer occurring across the boundary.

On a similar note, the chord reinforcement elements are as long as two bays. Therefore, moment is transferred across the pinned connections between bays. This further reduces the ability of bay connections to act as ideal pins, but rather can be more closely identified as a sort of spliced connection.

Finally, some stiffness is not modelled as a result of simplifying the welded plates at panel mid-height, as indicated in Figure G-4 [59]. The stiffness increase that may come from modelling these components could decrease the displacement that the model experiences during loading.

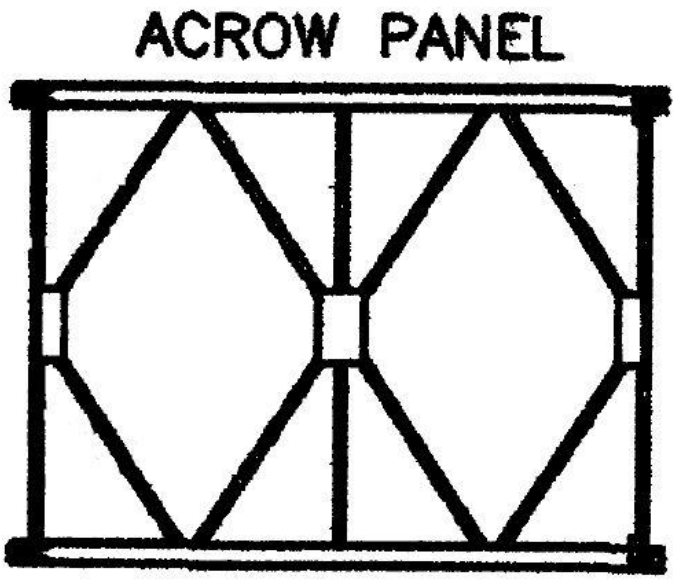

Figure G-4 - ACROW panel showing welded plates at mid-height [59]

APPENDIX H DATA FILTER CONVERGENCE TEST RESULTS

To determine the appropriate parameters to apply to low-pass data filters used during analysis, multiple filters (with different cut-off frequencies) were independently applied to raw strain data and the effects compared to each other using convergence tests. Cut-off frequencies of 0.25 Hz, 0.5 Hz, 1.0 Hz, and 2.0 Hz were used. With this comparison, it was determined that a low-pass data filter cut-off frequency of 1.0 Hz was appropriate. Convergence test results are given below.

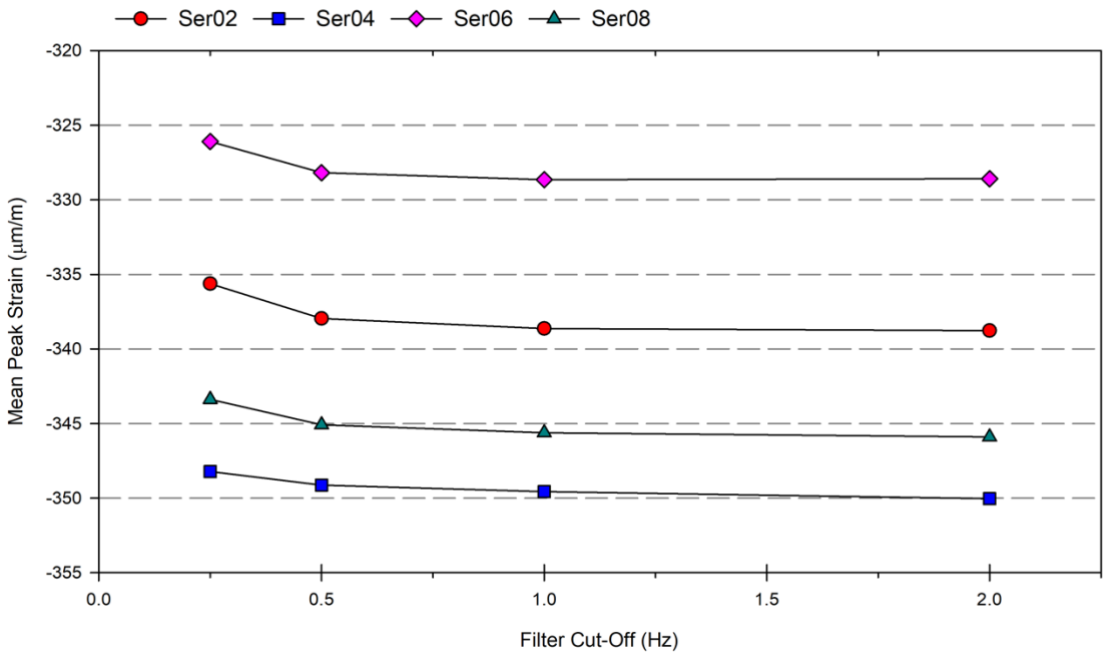

Figure H-1 - AEV data filter convergence test results

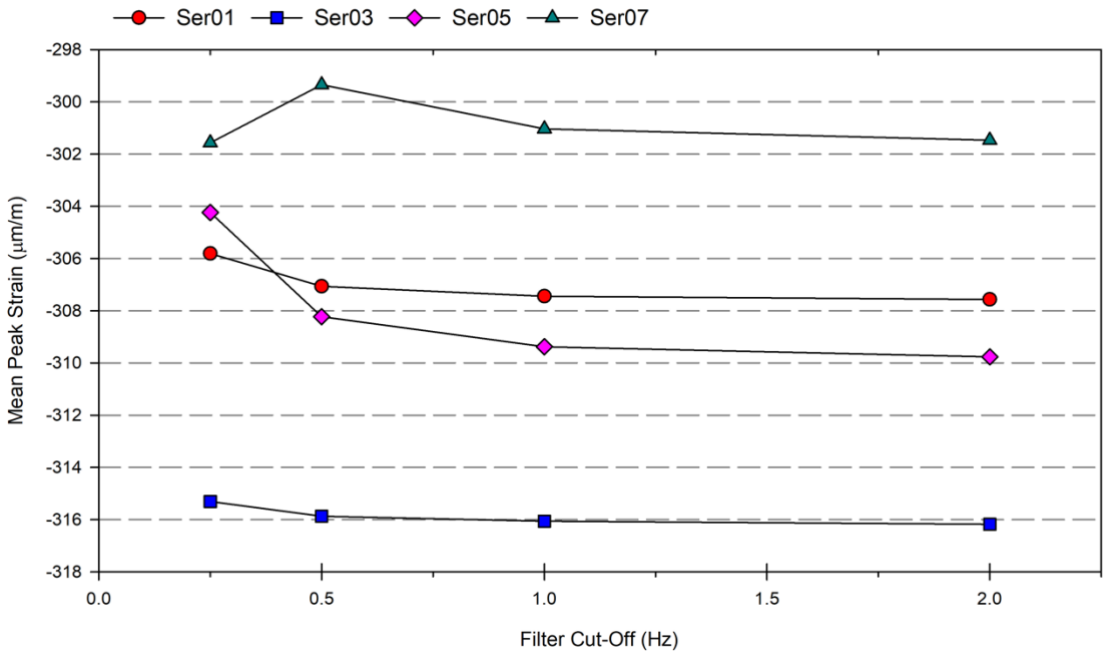

Figure H-2 - MBT data filter convergence test results

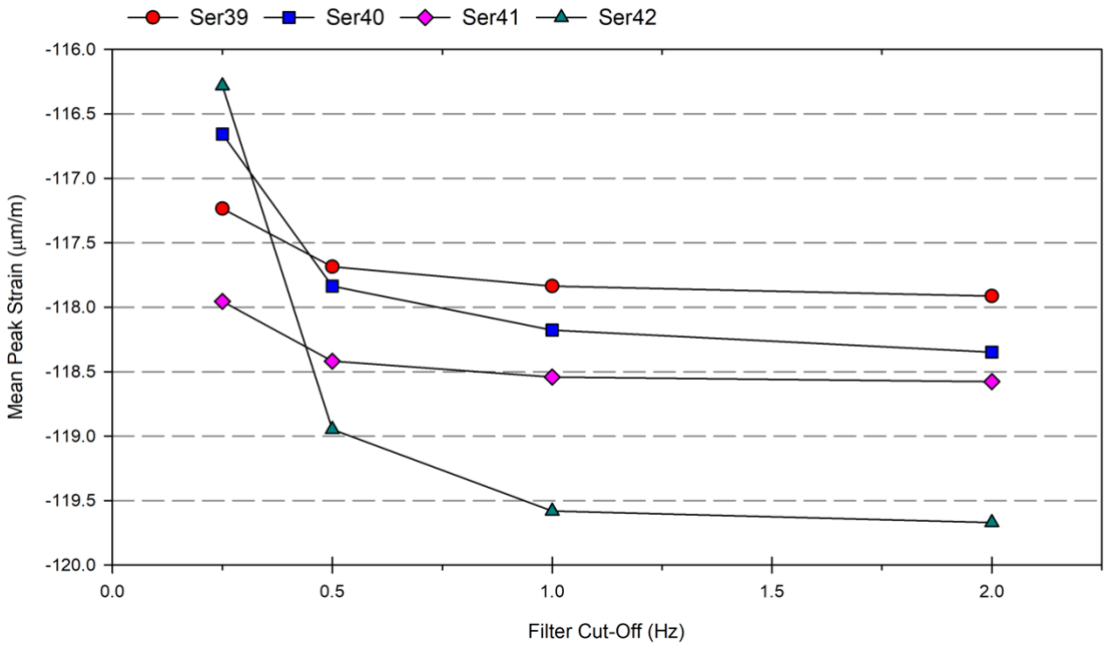

Figure H-3 - MSVS data filter convergence test results

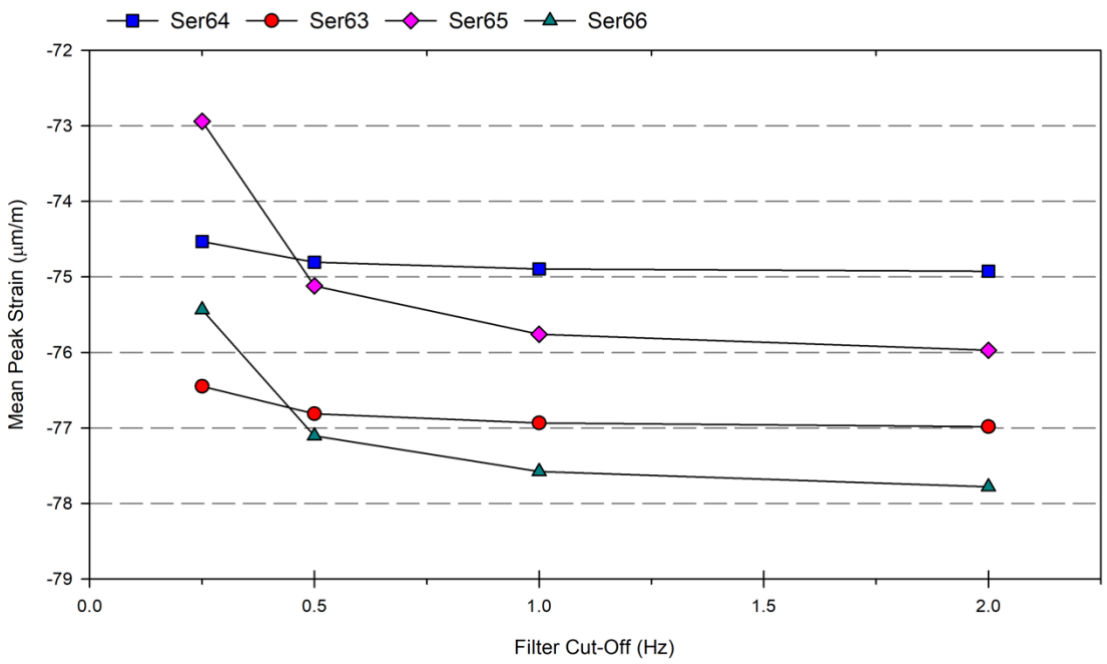

Figure H-4 - TAPV data filter convergence test results

APPENDIX I BRIDGE DYNAMIC LOAD ALLOWANCE COMPARISON

Table I-1 - Bridge DLA using national bridge codes and military bridge manuals

Source	DLA Specification	DLA	Note
CHBDC (three axles of the design truck) [2]	Specified	0.25	
OHBDC [4], [43]	See Figure 2.4	0.40	
AASHTO Standard Specification for Highway Bridges 1973 [20]	$I = \frac{15.24}{L + 38.1} \leq 0.30$	0.20	
AASHTO LRFD Bridge Design Specifications [15]	Specified	0.33	
Chinese General Code for Design of Highway Bridges and Culverts 1989 [21]	$IM = \frac{15}{37.5 + L}$	0.19	
Chinese General Code for Design of Highway Bridges and Culverts [21]	$IM = 0.1767 \ln f - 0.0157$	0.18	
NZTA Bridge Manual [22]	$DAF = 1 + \frac{15}{L + 38}$	0.19	1
Eurocode 1: Actions on Structures - Part 2: Traffic Loads on Bridges (single lane, moment) [21]	Specified	0.40	1
Eurocode 1: Actions on Structures - Part 2: Traffic Loads on Bridges (special vehicle model) [19]	$\phi = 1.40 - \frac{L}{500} > 1.0$	0.32	1
British BS 5400-2 [45]	Specified	0.25	
Japanese Specifications for Highway Bridges Part 1: Common Specifications [21]	$IM = \frac{20}{50 + L}$	0.22	
CAF Bridge Manual (B-GL-361-014/FP-001) [6]	Specified	0.15	
US Army Bridge Manual (FM 3-43.343) [7]	Specified	0.15	

Note:

1. Code specifies dynamic amplification term to be > 1.0; reduction of calculated term by a magnitude of 1.0 completed to show comparable DLA as defined in Section 2.3.1.